UNIVERSITY OF CALIFORNIA

Santa Barbara

Studies in Neoproterozoic Paleontology

A dissertation submitted in partial satisfaction of the

requirements for the degree Doctor of Philosophy

in Geological Sciences

by

Leigh Anne Smith Riedman

Committee in charge:

Professor Susannah M. Porter, Chair

Professor Stanley M. Awramik

Professor Bruce H. Tiffney

December 2014

The dissertation of Leigh Anne Smith Riedman is approved.

_____
Stanley M. Awramik

_____
Bruce H. Tiffney

_____
Susannah M. Porter, Committee Chair

December 2014

Studies in Neoproterozoic Paleontology

by

Leigh Anne Smith Riedman

NOMENCLATURAL DISCLAIMER

The present dissertation does not constitute a published work under Article 30 of the International Code of Nomenclature for algae, fungi, and plants (Melbourne Code), and no new names or nomenclatural acts are made available herein.

PRINCIPAL SEYMOUR SKINNER: "Ah, there's nothing more exciting than science. You get all the fun of sitting still, being quiet, writing down numbers, paying attention… Science has it all."

The Simpsons, *Bart's Comet*

"If you're looking for sympathy you'll find it between shit and syphilis in the dictionary."

David Sedaris, *Barrel Fever*

ACKNOWLEDGEMENTS

The greatest of thanks are due to my family. My parents have always supported my interest in the sciences in general and in geology in particular. They never suggested I should choose a more practical vocation. My kids cannot remember a time before I started graduate school— they have been supportive and proud of me and have taught me the importance of time management. My husband, John, is a big part of who I am today. I could not have done half of what I've done without his help, support and occasional pushes. He is my day, my night, my compass.

Susannah Porter has shown me what an advisor, mentor, teacher and friend can be. She took a chance on me and I will never forget it. I will strive to be as compassionate, generous and inspirational with colleagues and students and as clever, meticulous and precise in my science as she.

I am incredibly fortunate to have had the chance to share an office and seven years with John Moore, easily one of the smartest people on the planet (this, despite his unreasonable attachment to the Oxford comma). John has taught me much about taxonomy, the rules of nomenclature, languages and food and made the day-to-day time in the office a joy.

Many thanks are due to my friends Susannah Hoffman and Aashish Mehta for their willingness to listen and to help watch my kids while I worked. Thank you, Brooke Whittington, for convincing me to commit to running a half-marathon. Taking on a time-consuming training schedule while finishing a dissertation seems foolhardy but it has been a great outlet and gave me forced quiet time and perspective.

CURRICULUM VITÆ OF LEIGH ANNE SMITH RIEDMAN

Education

2014 (expected, December) Ph.D., Geological Sciences, with emphasis in paleontology, University of California, Santa Barbara, Dissertation: Studies in Neoproterozoic Paleontology

2004 M.S., Geology, with emphasis in paleontology, University of California, Los Angeles

2000 B.S., Geology with a minor in Mathematics, Louisiana Tech University

Publications

In prep Porter, S. M. and **Riedman, L. A.**, Systematic Paleontology of the mid-Neoproterozoic Chuar Group, Arizona.

In press Junium, C. K., Hurtgen, M. T., **Riedman, L. A.**, Porter, S. M., Halverson, G. P., Fueling the Snowball Earth Biogeochemical Recovery: Evidence for a Bio-inorganic Bridge.

In press **Riedman, L. A.**, Porter, S. M., Organic-walled microfossils of the early to mid-Neoproterozoic Alinya Formation, Officer Basin, Australia.

2014 **Riedman, L. A.**, Porter, S. M., Halverson, G. P., Hurtgen, M. T., Junium, C. K., Organic-walled microfossil assemblages from glacial and interglacial

Neoproterozoic units of Australia and Svalbard. *Geology* v. 42, pp. 1011–1014.

2011 Yin, C., Liu, P., Awramik, S. M., Chen, S., Tang, F., Gao, L., Wang, Z., **Riedman, L. A.**, 2011. Acanthomorphic Biostratigraphic Succession of the Ediacaran Doushantuo Formation in the East Yangtze Gorges, South China. Acta Geologica Sinica. 85:283-295.

Presentations

2013 Oral Presentation, Geological Society of America, Annual Meeting, "High Morphological Diversity of the Neoproterozoic Alinya Formation, Officer Basin, Australia"

2012 Oral presentation, Geological Society of America, Annual Meeting, "Fossil Evidence for a Cryogenian Diversity Crisis"

2012 Poster presentation, Fermor Meeting of Geological Society, London, "Fossil Evidence for a Cryogenian Diversity Crisis"

2012 Oral presentation- CalPaleo, UC Riverside, "The Cryogenian Crisis: A Story of Acritarchs and Aggregates"

2011 Poster presentation- Geological Society of America Annual Meeting, "Preliminary Paleontological Data for Five Cryogenian Siliciclastic Units"

Research and Instrumentation Experience

- Light microscopy and SEM of macerated organic-walled microfossils

    - Cryogenian units of Svalbard and Australia: Amadeus Basin, Officer Basin, Adelaide Rift Complex, northwestern Tasmania
- Light Microscopy of thin sections (chert, shale, carbonate)
    - Bambuí Group, Doushantuo Fm, Black River Dolomite, Svanbergfjellet Fm, Chuar Group
- SEM/EDS of Neoproterozoic vase-shaped microfossils
    - Chatkaragai Suite, Tien Shan; Chuar Group, USA; Togari Group, Tasmania
- Electron Microprobe of Neoproterozoic Vase-shaped microfossils
    - Chatkaragai Suite, Tien Shan

Field Experience

2010 Togari and Grassy Groups, NW Tasmania and King Island, field and core sampling

2010 Cryogenian of Officer Basin, Amadeus Basin, Adelaide Rift Complex, Australia, core sampling

2009 Doushantuo Formation, Yangtze Gorges Area, China, field sampling

Awards and Recognition

2013 UCSB Earth Research Institute Travel Award

2012 UCSB Department of Earth Science Wendell Phillips Woodring Memorial Graduate Fellowship for thesis proposal of highest merit

2012 Tappan and Loeblich Student Research Award, Cushman Foundation for Foraminiferal Research

2012 UCSB Affiliates Graduate Dissertation Fellowship

2012 Geological Society of London Travel Grant, Fermor meeting 2012

2010 Geological Society of America, Student Research Grant

2009 Sigma Xi, Grant-in-Aid of Research

2008 UCSB, Instructional Grant for laboratory development, Principles of Paleontology

2000-2004 6 quarters, Recognition for excellence in teaching, Dept of Earth Science, UCLA

2000 Fellowship, Center for the Study of Evolution and the Origin of Life, UCLA

1998-2000 Louisiana Space Fellowship, Louisiana Space Consortium

Service Activities within Academic community

2014 Organizer, GSA technical session 202: "The Tonian-Cryogenian World"

2013 Co-chair, GSA technical session 300: "Early Life and Taphonomy"

Service and Mentoring

2014-2015 Weekly Kindergarten classroom volunteer, outreach paleontology, science presentations, Mountain View Elementary, Goleta, CA

2010-2014 Science and career presentations, Mountain View Elementary School, Goleta, CA

2012-2013 Mentor to undergraduate scientists, UCSB

2012 Review committee for award of Gerald A. Soffen Travel Grant (NASA Academy Alumni Association)

2010-2011 Weekly Kindergarten classroom volunteer, outreach paleontology, science presentations, Mountain View Elementary, Goleta, CA

2009-2010 NASA Academy Alumni Association, NASA Academy selection committee

Chronology of Research and Teaching

2012 Fall Teaching Assistant, Earth 7, Dinosaurs, UCSB

2011	Spring	Guest lecturer, Earth 30, History of Life, UCSB
2009- 2013		Research Assistant, UCSB
2009	Spring	Lead Teaching Assistant, Earth 7, Dinosaurs, UCSB
2009	Winter	Teaching Assistant, Earth 111L, Principles of Paleontology, UCSB
2008	Fall	Teaching Assistant, Earth 144, Invertebrate Paleobiology, UCSB
2008	Spring	Teaching Assistant, Earth 7, Dinosaurs, UCSB
2008	Winter	Teaching Assistant, Earth 111L, Principles of Paleontology, UCSB
2007	Fall	Teaching Assistant, Earth 159C, Early Life on Earth, UCSB
2007	Spring	Lecturer, Physical Geology, California State University, Long Beach
2005	Spring	Lecturer, General Geology, California State University, Dominguez Hills
2004-2000		Research Assistant and Teaching Assistant, UCLA

ABSTRACT

Studies in Neoproterozoic Paleontology

by

Leigh Anne Smith Riedman

The Neoproterozoic Era was one of major biotic change against a background marked by fluctuations in oceanic and atmospheric chemistry, formation and rifting of the supercontinent Rodinia, and at least two global glaciations (Snowball Earth events). Presented here are three studies of differing aspects of those biological changes.

The first is a systematic study of the diverse and well-preserved, organic-walled microfossil assemblage of the Alinya Formation of eastern Officer Basin, Australia. The use of scanning electron microscopy (SEM) revealed an unexpected level of morphological detail not visible in transmitted light microscopy and led to the recognition of new species and emendation of existing species as well as establishment of degradational sequences. In total, thirty-three taxa are described here including nineteen previously named forms, five newly described species and two new combinations.

The second study describes the organic-walled microfossil assemblages from five successions that span the first (Sturtian) glaciation (~717 Ma) and interglacial interval (>635 Ma), and integrates those data with a critical evaluation of primary paleontological literature of units deposited from ~850 to 650 Ma. The described successions from Australia and Svalbard record low species richness throughout this interval and when placed in context of

all available body fossil data from the mid-Neoproterozoic, indicate global species richness may have decreased much earlier than previously realized. This finding of temporal decoupling between loss of richness and glacial onset suggests the extinctions previously associated with the Snowball Earth glacial events may not have been glacially driven.

The last of these three studies provides a broader view of the early to middle Neoproterozoic biosphere (1 Ga to 635 Ma) and describes application of the CONOP correlation and seriation algorithm to a new database of paleontological, geochemical and radiometric data. Paleobiological (first and last species appearances), geochemical and age events were placed into an ordinal sequence and calibrated to the geological time-scale to reveal a high-resolution species richness record for the first 80% of the Neoproterozoic Era. Major features of this record include an increase in species richness ~805 Ma, sustained high richness levels until a decrease ~770 Ma and a short-lived increase ~760 Ma before a steep decline ~750 Ma. The findings of the two studies described above can be placed within the context of this broader synthesis: the diverse assemblage of the Alinya Formation is representative of the richness peak between ~805 and 775 Ma and the successions recording the Sturtian glacial and interglacial assemblages in Australia and Svalbard are indicative of the extended nadir that began ~750 Ma with a recovery in species richness delayed until after the termination of the second (Marinoan) glacial event.

These three studies, together, describe a broad view of the early to middle Neoproterozoic Era and detail important vignettes within that story. From a more detailed and temporally constrained record of the Neoproterozoic biosphere, relationships between biotic and abiotic events during this transformative time can become better understood.

TABLE OF CONTENTS

ORGANIC-WALLED MICROFOSSILS OF THE EARLY TO MID-NEOPROTEROZOIC ALINYA FORMATION, OFFICER BASIN, AUSTRALIA[1]

ABSTRACT—Organic-rich shales and siltstones of the mid-Neoproterozoic upper Alinya Formation, eastern Officer Basin, Australia, preserve an abundant and diverse assemblage of organic-walled microfossils deposited in a low-latitude, shallow marine setting. Use of scanning electron microscopy (SEM) revealed an unexpected level of morphological detail not visible in transmitted light microscopy. This led to the recognition of new species and emendation of existing species as well as establishment of degradational sequences, which aid in fossil recognition. In total, thirty-three taxa are described here; these include nineteen previously named forms, five newly described species: *Caelatimurus foveolatus, Culcitulisphaera revelata*, *Karenagare alinyaensis, Morgensternia officerensis* and *Sulcatisphaera simiipugnus,* and two new combinations: *Vidalopalla verrucata* and *Lanulatisphaera laufeldii.*

The Alinya assemblage shares some taxa with both Mesoproterozoic and mid-Neoproterozoic units, but does not replicate any other previously described assemblages.

[1] This chapter has been accepted for publication as L. A. Riedman and S. M. Porter, in press. Organic-walled microfossils of the early to mid-Neoproterozoic Alinya Formation, Officer Basin, Australia. *Journal of Paleontology.*

The taxonomic overlap with these units supports the view of very long stratigraphic ranges for a number of these taxa.

INTRODUCTION

THE NEOPROTEROZOIC Era was marked by fluctuations in oceanic and atmospheric chemistry (Meyer and Kump, 2008; Canfield, 2014), dynamic shifts in climate (Pierrehumbert et al., 2011) and carbon cycling (e.g. Rothman et al., 2003; Swanson-Hysell et al., 2010), formation and rifting of the supercontinent Rodinia (Li et al., 2008), and major biological innovations such as the advent of biomineralization and multicellularity (reviewed in Knoll, 2011, and Javaux, 2011). Molecular clock analyses suggest divergences of extant eukaryotic groups occurred in the mid-Mesoproterozoic to early Neoproterozoic (Berney and Pawlowski, 2006; Zimmer et al., 2007; Lücking et al., 2009; Parfrey et al., 2011) and compilations of fossil data indicate that eukaryotic diversity and disparity increased steadily during this time, preceding the dramatic drop and biotic turnover associated with the Cryogenian glaciations (Huntley et al., 2006; Knoll et al., 2006).

These eukaryotic diversity trends are based largely upon the fossil record of the acritarchs, a polyphyletic group of sphaeroidal organic-walled microfossils that compose the bulk of the Precambrian fossil record. As a group acritarchs are prone to taxonomic problems such as inflation— multiple names given to ontogenetic or taphonomic variants of

a single biological taxon— or deflation— a lack of differentiation between similar (often simple) forms. Such taxonomic difficulties lead to uncertainty in the interpretations of eukaryotic diversity trends based upon this record.

Early and mid-Neoproterozoic acritarchs seem particularly prone to these taxonomic issues; pre-Ediacaran acritarchs are typically smaller and darker than Ediacaran taxa and they often appear to lack diagnostic morphological features. Traditionally, organic-walled microfossils have been studied by use of only transmitted light microscopy but during the course of this study the importance of characterizing micron-scale fossil morphology by use of scanning electron microscopy (SEM) became apparent. A number of taxa were found to have micro- and nano-scale morphological details that would have gone undetected by transmitted light (e.g. Figs. 8, 10, 11). Those specimens (e.g. *Culcitulisphaera revelata* n. sp.*, Lanulatisphaera laufeldii* [=*T. laufeldii*] n. comb.) would have been counted within form taxa such as *Leiosphaeridia* or mistakenly split into several separate taxa based on taphonomic alteration. Thus, it appears that early to mid-Neoproterozoic acritarchs do, in fact, possess taxonomically important morphological details but they are manifest on a smaller scale than seen in younger forms. This offers hope that acritarch taxonomic difficulties can be ameliorated, although perhaps not eliminated, leading to more robust assessments of Precambrian eukaryotic diversity trends.

An additional benefit to the increased use of SEM in acritarch studies is the opportunity to characterize taphonomic sequences of these taxa (Fig. 3). This not only

allowed poorly preserved specimens be assigned to their proper taxonomic homes but also provided additional information about the structure of the vesicle walls (e.g. remarks in *C. revelata*).

Here we present a systematic description of the organic-walled microfossils of the upper Alinya Formation, an early to mid-Neoproterozoic siliciclastic unit from eastern Officer Basin, Australia. This fossil assemblage includes common and long-ranging taxa such as *Valeria lophostriata*, taxa such as *C. revelata* that are restricted to just a few other units, and new taxa for which additional occurrences are equivocal. The Alinya assemblage provides a glimpse of a diverse ecosystem inhabiting a low-latitude (Pisarevsky et al., 2001; 2007), shallow intertidal marine environment during early to mid-Neoproterozoic time.

GEOLOGICAL SETTING AND AGE

The Officer Basin (Fig. 1) spans more than 3.5×10^5 km^2 in the states of Western and South Australia and contains ~7 km of Proterozoic sediments partially overlain by ~1km of Phanerozoic sediments including the modern Gibson and Great Victoria Deserts (Grey, 2005). The Officer Basin composes the southwestern portions of a large depositional system known as the Centralian Superbasin (Walter et al., 1995), sedimentation in which initiated in the early Neoproterozoic Era during intracratonic subsidence perhaps related to rifting associated with break-up of Rodinia (Lindsay and Leven, 1996). The late-Neoproterozoic to

early Cambrian Petermann Orogeny and Paleozoic Alice Springs Orogeny led to fragmentation of the Centralian Superbasin into the present-day Officer, Amadeus, Ngalia and Georgina basins (Walter et al., 1995).

The Alinya Formation is a predominantly fine-grained siliciclastic unit that prior to the drilling of the Giles-1 wildcat petroleum well in 1985 was known only from sporadic and deeply weathered outcrops along the northeastern margins of Officer Basin (Zang and McKirdy, 1994). Seismic interpretations suggest the Alinya Formation is 230 m thick in the northern reaches of the basin, thins to ~57 m in the area of Giles-1 and may extend into the Nullarbor Plain to the south (Morton, 1997). Together with the underlying Pindyin Sandstone and locally overlying Coominaree Dolomite and Cadlareena Volcanics, the Alinya Formation is considered an equivalent of the Callanna Group of the Adelaide Rift Complex and Stuart Shelf (Morton, 1997).

Zang (1995) divided the Alinya Formation into two units, the lower of which is characterized by red-brown to pale green siltstones with sandstone interbeds and common anhydrite, suggesting deposition on an intertidal flat. The upper unit (from which the samples discussed here were collected) comprises stacked cycles of organic-rich siltstones grading into black shales, siltstones with interbedded evaporite deposits, and terminating in aeolian sandstones. The upper unit of the Alinya Formation is interpreted to have been deposited in a coastal sabkha setting (Zang, 1995; Morton, 1997). Zang (1995) also

described an assemblage of acritarchs from the Alinya Formation; comparisons with that study are discussed below.

Samples of the Alinya Formation were collected from the Giles-1 drill core, currently housed in the Glenside Core Facility, Adelaide. Giles-1 was drilled by Comalco Ltd. as a wildcat exploratory petroleum well in eastern Officer Basin (Fig. 1), South Australia (28°25'54" S, 132°23'12"E) and reached a total depth of 1326.8 meters, terminating in the Tonian to Cryogenian (Grey et al., 2011) aeolian Pindyin Sandstone. In the Giles-1 drillcore the Alinya Formation conformably overlies the Pindyin Sandstone and is, in turn, unconformably overlain by the Ediacaran Tarlina Sandstone; no Cryogenian glacial units are preserved.

Age constraints.—There are no direct age constraints on the Alinya Formation. Deposition preceded the Cryogenian glaciations; although absent from the Giles-1 drillcore, the Sturtian Chambers Bluff Tillite is found higher in the sequence elsewhere in eastern Officer Basin. Debris of the late Neoproterozoic Acraman bolide impact (Hill et al., 2004) and distinctive Ediacaran acritarch taxa (Willman and Moczydłowska, 2008) are found in the Ungoolya Group stratigraphically above the Alinya Formation within the Giles-1 drillcore, providing additional, if broad, minimum age constraints.

Based on lithological correlations the upper unit of the Alinya Formation is considered a lateral facies equivalent of the Coominaree Dolomite, a unit restricted to the

Manya Trough in the eastern part of Officer Basin and to the western portions of the Adelaide Rift Complex (Morton, 1997; Hill, 2005). Rocks from the Coominaree Dolomite (Manya 5 drillcore) have been correlated with those of the lower Bitter Springs Formation of the Amadeus Basin (upper Gillen Member + lower Loves Creek Member by Hill and Walter (2000) and with the lower two-thirds of the Loves Creek Member by Grey and colleagues (2011)) based on carbon and strontium isotopes and stromatolite biostratigraphy (*Acaciella australica* assemblage). The Bitter Springs negative carbon isotope anomaly, constrained to be no older than 811.5 Ma (Macdonald et al., 2010) occurs at the boundary of the Gillen and Loves Creek members of the Bitter Springs Formation (Halverson et al., 2005; Swanson-Hysell et al., 2010). Thus the above correlations imply an age of <811.5 Ma for the Coominaree Dolomite and Alinya Formation.

DISCUSSION

Comparison with previous study of the Alinya Formation.—A previous study of the Alinya Formation by Zang (1995) revealed some of the diversity documented here. Certain forms are held in common between these works and others are not; newly described forms include *Caelatimurus foveolatus* n. sp., *Culcitulisphaera revelata* n. sp., *Karenagare alinyaensis* n. sp., *Morgensternia officerensis* n. sp. and *Sulcatisphaera simiipugnus* n. sp. Biostratigraphically significant forms reported by Zang but not recovered in this study

include: *Trachyhystrichosphaera aimika*, *T. stricta, T. vidalii, Cymatiosphaeroides kullingii* and *Vandalosphaeridium* sp. cf. *V. reticulatum* as well as vase-shaped microfossils (VSMs).

One of the forms recovered in both studies is "*Comasphaeridium" tonium*, a species named by Zang (1995) from Alinya sediments (the generic assignment is considered dubious by the present authors and placed in quotation marks). Some authors (Willman and Moczydłowska, 2008; Grey et al., 2011) have expressed concern about the occurrence of this fossil in the early to mid-Neoproterozoic Alinya Formation, arguing that its acanthomorphic ornamentation is more consistent with acritarchs of the Ediacaran Period. However, the specimens illustrated do not conform to any recognized Ediacaran acritarch taxa (Grey et al., 2011), and the concern over these fossils may speak more to an unwarranted assumption that certain morphological characters— rather than monophyletic taxa— define chronostratigraphic intervals (cf. Xiao et al., 1997).

Zang (1995; p. 147) reported large acritarchs attributed to *Trachyhystrichosphaera aimika* with vesicle diameters from 50 to 400 μm and hollow processes up to 70 μm in length, as well as the occurrence of *T. stricta* (synonymized with *T. aimika* by Butterfield et al., 1994), which exhibits vesicle diameters up to 800 μm. No specimens attributable to *Trachyhystrichosphaera,* or with such great dimensions were observed during the present study. Specimens attributed to *Trachyhystrichosphaera* spp. and figured by Zang (1995) appear to be forms comparable to *Pterospermopsimorpha* sp. (figs. 25H-J; the "processes" appear to be folds of the outer envelope), fragments of smooth-walled acritarchs overlain by

filaments of *Siphonophycus* spp. (figs. 26A-B), and specimens that may bear processes but share no similarity with *Trachyhystrichosphaera* spp. (figs. 26E-G). Similarly, in contrast to Zang's study, no specimens attributable to the genus *Vandalosphaeridium* were observed. Those figured by Zang (*Vandalosphaeridium* sp. cf. *V. reticulatum*; figs. 23F–H) do not conform to the specific diagnosis provided by Vidal and Ford (1985), who described a vesicle bearing widely spaced, funnel-shaped processes supporting an outer membrane. Rather, they appear to be degraded leiosphaerids or portions of colonial aggregates.

Another fossil group recorded in Zang's (1995) study that is of great potential biostratigraphic significance is the vase-shaped microfossils (VSMs). As a group, VSMs, allied with modern amoebozoan and, possibly, rhizarian testate amoebae (Porter and Knoll, 2000; Porter et al., 2003), are found abundantly and globally in Cryogenian-age rocks. Work by Nagy and colleagues (2009; as well as others cited therein) indicates the acritarch assemblage associated with VSMs is a taxonomically depauperate one dominated by long-ranging taxa such as small leiosphaerids; this is true not only for the Chuar Group, but for other globally distributed assemblages as well. Thus the discovery of VSMs in the diverse acritarch assemblage of the Alinya Formation would be noteworthy for paleoecological as well as biostratigraphic reasons. Zang (1995) reported recovery of three VSM specimens in association with spiny acritarchs from a chert of the lower Alinya Formation collected in outcrop at North Pindyin Hills, northeastern Officer Basin. Although it is possible that the specimens reported by Zang do represent VSMs, it seems more likely (judging from the two

figured specimens) that these are torn elongate acritarchs such as *Navifusa* sp. No VSM specimens were recovered during the present study; note, however, this study was restricted to the upper Alinya Formation of the Giles-1 drillcore and comparison of the stratigraphic position of Zang's chert sample with depths in the Giles-1 drillcore is not straightforward.

Biostratigraphy.—Those taxa from the Alinya Formation that have biostratigraphic potential (i.e. they are morphologically distinctive and confidently identified in other units) include *Valeria lophostriata, Culcitulisphaera revelata*, *Caelatimurus foveolatus* and *Lanulatisphaera laufeldii*. However, all but one of these taxa have long stratigraphic ranges: *V. lophostriata* is seen in the ca. 1.8 Ga Changcheng Group, China (Yan and Liu, 1993), and the 770-742 Ma Chuar Group, USA (Vidal and Ford, 1985; Nagy et al., 2009) and *C. revelata* occurs in the ca. 1 Ga Lakhanda Formation, Siberia (Schopf, 1992), and the 770-742 Ma Chuar Group (Nagy et al., 2009). *C. foveolatus* is a new species described here, but was reported as a sphere with a reticulated surface from the Mesoproterozoic Roper Group of Australia (Peat et al., 1978) and under the name *Turuchanica maculata* from the poorly constrained but probably Mesoproterozoic Muhos Formation of Finland (Tynni and Uutela, 1984). *L. laufeldii* may have the shortest range as it has not been recorded in units older than the mid-Neoproterozoic in age, namely, the Visingsö (Vidal, 1976), Chuar and Uinta Mountain (Vidal and Ford, 1985; Nagy et al., 2009) and Kildinskaya (Samuelsson, 1997) groups. Although their presence in the Alinya assemblage is still equivocal, if VSMs were

present, this would help constrain the age of the unit as they are not known from units older than about 800 Ma or younger than the onset of the first Cryogenian glaciation ca. 717 Ma (Porter and Knoll, 2000; Strauss et al., 2014).

Also possibly informative is the absence of certain taxa considered to be index fossils, in particular, *Cerebrosphaera buickii* (Hill and Walter, 2000; Hill et al., 2000; Grey et al., 2011), *Trachyhystrichosphaera aimika* (Butterfield et al., 1994, Samuelsson and Butterfield, 2001; Tang et al., 2013) and *Cymatiosphaeroides kullingii* (Kaufman et al., 1992; Butterfield et al., 1994). Of these, however, *T. aimika* is the least useful as an index taxon as it has a very long-stratigraphic range, occurring in the 811-717 Ma upper Fifteenmile Group (formerly Tindir Group) (Allison and Awramik, 1989; Macdonald et al., 2010a,b) as well as the >1005±4 Ma Lakhanda Formation (Hermann *in* Timofeev et al., 1976; Rainbird et al., 1998). *C. kullingii* also occurs in the upper Fifteenmile Group, and may be present (noted as only *Cymatiosphaeroides* sp.) in the 900-800 Ma Miroyedikha Formation (Veis et al., 1998). The distinctively wrinkled ornamented acritarch *C. buickii* appears to have the shortest ranges of these possible index taxa; its first appearance in Australia is constrained to be ca. 800 Ma (Grey et al., 2011) and the youngest occurrence is in the lower Chuar Group (770-742 Ma).

Although absence of VSMs from the Alinya assemblage could potentially be caused by laboratory processing, the lack of *C. buickii*, *T. aimika* and *C. kullingii* from the Alinya assemblage likely reflects a primary absence from the biota. These fossils are relatively

large (usually >100 μm, often as large as 700 μm) and conspicuous, and even fragments of them should be recognizable. This argument is particularly apt with regards to *C. buickii,* which is both robust and distinctive; even very small fragments of *C. buickii* can be recognized and identified.

Absence of these taxa from this assemblage could reflect paleogeographic distribution or environmental preferences of the biota. However, during the Neoproterozoic, Officer Basin was in a low-latitude position (Pisarevsky et al., 2001; 2007) and the Alinya Formation was deposited in an intertidal to shallow subtidal environment, similar to units that do host these globally distributed taxa. Additionally, *C. buickii* has been reported from farther west in Officer Basin (Hussar and Kanpa fms; Cotter, 1999).

Assuming the absence of these taxa from the Alinya Formation is not taphonomically driven and it reflects stratigraphic rather than geographic or environmental distributions, then the deposition of the Alinya Formation either preceded the appearance of these taxa or postdated their extinctions. If the former, then this assemblage is older than ~1 Ga and the taxa shared with units such as the well-constrained Chuar Group (e.g. *C. revelata* and *L. laufeldii*) must be very long-ranging and for some reason absent from intervening, well-preserved units such as the Wynniatt, Svanbergfjellet, Draken formations (note this would also conflict with lithologic correlations for the Alinya Formation, see "Geology Section" above). If the latter, then this formation must be younger than at least the lower Chuar Group in which *C. buickii* is found and younger than the Fifteenmile Group acritarch

assemblage constrained to be 811–717 Ma (note that Macdonald and colleagues (2010b) suggest the age of this unit is likely to be nearer the older end of this range). The most parsimonious interpretation is that the Alinya Formation was deposited between 717 Ma and ca. 770 Ma, recording the diverse biota present before the onset of the Cryogenian glaciations.

Diversity patterns from this study.—Fossil abundance and taxonomic diversity covary throughout the sample suite (Fig. 2), suggesting diversity changes may simply be artifacts of changes in fossil abundance. However, standardized diversity—measured as the taxonomic diversity of a subsample composed of the first twenty specimens encountered during light microscopy—is also positively correlated with sample diversity. This suggests that fluctuations in diversity are genuine.

The greatest taxonomic diversity was found in the lowest part of the upper Alinya Formation (1265.36–1265.71m; Figs. 1, 2). Samples from the uppermost parts of this formation host a greater proportion of smooth-walled sphaeroids (leiosphaerids), colonies of cells, and simple filaments; few ornamented acritarchs occur in these rocks. We suspect that the absence of ornamented acritarchs in younger samples is primary rather than taphonomically driven given that they appear to be relatively robust (i.e. thicker walled) compared to many of the leiosphaerids that are present in these samples. Whether this shift reflects local factors such as a change in water depth or global factors such as extinction is

not known. The whole unit is interpreted to record deposition in a shallow subtidal to sabkha environment, and forms considered to have been benthic mat-formers (i.e. *Synsphaeridium* spp. and the various filamentous species) are seen throughout the unit, thus any change in water depth is likely to have been relatively little.

MATERIALS AND METHODS

All samples for this study were processed by standard hydrofluoric maceration by Waanders Palynology Consulting, following protocols outlined by Grey (1999). Macerate samples are stored in 200 proof ethyl alcohol to discourage fungal and bacterial growth.

For SEM study, drops of sample macerate were strewn on glass slides or on SEM stubs and allowed to air dry. Transmitted light microscopy (using a Zeiss Axioskop 40) was performed on the glass slide preparations in order to locate specimens, note coordinates, and circle them with a fine-point marker so they could be located during SEM study. A 20 to 30 nm-thick carbon coat was applied with a high-vacuum carbon coater to reduce the effects of charge build-up. SEM was performed with a FEI Quanta 400 field-emission, environmental SEM using a voltage of 5 kV and working distances from 7 to 9 mm. After SEM analyses, glass coverslips were epoxied to the glass slides (using Petropoxy 154) and photographed under high magnification transmitted light microscopy using QImaging camera and

Qcapture™ software. This allowed comparison of the same specimens in SEM and light microscopy (e.g. Figs. 4, 12.6 and 12.7).

Cross-sectioning by Focused Ion Beam Electron microscopy (FIB-EM) was performed on *C. revelata* specimens partially embedded in epoxy using FEI DB235 Dual-Beam FIB (Fig. 9). Samples were prepared by applying a drop of epoxy (Petropoxy 154) to an SEM stub and then holding the stub with the stem in contact with a hot plate in order to begin curing before a drop of fossil macerate was applied. The goal was to apply the fossils to epoxy that was not completely cured but would cure by virtue of residual heat of the stub. When the epoxy reached a tacky texture, the stub was removed from the heat and a drop of fossil macerate was applied by pipette. The stub was then allowed to cool. After carbon coating (20 to 30 nm) fossils were located by SEM. Relocation of fossils for FIB sectioning was expedited by creation of high-resolution montages of stubs during SEM. FIB is most efficient and least likely to produce slicing artifacts when used on smooth surfaces; this was achieved by selecting regions of low topographic relief and applying a ~500 nm coat of platinum to the 10 µm x 10 µm square region to be sliced (Fig. 9.2). Near the target region a 2 x 2 µm square of platinum (Fig. 9.2) was applied and an "X" marked into the surface to act as a fiducial marker, used after sectioning was complete in order to align images. The FIB milled away 80 ~120 nm- thick sections of the fossil; after each slice, an electron image of the milled edge of the fossil was captured.

SYSTEMATIC PALEONTOLOGY

All illustrated specimens have been reposited in the collections of the South Australian Museum (SAM), Adelaide under the accession numbers SAM P49464–P49558. Fossil coordinates (generated using England Finder graticule with sample slide label to the left for all slides except 1265.46-Feb6 and 1265.46-2_28B for which the label is to the right) are noted in captions following slide numbers. A table of all specimens, their accession numbers, slides or stubs and coordinates is available in the supplemental data file. Coordinates are unavailable for specimens on stubs. The International Code of Nomenclature for Algae, Fungi and Plants (Melbourne Code, 2011) is followed.

Group ACRITARCHA

Genus CAELATIMURUS new genus

Type species.—Caelatimurus foveolatus, n. sp., by monotypy.

Diagnosis.—As for type species

Etymology.—From the Latin, *caelatum,* meaning "embossed or engraved" and *murus*, meaning "wall" for the embossed appearance of the vesicle. Pseudo-compounding is

intentional (recommendation 60G.1(c) of the ICN) and used to indicate etymological difference with the Latin *caelum*, meaning sky or heaven.

CAELATIMURUS FOVEOLATUS new species

Figures 5.6–5.7

1978 Sphere with type I reticulate surface PEAT, MUIR, PLUMB, MCKIRDY AND NORVICK, p. 5, fig. 3A.

1984 *Turuchanica maculata* TYNNI AND UUTELA, p. 24, ?fig. 175, fig. 176, *non* 177, *nec* 178–179, ?180–182, *nec* 183–186.

Diagnosis.—Optically dense sphaeroidal to ellipsoidal organic-walled microfossils ~40 µm in diameter bearing frequent (16 to 20 per 10 μm^2), small (0.9 to 1.2 µm wide and ~2 µm long) light-colored ellipsoidal depressions upon the vesicle.

Description.—Optically dense sphaeroidal to ellipsoidal organic-walled microfossils of an average diameter of 41.3 µm (s=15.6, N=3) bearing lighter-colored ellipsoidal marks 0.9 to 1.2 µm wide and typically ~2 µm in length that appear to be impressions in the vesicle wall.

Etymology.—From the diminutive of *fovea*, meaning "minutely pitted".

Holotype.—SAM Collection number P49508, (Fig. 5.6 and 5.6a) from sample 1265.57 m, Giles-1 drillcore, Alinya Formation. Slide 1265.57-19A, coordinate G27-2.

Occurrence.—This form has been reported from the Mesoproterozoic Roper Group and in the poorly constrained, but probably Mesoproterozoic Muhos Formation of Finland.

Remarks.—This species occurs in the Muhos Formation of Finland (Tynni and Uutela, 1984) but the name assigned in that paper, *Turuchanica maculata*, is not employed here. The new species erected by Tynni and Uutela was placed within the genus *Turuchanica*, a genus distinguished by radial cracking of the vesicle, a taphonomically imposed feature, and was synonymized with the smooth-walled *Leiosphaeridia* by Jankauskas and colleagues (1989). Tynni and Uutela mentioned the patterned wall of the fossil, but this feature—considered here to be a diagnostic feature—is not obvious in the holotype (Tynni and Uutela, fig. 175). It is clearly visible in only one (fig. 176) and possibly present in another (fig. 180–182) three of the twelve specimens figured. Should restudy of the holotype of *T. maculata* indicate the presence of this texture, the species erected here, *C. foveolatus,* should be synonymized with it, although in a new combination in light of the transfer of *Turuchanica* to *Leiosphaeridia.*

Material examined.—Three specimens from the Alinya Formation, Giles-1 drill core depth 1265.46 and 1265.57 meters.

Genus CONEOSPHAERA Luo, 1991

?CONEOSPHAERA ARCTICA Hofmann, 1994

Figures. 6.1 and 6.2

1976 nannocyst formation TIMOFEEV, HERMANN AND MIKHAILOVA, pl. 9, figs. 6–7.

?1978 cells and endospores PEAT, MUIR, PLUMB, MCKIRDY AND NORVICK, figs. 5B and D.

1990 *Aimia delicata* HERMANN, pl. 12 figs. 1 and 7 (*non* fig. 2).

1994 *Coneosphaera arctica* HOFMANN AND JACKSON, p. 28, figs. 19.1-19.3.

?1994 *Leiosphaeridia* sp. KNOLL, fig 4A.

1999 *Coneosphaera* sp. cf. *C. arctica* COTTER, p. 72, fig. 7E.

Description.—Sphaeroidal organic-walled microfossils 22.3 to 33.0 µm in diameter ($\bar{x}$=28.6 µm, s=5.7 µm, N=5), bearing smaller sphaeroids 2.5 to 4.5 µm in diameter ($\bar{x}$=3.6 µm, s=1.0 µm, N=5) on ?exterior of vesicle.

Remarks.—The vesicle diameters of the Alinya specimens (22 to 33 μm) are considerably smaller than those of the Bylot Group population (79 to 130 μm; Hofmann and Jackson, 1994). Similarly, the sphaeroids attached to the vesicle are smaller in the Alinya population than in the Bylot specimens (2.5 to 4.5 μm as opposed to 8 to 11 μm). The ratios of sphaeroid diameter to vesicle diameter, however, are similar in the two groups, with the Alinya forms exhibiting a slightly broader range (1/5 to 1/12 vs. 1/8 to 1/10)

In images of the type material, the surface sphaeroids appear to be hollow (a character not discussed by Hofmann and Jackson (1994)); for some of the Alinya specimens this seems to be the case (Fig. 6.2) but for others the hollow nature cannot be determined (Fig. 6.1). Because of the differences in dimension, the questionable hollowness of the attached sphaeroids in the Alinya material and the low numbers of specimens recovered, this form is here left in open nomenclature.

Material examined.—Five specimens from the Alinya Formation, Giles-1 drill core depths 1255.43, 1265.57 and 1265.71 meters.

Genus COMASPHAERIDIUM Staplin, Jansonius and Pocock, 1965

"COMASPHAERIDIUM" TONIUM Zang, 1995

Figures 7.2–7.4

1995 *Comasphaeridium tonium* ZANG, p. 162, figs. 24A–G.

Description.—Sphaeroidal organic-walled microfossils ranging in vesicle diameter from 42.5 to 57.9 µm ($\bar{x}$=51.3 µm, s= 5 µm, N=7) and bearing frequent (12-20 visible in 10 µm section of vesicle perimeter), short and fine processes (length range 0.8–2.4 µm, $\bar{x}$= 1.5 µm, s= 0.6; width range 0.4 to 0.7 µm, $\bar{x}$= 0.5 µm, s=0.1 µm). No outer envelope has been seen. Processes appear to be solid, as determined from the consistent optical density of processes viewed from the side and head-on; they do not appear to be a lighter shade in the center of the process. No branching has been observed.

Remarks.—The specimens recovered in this study conform to Zang's (1995) description of *C. tonium* from the Alinya Formation. However, the generic assignment of this species is considered dubious (see below). Unfortunately, the current fossil material is not sufficient to recommend a new nomenclatural combination or erection of a new genus.

Comasphaeridium is a broadly defined and incredibly (in the literal sense) long ranging genus: Fensome and colleagues (1990) list thirty-one validly named species that range in age from the early Cambrian to the Oligocene. The generic diagnosis indicates members are "… spherical to ellipsoidal, sometimes of large size with densely crowded, thin, solid, usually simple, more or less flexible hair-like spines" (Staplin et al., 1965, p.

192). The broadness of the diagnosis makes the biological coherence of the genus unlikely, thus, great caution is warranted in making assumptions about genus longevity.

Occurrence.—First reported from the Neoproterozoic Alinya Formation (Zang, 1995). Singh and Babu (2013) also reported *C. tonium* from the Neoproterozoic Raipur Group of India, however the fossil figured is too poorly preserved to provide an unequivocal identification.

Material examined.—Seven specimens from the Alinya Formation, Giles-1 drill core depths 1255.43, 1255.76, 1265.57 and 1265.71 meters.

Genus CULCITULISPHAERA new genus

Type species.—Culcitulisphaera revelata n. sp., by monotypy.

Diagnosis.—As for type species.

Etymology.—From the Latin *culcitula*, meaning small pillow, and *sphaera*; a sphere covered by small pillows

Remarks.—The distinctiveness of the pillow elements of the vesicle exterior warrants the erection of a new genus.

CULCITULISPHAERA REVELATA new species

Figures 3, 4.4–4.6, 8, 9

1979 *Kildinella* sp. VIDAL, pl. 4, figs. C and D.

?1982 *Chuaria* aff. *circularis* JANKAUSKAS, p. 103, pl. 41, fig. 7.

?1985 *Trachysphaeridium laminaritum* VIDAL AND FORD, p. 373, figs. 8A, 8C.

?1985 *Trachysphaeridium* sp. A VIDAL AND FORD, p. 377, figs. 8B, 8D.

?1989 *Chuaria circularis* JANKAUSKAS *in* JANKAUSKAS, MIKHAILOVA AND HERMANN, p. 67, pl. 12, fig. 1, *non* pl. 12, fig. 2.

Non 1989 *Leiosphaeridia laminarita* JANKAUSKAS *in* JANKAUSKAS, MIKHAILOVA AND HERMANN, p. 78, pl. 11, figs. 11–13.

?1990 *Leiosphaeridia laminarita* Hermann, pl. 1, fig. 4, *non* pl. 1, fig. 6.

1992 *Trachysphaeridium laminaritum* SCHOPF, pl. 14, fig. A.

?1994 *Lophosphaeridium granulatum* HOFMANN AND JACKSON, p. 22, figs. 17.8, 17.9.

?1994 *Spumosina rubiginosa* HOFMANN AND JACKSON, p. 30, figs. 19.5, 19.6, 19.8, *non* fig. 19.7.

2009 *Trachysphaeridium laminaritum* NAGY, PORTER, DEHLER AND SHEN fig. 1H.

Diagnosis.—Optically dense sphaeromorphic organic-walled microfossil distinguished by a surface ornament of tightly packed 1 to 3 μm cushion-shaped outpockets of the vesicle that may appear only as ~1 μm diameter light spots or alveolae under light microscopy.

Description.—Optically dense organic vesicle circular to ellipsoidal in outline, ranging in diameter from 34.6 to 88.4 μm ($\bar{x}$= 60.3 μm, s=15.6, N=24); likely reflecting an originally sphaerical to sub-sphaerical shape. Vesicle surface consists of small circular to sub-circular outpockets. The outpocket elements range in diameter from 1.3 to 2.7μm ($\bar{x}$= 1.8μm, s=0.6, N=17; measurement unavailable in specimens viewed only by transmitted light microscopy). Vesicular elements are unlikely to have been surficial scales as none has yet been found separated from the vesicle surface and inspection of all specimens suggests full attachment to the vesicle. Thus far these vesicular elements have been recognized only under SEM; specimens viewed under light microscopy appear to have small (~0.7μm) alveolae or hemisphaerical depressions in the vesicle. Occasionally these alveolar structures can be recognized as cushion-shaped elements along the periphery of a specimen as viewed under light-microscopy (Fig. 8.1–8.5).

A spectrum of taphonomic variation is seen in *C. revelata* specimens. Study of these variants has been informative for developing an understanding of the vesicle morphology (for example, by providing evidence of the hollow nature of the pillow-shaped elements and

indication that the wall is composed of individual blisters rather than bearing only a textured surface). The flexibility of the vesicle wall is indicated in the folding that occurs in the elements along the perimeter of the flattened fossil, giving an imbricated appearance (Fig. 3.4). During degradation the pillow elements of the vesicle appear to "deflate"; the outer wall of the element sinks into the underlying cavity (Fig. 3.3, 8.6a, 8.8b), creating a honeycomb-like appearance. Occasionally the outermost skin of the pillows shows rupture (Figs. 3.1 and 3.2) or appears to have been sheared away from the fossil (arrows in Fig. 3.5), revealing a smooth surface within the 'blister'. Several of the fossils studied here also show a wart-like crater that excavates through the vesicle layers (Figs. 8.6, 8.8b); this feature is not interpreted as an excystment structure, but more likely represents post-mortem degradation.

FIB-EM sectioning and analysis by energy-dispersive X-ray spectroscopy (EDS) of *C. revelata* specimens (Fig. 9) indicates a homogeneous carbon composition with no discernable boundaries between vesicle layers, likely to be a product of compaction and diagenesis. FIB-EM nanotomography of these samples did, however, reveal the presence of frequent 30 to 600 nm nanopores within the vesicle (Figs. 9.4 and 9.5). Similar nanopores are seen in FIB serial sections of the Mesoproterozoic acritarch, *Shuiyousphaeridium macroreticulatum* (Schiffbauer and Xiao, 2009). The occurrence of these features is unlikely to represent artifacts of processing and may speak to a spongy, woven or reticulated subsurface in this taxon.

Etymology.—From the Latin *revelatum*, meaning "revealed", referring to the fact that the pillow elements of the vesicle were unknown until revealed by SEM.

Holoype.—SAM Collection number P49519, (Fig. 8.1) from sample 1265.56 m, Giles-1 drillcore, Alinya Formation. Slide 1265.57-19A, coordinate N24-1.

Occurrence.—Appears in late Mesoproterozoic to middle Neoproterozoic units: the uppermost Limestone Dolomite "series" (beds 19-20) of the Eleonore Bay Group of East Greenland, the Chuar Group of southwestern United States and the Lakhanda Formation of Siberia.

Remarks.—C. revelata is not considered here to be conspecific or congeneric with *Trachysphaeridium laminaritum,* although this was thought a likely taxonomic home for these specimens in the early stages of this study owing to similarities with specimens figured in Vidal and Ford (1985) and Schopf et al. (1992). The original diagnosis and description of *T. laminaritum* (Timofeev, 1966) are vague and do not mention features considered diagnostic of *C. revelata* (i.e. alveolae or circular to cushion shaped vesicular elements), instead describing a thick-walled vesicle with a chagrinate texture. Additionally, the fossil

images of *T. laminaritum* (plate 7, figure 3; hand drawn illustrations), do not conclusively illustrate diagnostic features of this taxon.

The fossil imaged in plate 14, figure A, p. 1075 of Schopf et al. (1992) appears to be *C. revelata*. The caption reads, "*Trachysphaeridium laminaritum* Timofeev in press HOLOTYPE" and the fossil is indicated as being from the Lakhanda Formation of Siberia (the publication "in press" is unclear and not listed in the bibliography). The "holotype" designation in the caption is apparently incorrect as the holotype Timofeev (1966) designated for *T. laminaritum* was from a drill core taken from northern Moldova, not from the Lakhanda Formation. Differences in diameter and outline indicate these are two distinct specimens. There would have been no need to have designated a neotype in 1992 as Timofeev's original specimens were still available for study as of 1996 (Knoll, 1996; *contra* Jankauskas et al., 1989). In any case, the specimen figured by Schopf (1992) indicates that *C. revelata* was a part of the ca. 1 Ga Lakhanda biota, extending this form's geographic and stratigraphic range.

In Vidal's (1976) monographic treatment of the Visingsö Formation of southern Sweden, he emended the diagnosis of *T. laminaritum* (using specimens from Timofeev's collection) to include an alveolar surface texture of the vesicle. Despite the fact that this emended diagnosis is consistent with the morphology of *C. revelata*, the fossils figured from the Visingsö material (figs. 20A–B, D–H) do not resemble those described in the present

study. Instead, most (figs. 20A–B, F–H) are specimens of *L. laufeldii* (=*T. laufeldi*) that are in possession of the outer envelope (see below).

Fossils assigned to *T. laminaritum* and *Trachysphaeridium* sp. A from the Chuar and Uinta Mountain groups by Vidal and Ford (1985) may be examples of *C. revelata*, but the images are inconclusive. However, this species is known from the Chuar Group (unpublished observations, S.M.P.).

Material examined.—Twenty-seven specimens from the Alinya Formation, Giles-1 drill core depths 1265.36, 1265.46 and 1265.57 meters.

Genus KARENAGARE new genus

Type species.—Karenagare alinyaensis n. sp., by monotypy

Diagnosis.—As for type species.

Etymology.—*Karenagare* is from the Japanese name for the element of raked sand or gravel in Zen rock gardens forming impressionistic water-less streams. It applies here to the resemblance of the fossil's ridged ornament to the lines of sand or gravel composing the "stream".

Remarks.—The fossils of this genus are distinguished from other striated acritarch taxa by undulating nature of the striations rather than by sharp grooves as seen in *Sulcatisphaera simiipugnus* or narrow ridges (~0.5 μm from crest to crest) as in *Valeria lophostriata*. Additionally, these undulations are seen on the exterior of the vesicle as opposed to the interior linear ornamentations of *V. lophostriata* (Javaux et al., 2004). Although these species share superficial similarity, there is no reason to presume they may have been closely related. Thus, the decision to erect a new genus for this species (rather than a new species within *Valeria or Sulcatisphaera*) is based on an intent to create a biologically meaningful generic concept.

KARENAGARE ALINYAENSIS new species

Figures 5.1–5.5

?1996 Unnamed acritarch, KNOLL, pl.4, fig 11.

Diagnosis.—Sphaeroidal to ellipsoidal organic-walled microfossils bearing 2–3 μm wide, parallel, undulatory, ripple-like external striations.

Description.—Sphaeroidal to ellipsoidal organic-walled microfossils with vesicles of varying opacity and distinctive ornamentation of wide parallel, undulating, ripple-like striations measuring 2–3 μm from crest to crest of ridges (the darker lineations). Vesicles range in diameter from 32.2 to 86.7 μm ($\bar{x}$=42.7μm, s=16.2 μm, N=10). On certain specimens (Figs. 5.2 and 5.3), the striations are visible on only a small part of the vesicle, but others exhibit striations over all visible vesicle surface; whether this is indicative of ontogenetic or taphonomic variation is not yet clear. One specimen may exhibit an outer envelope (Fig. 5.1). Striations appear to ornament the external surface of the vesicle as suggested by their appearance along the periphery of the vesicle (lower portion of Fig. 5.4).

Etymology.—For the fossil's discovery in the Alinya Formation of Officer Basin, South Australia.

Holoype.—SAM Collection number P49493**,** (Fig. 5.4) from sample 1265.46 m, Giles-1 drillcore, Alinya Formation. Slide 1265.46-18B, coordinate H18-3.

Occurrence.—Neoproterozoic Alinya Formation of Officer Basin, South Australia and perhaps an unspecified Neoproterozoic unit of Russia (Knoll, 1996).

Remarks.—The "unnamed acritarch" of Knoll (1996) appears similar to *K. alinyaensis* but as measured from the image is ~25 μm in diameter with striations ~1 μm from crest to crest, somewhat smaller with more closely spaced ridges than the population recovered here.

There is an intriguing morphological similarity between *K. alinyaensis* and species of *Dactylofusa* (senior synonym of "*Moyeria*"; Fensome et al., 1990), early Paleozoic organic-walled microfossils interpreted as possible euglenoids (Gray and Boucot, 1989). The size and curvature of the undulations in the vesicle of *K. alinyaensis* are consistent with the appearance of the ridges in *Dactylofusa* sp.; these have been interpreted as pellicle strips in the latter (Gray and Boucot, 1989). At this time nothing more than a mention of morphological similarity is possible, but if further study were to establish a euglenoid affinity for *K. alinyaensis*, this would be the oldest known record of this clade.

Material examined.—Ten specimens from the Alinya Formation, Giles-1 drill core depths 1265.46 and 1265.57 meters.

Genus LANULATISPHAERA new genus

Type Species.—*Lanulatisphaera laufeldii* by monotypy.

Diagnosis.—As for type species.

Etymology.—From the Latin *lanulata*, a diminutive for "woolly", referring to the dense, matted appearance of the filaments between the vesicles; and *sphaera* in reference to the shape of the whole of the fossil.

Remarks.—New morphological data require the placement of *"Trachysphaeridium" laufeldii* into a new genus. The original description of *Trachysphaeridium* (Timofeev, 1959) lacked a diagnosis but was described as "thick, dense vesicle with shagreen surface" (translated from Timofeev, 1959, p. 28) and as "single-layered sphaerical vesicles 60 to 250 μm in diameter of varying thickness and density with shagreen surface that is usually compressed into folds" (translated from Timofeev, 1966, p. 36). The genus *Trachysphaeridium* was synonymized with *Leiosphaeridia* by Jankauskas and colleagues (1989) because features Timofeev used to distinguish these two genera, such as folding and a rough-textured vesicle, were considered to be taphonomically induced. This is likely to be the correct placement for some species of *Trachysphaeridium*, including the type species, *T. attenuatum*. However, forms attributed to *T. laufeldii* possess morphological features inconsistent with a placement in *Leiosphaeridia*, a form genus of smooth-walled sphaeroids. Additionally, no existing genus is known that can accommodate the features diagnostic of *T. laufeldii*, thus a new genus and combination is established here.

LANULATISPHAERA LAUFELDII (Vidal) new comb.

Figures 4.1–4.3, 10.7, 10.8, 11

1976 *Trachysphaeridium laufeldi* VIDAL, p. 36, figs. 21A–21N.

1985 *Trachysphaeridium laufeldi* VIDAL AND FORD, p. 375, figs. 7 A, B, D, F.

?1985 *Trachysphaeridium laminaritum* VIDAL AND FORD, p. 373, figs. 8A, 8C.

1997 *Lophosphaeridium laufeldii* SAMUELSSON, p. 174, figs, 7 F, H, I.

2009 *Lophosphaeridium laufeldi* NAGY, PORTER, DEHLER AND SHEN, fig. 1J.

Emended diagnosis.—Double-walled, originally sphaeroidal, organic-walled microfossil bearing abundant, solid, sub-micron diameter solid processes that emanate from the exterior of the inner vesicle and fuse distally forming cones ~1-3 μm long, or fuse and branch forming complex networks. Surface of outer envelope bearing ~50 to 100 nm diameter mammillae; filamentous processes appear to make no contact with outer envelope.

Description.—Small, sphaeroidal, organic-walled microfossils ranging in diameter from 26.5 to 46.1 μm ($\bar{x}$=33.1 μm, s=4.6 μm, N=21) and bearing abundant, solid, thin ($\bar{x}$=0.4 μm, s=0.1 μm, N=21), filamentous structures that emanate from the external surface of the inner vesicle and fuse distally. Outer vesicle envelops— but does not appear to make contact with— the inner vesicle or reticulate filamentous structures. Outer vesicle exhibits a fine-

scale (~ 50 to 100 nm diameter) mammillar ornament (Figs. 10.7a, 11.1, 11.2). Filamentous processes not typically visible in transmitted light microscopy but are easily identifiable by SEM. In transmitted light, fossils appear very dark and often mottled; double-vesicle construction not always easily determined due to optical density of outer vesicle.

During taphonomic degradation the filaments become flattened and shortened by breakage, but still visibly fused (Fig. 4.3).

The occasional spiny protuberances and circular openings surrounded by raised rims reported by Vidal (1976), Vidal and Ford (1985) and seen in Nagy et al (2009; fig. 1j) were not observed in the present material.

Basionym.—Trachysphaeridium laufeldi Vidal (*in* Vidal, 1976. Fossils and Strata, 9, p. 36–38).

Holotype.—Specimen BV/83.60—1:X/53.3 from the Visingsö Group, middle unit, Kumlaby borehole— in keeping with the original designation by Vidal (1976).

Occurrence.—Occurs in early Neoproterozoic units including Visingsö Group of southern Sweden, the Kildinskaya Group, northwestern Russia, and the Chuar and Uinta Mountain groups of southwestern United States.

Remarks.—The original diagnosis of Vidal (1976) is emended here to accommodate new morphological information made available by SEM study. Vidal's (1976) diagnosis stated, "The vesicle surface is tightly covered with very short conical spines", but SEM study of the present material indicated the "cones" are in fact the convergence of several of the filamentous processes.

Samuelsson (1997) corrected the orthography of the specific epithet from the original *laufeldi* to *laufeldii* (. In the same work he interpreted the processes of *T. laufeldii* to be tubercles upon the vesicle and transferred this species to *Lophosphaeridium* Timofeev 1959 ex Downie 1963, a genus diagnosed by a thick vesicle with a knobby, tuberculate surface sculpture. That transfer is rejected here as a tuberculate sculpture has not been borne out by SEM study.

Similarities are seen between *L. laufeldii* and *M. officerensis* (both Fig. 10); these species may be distinguished by differences in process character. Whereas the conical processes of *M. officerensis* are clearly apparent in transmitted light, the reticulated filaments of *L. laufeldii* do not project as far from the surface and may be difficult to recognize in transmitted light. Additionally, as viewed by SEM, processes of *L. laufeldii* are constant in diameter and anastomose distally with neighboring processes whereas *M. officerensis* processes are conical, tapering distally and do not anastomose. Both forms possess external envelopes, however the nano-scale mammillar ornament of *L. laufeldii* has not been observed on specimens of *M. officerensis*.

Material examined.—Twenty-one specimens from the Alinya Formation, Giles-1 drill core depths 1265.46 and 1265.57 meters.

Genus LEIOSPHAERIDIA Eisenack, 1958a,

emend. Downie and Sarjeant, 1963

Type Species.—*Leiosphaeridia baltica* Eisenack, 1958a.

Remarks.—Leiosphaeridia is a form genus comprising morphologically simple, smooth organic-walled microfossils. Recent ultrastructural analyses have illustrated the polyphyletic nature of this group (e.g. Talyzina and Moczydłowska, 2000; Javaux et al., 2004; Willman, 2009).

The formal designations of *Leiosphaeridia* species given by Jankauskas and colleagues (1989) are followed here. Species are differentiated on the basis of diameter and opacity of the vesicle. *L. crassa* and *L. jacutica* possess an optically dense vesicle and are differentiated by being less than (*L. crassa*) or greater than (*L. jacutica*) 70 μm in diameter. Similarly, *L. minutissima* and *L. tenuissima* possess vesicles of low optical density and are differentiated based on being less than (*L. minutissima*) or greater than (*L. tenuissima*) 70 μm in diameter.

LEIOSPHAERIDIA CRASSA (Naumova, 1949),

emend. Jankauskas (*in* Jankauskas et al., 1989)

Figure 6.5

1989 *Leiosphaeridia crassa* JANKAUSKAS *in* JANKAUSKAS, MIKHAILOVA AND HERMANN, p. 75, pl. 9, figs. 5-10.

1994 *Leiosphaeridia crassa* BUTTERFIELD, SWETT AND KNOLL, p. 40, figs. 16F, 23K.

1994 *Leiosphaeridia crassa* HOFMANN AND JACKSON, p. 22, figs. 13.3, 15.19–15.29.

1999 *Leiosphaeridia crassa* BUICK AND KNOLL, p. 756, figs. 5.2–5.4.

2005 *Leiosphaeridia crassa* GREY, 2005, p. 179, figs. 63A–C, 64 A, ?B, ?C, D.

2008 *Leiosphaeridia crassa* MOCZYDŁOWSKA, p84, figs. 7A, 8G.

(For additional synonymy, see Jankauskas et al., 1989.)

Description.—Solitary, sphaeroidal, smooth, single-walled vesicles 18 to 70µm in diameter ($\bar{x}$=36.5 µm, s=13.4 µm, N=132). Vesicle dark but translucent.

Occurrence.—Ubiquitous in Precambrian and Phanerozoic organic-walled microfossil assemblages.

Material examined.—One hundred sixty-seven specimens measured (many more present but uncounted) from the Alinya Formation, Giles-1 drill core depths 1237.74, 1242.84, 1244.17, 1248.91, 1255.43, 1255.76, 1257.73, 1265.36, 1265.46, 1265.57, 1265.71 and 1266.31 meters.

LEIOSPHAERIDIA JACUTICA (Timofeev, 1966),

emend. Mikhailova and Jankauskas

(*in* Jankauskas et al., 1989)

Figure 6.7

1966 *Kildinella jacutica* TIMOFEEV, p. 30, pl. 7, fig. 2.

1989 *Leiosphaeridia jacutica* MIKAILOVA AND JANKAUSKAS *in* JANKAUSKAS, MIKHAILOVA AND HERMANN, p. 77, pl. 12, figs. 3, 7, 9.

1994 *Leiosphaeridia jacutica* BUTTERFIELD, KNOLL AND SWETT, p. 42, fig. 16H.

1994 *Leiosphaeridia jacutica* HOFMANN AND JACKSON, 1994, p. 22, figs. 17.1–17.4.

2005 *Leiosphaeridia jacutica* GREY, 2005, p. 183, fig 63G.

2009 *Leiosphaeridia jacutica* VOROB'EVA, SERGEEV AND KNOLL, p. 185, fig. 14.13.

(For additional synonymy, see Jankauskas et al., 1989.)

Description.—Solitary, sphaeroidal, smooth, single-walled vesicles 70 to 317 µm in diameter ($\bar{x}$=137.3 µm, s=48.4 µm, N=35). Vesicle dark but translucent.

Occurrence.—Ubiquitous in Precambrian and Phanerozoic organic-walled microfossil assemblages.

Material examined.—Thirty-six specimens from the Alinya Formation, Giles-1 drill core depths 1242.84, 1244.17, 1248.91, 1255.76, 1265.36, 1265.46 and 1265.57 meters.

LEIOSPHAERIDIA MINUTISSIMA (Naumova, 1949),

emend. Jankauskas (*in* Jankauskas et al., 1989)

Figure 6.6

1989 *Leiosphaeridia minutissima* JANKAUSKAS *in* JANKAUSKAS, MIKHAILOVA AND HERMANN, p. 79, pl. 9, figs. 1–4, 11.

1994 *Leiosphaeridia minutissima* HOFMANN AND JACKSON, p. 21, figs. 15.9–15.15.

1999 *Leiosphaeridia minutissima* BUICK AND KNOLL, p. 756, figs. 5.3–5.6.

2005 *Leiosphaeridia minutissima* GREY, 2005, p. 184, fig. 63D.

2008 *Leiosphaeridia minutissima* MOCZYDŁOWSKA, p. 84, fig. 8H.

(For additional synonymy, see Jankauskas et al., 1989.)

Description.—Solitary, sphaeroidal, smooth, single-walled vesicles 10 to 70 μm in diameter ($\bar{x}$=35.7 μm, s=13.4 μm, N=79).

Occurrence.—Ubiquitous in Precambrian and Phanerozoic organic-walled microfossil assemblages.

Material examined.—One hundred specimens measured (many more present but uncounted) from the Alinya Formation, Giles-1 drill core depths 1237.74, 1242.84, 1244, 1244.17, 1255.76, 1257.73, 1265.36, 1265.46, 1265.57, 1265.71 and 1266.31 meters.

LEIOSPHAERIDIA TENUISSIMA Eisenack, 1958b

Figure 6.10

1989 *Leiosphaeridia tenuissima* JANKAUSKAS *in* JANKAUSKAS, MIKHAILOVA AND HERMANN, p. 81, pl. 9, figs. 12–13.

1994 *Leiosphaeridia tenuissima* BUTTERFIELD, SWETT AND KNOLL, p. 42, figs. 16I.

1994 *Leiosphaeridia tenuissima* HOFMANN AND JACKSON, 1994, p. 22, figs. 15.16–15.18.

2005 *Leiosphaeridia tenuissima* GREY, p. 184, fig. 63H.

Description.—Solitary, sphaeroidal, smooth, single-walled vesicles 70 to 144 μm in diameter ($\bar{x}$=95.9 μm, s=23.1 μm, N=11).

Occurrence.—Ubiquitous in Precambrian and Phanerozoic organic-walled microfossil assemblages.

Material examined.—Seventeen specimens from the Alinya Formation, Giles-1 drill core depths 1237.74, 1244.17, 1255.76, 1265.36, 1265.46, 1265.57 and 1265.71 meters.

LEIOSPHAERIDIA sp. A

Figures 12.4, 12.5, 12.9

Description.—Small (~36 μm), sphaeroidal organic-walled microfossils bearing a ring (~3 μm wide) about the perimeter. Vesicle diameters range from 28.6 to 48.0 μm including the ring ($\bar{x}$ =35.8 μm, s=6.7 μm, N=7) and ring widths range from 2.6 to 3.8 μm ($\bar{x}$ =3.1, s=0.4 μm, N=7). This ring is not considered a happenstance of concentric folding as there is no evidence of radial cracking and in one fossil (Fig. 12.9) the ring is no darker than the interior, arguing against the presence of more layers of vesicle in the periphery. This group may be another example of a winged, or pteromorphic, morphotype.

Material examined.—Seven specimens from the Alinya Formation, Giles-1 drill core depths 1265.46 and 1265.57 meters.

LEIOSPHAERIDIA sp B

Figures 12.1– 12.3, 12.11, 13

Description.—Sphaeroidal organic-walled microfossils bearing (typically one, occasionally more than one) optically dense spot as a part of the vesicle. This is distinct from reports of dark bodies *within* vesicles that are interpreted to represent condensed cytoplasm (e.g. Knoll and Barghoorn, 1975). Vesicles range in diameter from 19.7 to 285.0 µm ($\bar{x}$= 54.6 µm, s=43.3 µm, N=52) and dark spots range from 3.1 to 142.7 µm ($\bar{x}$= 21.9 µm, s=23.3 µm, N=52). Three specimens exhibit more than one spot upon the vesicle and in one of those cases the vesicle appears to be in the process of fission (Fig. 12.1).

Remarks.—The spots appear to be a (probably thickened) part of the vesicle, rather than a separate body within the vesicle as with the vesicle-within-a-vesicle construction of *Pterospermopsimorpha* or in cases of shrunken cell contents of forms such as *Caryosphaeroides* and *Glenobotrydion* (e.g. Knoll and Barghoorn, 1975). The surficial nature is indicated in observation by light microscopy in that the spots are in the same focal plane as the rest of the vesicle as well as by the fact that occasional torn specimens show

tearing across the spots (Fig. 12.3) and in some instances, degradation of the spot allows the viewer to see through the fossil to the back wall of the vesicle (Figs. 12.2 and 12.11).

This group appears to comprise one taxon; the distribution of vesicle diameters (Fig. 13) is weakly bimodal with a major mode at 20 to 30 µm and a minor mode from 60 to 80 µm and the population shows a linear relationship between vesicle diameters and spot diameters ($m=0.51$, $R^2= 0.90658$; Fig. 13). This linear relationship in spot and vesicle diameters is also seen in *Leiosphaeridia* species A of Nagy et al (2009) (S.M.P., unpublished observations). In that form, the body or "spot" upon the vesicle is clearly an operculum. It is unclear if variability reflects an ontogenetic sequence or simply variation within a population.

The function of the spots is unclear; were they opercula, one would reasonably expect to find a number of specimens opened, either with opercula attached or detached and showing distinctive holes, or even loose opercula within the strewn mount. None of these has been observed.

It is worth noting that similar features are seen in some specimens of *Synsphaeridium* spp. reported here (Figs. 12.6-12.7, 12.13, 12.14). It is conceivable that *Leiosphaeridia* sp. B and *Synsphaeridium* spp. are conspecific, their differences perhaps indicative of ontogenetic or ecophenotypic variation.

Material examined.—Sixty-two specimens from the Alinya Formation, Giles-1 drill core depths 1237.74, 1242.84, 1244.17, 1248.91, 1255.43, 1255.76, 1257.73, 1265.36, 1265.46 and 1265.71 and 1266.31 meters.

Genus MORGENSTERNIA new genus

Type Species.—Morgensternia officerensis n. sp., by monotypy.

Diagnosis.—As for type species.

Etymology.—The German, *morgenstern*, meaning "morning star" and referring to the fossil's resemblance to the medieval weapon of that name composed of a metal ball bearing frequent spikes.

Remarks.—Similar fossils have been assigned in open nomenclature to the genus *Gorgonisphaeridium*, however, due to significant differences in diagnostic characters, the new genus *Morgensternia* is erected here for the new species *M. officerensis* rather than including this species in the existing genus *Gorgonisphaeridium*. *M. officerensis* processes are straight rather than sinuous; and consistently conically tipped, rather than the occasional branched processes seen in species of *Gorgonisphaeridium,* including the type species, *G.*

winslowiae. Additionally, *M. officerensis* possesses an outer vesicle, a feature not found in *Gorgonisphaeridium* species. The combination of diagnostic characters seen in *M. officerensis* is not found in previously erected genera.

MORGENSTERNIA OFFICERENSIS new species

Figures 10.1–10.6

?1991 *Gorgonisphaeridium maximum* KNOLL, SWETT AND MARK, p. 557, fig. 21.12.

?1992 *Baltisphaeridium* sp. A ZANG AND WALTER, p. 280, pl. 5, figs. A–J.

?1992 *Baltisphaeridium* sp. B ZANG AND WALTER, p. 281, pl. 5, figs. K–L, (*non* M–O).

?1994 *Gorgonisphaeridium* sp. BUTTERFIELD, KNOLL AND SWETT, p. 40, figs. 14I–J.

?2009 *Cymatiosphaeroides* cf. *C. kullingii* NAGY, PORTER, DEHLER AND SHEN, fig. 1.I.

Diagnosis.—Optically dense, organic-walled microfossils with abundant (7 to 10 processes visible in a 10 μm section of vesicle periphery), processes that are ~2 μm long, solid, and conical, narrowing from a ~0.8 μm diameter base to a ~0.4 μm diameter tip. Smooth-walled outer envelope occasionally preserved. Processes do not support or connect to the outer envelope.

Description.—Organic-walled microfossils with optically dense vesicles ranging in diameter from 23.7 to 59.6 μm ($\bar{x}$=36.3 μm, s=8 μm, N=37), bearing abundant short, solid, conical processes that range in length from 1.0 to 3.3 μm ($\bar{x}$=1.9 μm, s=0.6 μm, N=37). Solid character was determined in SEM by observation of stumps upon the vesicle left by broken processes (e.g. arrow in Fig. 10.6a). Processes narrow from the base (0.8 μm) to a blunt tip (~0.4 μm); rarely, individual specimens are seen to possess processes with conical and bulbous terminations (Fig. 10.4). Processes are typically straight, but rarely a few are seen to be bent (not broken; arrows in Figs. 10.2 and 10.3), possibly indicating a plastic, rather than brittle, character. Smooth outer envelope is occasionally preserved (Fig. 10.1, 10.2).

Etymology.—In reference to the fossil's discovery in units of Officer Basin, Australia.

Holotype.—SAM collection number P49520, (Fig. 10.1) from sample 1265.57 m, Giles-1 drillcore, Alinya Formation. Slide 1265.57-19A, coordinate V32-4.

Occurrence.—See Remarks section for details of possible occurrences.

Remarks.—The specimens described here from the Alinya Formation resemble fragmentary acritarch fossils from the Draken (Knoll et al., 1991) and Svanbergfjellet

formations (Butterfield et al., 1994) in that all of these forms bear small, solid, conical processes. The Draken and Svanbergfjellet specimens were assigned to the genus *Gorgonisphaeridium,* an almost entirely Paleozoic genus with a broad diagnosis that indicates the spines are "solid, usually sinuous, slender or broad… tips simple or distally branched, flexible, bases may be slightly bulbous" (Staplin et al., 1965). Knoll and colleagues (1991) created a new combination, *Gorgonisphaeridium maximum,* based on the single, solid-process bearing Draken specimen and seemingly similar fossils from the Ediacaran age Doushantuo Formation. However, subsequent study of the Doushantuo specimens revealed a hollow character to the processes and the combination was recognized as invalid (Knoll, 1992, p. 765). The genus, *Echinosphaeridium* (later renamed *Knollisphaeridium* by Willman and Moczydłowska, (2008)), was then erected for large acritarchs with densely arranged, hollow processes, excluding the solid-process bearing Draken specimen. Butterfield and colleagues (1994) left a similar form in open nomenclature, *Gorgonisphaeridium* sp. Both the Draken and Svanbergfjellet specimens resemble those described here, save the near order-of-magnitude difference in vesicle diameters.

The new genus *Morgensternia* is erected here to accommodate the new species *M. officerensis* due to dissimilarity with species of *Gorgonisphaeridium* such as the presence of an outer envelope, a general lack of flexibility to the spines, an absence of branching, and shorter and more numerous processes in this new species.

Cymatiosphaeroides kullingii is another form bearing short, thin, solid processes and having an outer envelope (up to twelve envelopes according to the emended diagnosis of Butterfield and colleagues (1994)). However, *C. kullingii* differs from *Morgensternia* not only by its tendency towards much greater vesicle dimensions (30–350 μm) but more importantly by its diagnostic thickening of its processes at both the base and apex and the connection of the processes to the outer vesicle (Knoll et al., 1991). *M. officerensis* specimens do not indicate connection between the processes and outer vesicle.

Certain specimens illustrated from the Neoproterozoic Liulaobei and Gouhou formations of North China (plate 5, figs. A–L; Zang and Walter, 1992) appear comparable to the forms described here as *M. officerensis*. However, Zang and Walter describe the processes as hollow in character and communicating freely with the vesicle interior, an interpretation difficult to reconcile with the images provided. This interpretation contrasts with that of solid processes in *M. officerensis* of the Alinya Formation. These fossils would be placed in synonymy only if future investigation reveals a shared hollow or solid character for processes of both the Australian and Chinese forms.

M. officerensis is considered to fall outside of *L. laufeldii* due to its conical and non-fusing processes, more optically dense vesicle and somewhat smaller vesicle diameter of the former. Additionally, the nano-scale mammillar ornament of *L. laufeldii* (Figs. 10.7a, 11) is not seen in *M. officerensis*.

Material examined.—Thirty-seven specimens from the Alinya Formation, Giles-1 drill core depths 1265.46, 1265.57 and 1265.71 meters.

Genus NAVIFUSA Combaz, Lange and Pansart, 1967 ex Eisenack, 1976

NAVIFUSA MAJENSIS Pyatiletov, 1980

Figures 6.8, 6.9

1980 *Navifusa majensis* PYATILETOV, p. 144, fig 1.

1994 *Navifusa majensis* HOFMANN AND JACKSON, p. 20, figs. 15.1-15.4.

1995 *Lakhandinna dilatata* ZANG, p. 165, fig 29A, ?D, ?G.

1995 *Archaeoellipsoides karatavicus* ZANG, p. 162, figs. 29H, J, K.

1999 *Navifusa majensis* SAMUELSSON, DAWES AND VIDAL, fig 5A.

2001 *Navifusa majensis* SAMUELSSON AND BUTTERFIELD, fig. 5A.

2005 *Navifusa majensis* PRASAD, UNIYAL AND ASHER, figs. 3.10, 5.15, ?7.1.

2011 *Navifusa majensis* COUËFFÉ AND VECOLI, fig. 6.7.

2013 *Navifusa majensis* TANG, PANG, XIAO, YUAN, OU AND WAN, fig 5H.

Description.—Ellipsoidal organic-walled microfossils with a mean length of 63.3 µm and width of 28.0 µm (length range: 39.9 to 118.0 µm, width range 16.2 to 78.9 µm). Mean length to width ratio is 2.5, varying from 1.5 to 4.1 (N=9).

Remarks.—One specimen (Fig. 6.8, 6.8a) bears subtle transverse annulations in its center, a feature suggestive of *Pololeptus rugosus* described from the Liulaobei Formation (Yin and Sun, 1994; Tang et al., 2013). The genus *Pololeptus* was erected by Yin (*in* Yin and Sun, 1994) to accommodate oval-shaped, organic-walled microfossils with patches of characteristic "worm-like or netted sculptures". Tang and colleagues (2013) synonymized the three species of this genus and emended the diagnosis of the remaining species, *P. rugosus*, to include the newly discovered character of transverse annulations. The single annulated specimen recovered from the Alinya Formation does not bear the characteristic terminal sculpture described by Yin and Sun (1994) and Tang et al., (2013) and is narrower than the Liulaobei specimens (19 μm wide, 53 μm long as compared to 30-145 μm wide and 40-280 μm long in Liulaobei Fm.). For these reasons we are hesitant to assign the name *P. rugosus* to this one specimen.

Occurrence.—*N. majensis* is widely distributed in units of late Mesoproterozoic to early Neoproterozoic age including the Lakhanda Formation of Siberia, the Bylot Supergroup of arctic Canada, the Lone Land Formation of northwestern Canada, the Thule Supergroup of Greenland, the Vindhyan Supergroup of Central India, the Kwahu Group of Ghana and the Liulaobei Formation of North China.

Material examined.—Nine specimens from the Alinya Formation, Giles-1 drill core depths 1255.43, 1265.57 and 1266.31 meters.

Genus PTEROSPERMOPSIMORPHA (Timofeev, 1966)

emend. Mikhailova and Jankauskas (*in* Jankauskas et al., 1989)

Type Species.—Pterospermopsimorpha pileiformis

Remarks.—The diagnosis followed here is from Jankauskas and colleagues (1989). The fossils are described as consisting of two sphaeroidal to ellipsoidal vesicles, one within the other. The diameter of the inner vesicle is not less than two-thirds the diameter of the outer. Vesicle diameters range from 10 to 500 μm for the outer and 8 to 400 μm for the inner.

This genus, like many morphologically simple acritarch genera, is almost certainly polyphyletic. Thus interpretations of biological or ecological significance of the presence or absence of members of this genus warrant a large degree of caution.

Pterospermopsimorpha, a disphaeromorph, is often confused with the pteromorph genus, *Simia*. See *Simia* remarks section for details.

PTEROSPERMOPSIMORPHA INSOLITA (Timofeev, 1969)

emend. Mikhailova (*in* Jankauskas et al., 1989)

Figures 14.6–14.9

1969 *Pterospermopsimorpha insolita* TIMOFEEV, p. 16, pl. 3, fig. 8.

1989 *Pterospermopsimorpha insolita* MIKHAILOVA *in* JANKAUSKAS, MIKHAILOVA AND HERMANN, p. 49, pl. 3, figs. 5, 6.

1994 *Pterospermopsimorpha insolita* HOFMANN AND JACKSON, p. 24, figs. 17.10–17.13.

?1997 ?*Pterospermopsimorpha* sp. COTTER, p. 266, fig. 8H.

1999 *Pterospermopsimorpha insolita* COTTER, p.76, fig 7B.

?1999 *Simia annulare* SAMUELSSON, DAWES AND VIDAL, fig. 7A.

2005 *Pterospermopsimorpha insolita* PRASAD, UNIYAL AND ASHER, pl. 3, figs. 7 and 9, pl.5, fig 17.

2009 *Pterospermopsimorpha insolita* NAGY, PORTER, DEHLER AND SHEN, fig. 1E.

?2011 *Pterospermopsimorha insolita* COUËFFÉ AND VECOLI, fig. 6.6.

(For additional synonymy, see Jankauskas et al., 1989.)

Description.—Diameters of inner vesicles range from 16.9 to 64.3 µm ($\bar{x}$=35.7 µm, s=12.7 µm), diameters of outer vesicles from 25.0 to 97.4 µm ($\bar{x}$=42.5 µm, s=16.9 µm).

Remarks.—Specimens are placed into *P. insolita* due to accord with the illustrated holotype and with stated vesicle diameter ranges. Many *Pterospermopsimorpha* species are

distinguished by textural features of the outer vesicle (e.g. shagrinate and granular) that are considered likely to be of taphonomic origin. Thus here a conservative approach is adopted in which such textural features of the vesicle are largely discounted in taxonomic assignment.

Occurrence.—A common and widely distributed component of organic-walled microfossil assemblages ranging from Mesoproterozoic to early Paleozoic in age (discussed in Hofmann and Jackson, 1994). Reported occurrences include Bylot and Vindhyan supergroups of Canada and India, respectively; Chuar Group of western United States; and Kanpa, Hussar and Browne formations of western Officer Basin, Australia.

Material examined.—Thirty-seven specimens from Alinya Formation, Giles-1 drill core depths 1237.74, 1244.17, 1248.91, 1255.76, 1257.73, 1265.36, 1265.57, 1265.71 and 1266.31 meters.

Genus SIMIA Mikhailova and Jankauskas, 1989

(*in* Jankauskas et al., 1989)

Type Species.—Simia simica (Jankauskas, 1980) Jankauskas, 1989.

Description.—Organic-walled microfossils with sphaeroidal to discoidal central bodies 20 to 300 μm in diameter and bearing an equatorial flange of widths 5 to 30 μm.

Remarks.—There is much confusion in the literature regarding the genus *Simia* and how it differs from the genus *Pterospermopsimorpha.* The main difference between these two genera is easily recognized in principle; *Simia* is a spheroidal to discoidal body bearing an equatorial flange, not unlike a ballerina's tutu, whereas *Pterospermopsimorpha* is a disphaeromorph, an acritarch composed of sphere-within-a-sphere construction. However, accurate fossil identification is problematic due to the fact that *Simia* fossils are preserved as flattened bodies viewed from the poles, not the equator (as the 'equator' is represented by the great circle of the flange or 'tutu'). Part of this confusion may likely be attributed to the unfortunate choice of the name *Pterospermopsimorpha*, a name misleadingly suggestive of the pteromorph (wing or flap-bearing) acritarchs (Downie et al., 1963).

In practical terms, certain characters aid in distinguishing these two forms. Convenient wrinkles, folds and tears (e.g. radial cracking of the internal body independently of the external envelope; Figs. 14.8, 14.9) can often suggest the presence of two nested vesicles**.** Additionally, if the fossil's opacity remains more or less consistent from the center to the edge, one would expect this to be indicative of *Simia*. In a disphaeromorph such a *Pterospermopsimorpha*, one would expect the central region to be darker in transmitted light; in this area the light must pass through four vesicle layers, as opposed to only two

nearer its edges. This is in contrast to the two layers in the central body of a pteromorph such as *Simia* and the one or two layers at its edges.

SIMIA ANNULARE (Timofeev, 1969),

emend. Mikhailova (*in* Jankauskas et al., 1989)

Figures 14.1–14.5

1969 *Pterospermopsimorpha annulare* TIMOFEEV, p17, pl. 3, fig. 9.

1989 *Simia annulare* MIKHAILOVA *in* JANKAUSKAS, MIKHAILOVA AND HERMANN, p. 66, pl. 6, figs. 5–8.

?1992 *Simia annulare* ZANG AND WALTER, p. 307, pl. 7, figs. A–B.

1995 *Simia annulare* ZANG, fig 28E.

1999 *Simia annulare* COTTER, 1999, p. 77, fig 7H.

1999 *Simia annulare* SAMUELSSON, DAWES AND VIDAL (*in part*), figs. 7B–E, *non* 7A.

?2005 *Simia annulare* PRASAD, UNIYAL AND ASHER, p. 46, pl. 3, fig. 8, pl. 5, fig. 9.

2009 *Ostiumsphaeridium complitum* VOROB'EVA, SERGEEV AND KNOLL, p. 186, figs. 14.1–14.5.

2013 *Simia annulare* TANG, PANG, XIAO, YUAN, OU AND WAN, figs. 4 F–G.

Description.—Organic-walled microfossils 20.4 to 209.5 μm in diameter ($\bar{x}$=81.4, s=37.5 μm, N=44), sphaeroidal to discoidal central bodies bearing an equatorial flange of width 3.3 to 32.4 μm ($\bar{x}$=9.4 μm, s=5.6 μm) that is five to twenty percent the diameter of the central body.

Remarks.—Specimens of *Simia annulare* described in this study are closely comparable to those identified as *Ostiumsphaeridium complitum* (Vorob'eva et al., 2009), which is considered here to be a junior synonym of *S. annulare*. *O. complitum* was described as a spheroidal to sub-sphaeroidal vesicle with a distinctive slit-like opening that causes the vesicle to pop open and "forms a flap that surrounds [the] vesicle like a halo 10–30 μm wide with a fringed margin" (Vorob'eva et al., 2009; p.186). The formation of this halo or flange is problematic as even a flexible sphaeroidal membrane, when everted, will exhibit radial splits, not form a continuous border. Additionally, if the equatorial flange is formed by the opened vesicle, the split, itself, should no longer be visible on the specimen; instead there should be only a roughly circular sheet of vesicle with radial splitting that occurred during eversion. Instead, specimens of *O. complitum* exhibit a sphaeroidal central body surrounded by a fringed border; this accords well with the diagnosis of *S. annulare*, although requiring an increase in diameter for the species description. (The identification of these forms with the larger *Simia* species, *S. nerjenica,* was rejected due to their lack of the characteristic 4 to 6 concentric folds surrounding the central body and a general dissimilarity with the *S.*

nerjenica holotype [Jankauskas et al., 1989 pl. 9, fig. 10].) Specimens from the Alinya Formation lack the slit-like opening that Vorob'eva and colleagues considered diagnostic of *O. complitum* but these forms are similar in dimension and presence of a fringed equatorial border.

Occurrence.—Due to confusion regarding the differences between *Simia* and *Pterospermopsimorpha* species, occurrences are often difficult to establish from published reports. *S. annulare* appears to range from the late Mesoproterozoic into at least the mid-Ediacaran. This form has been reported from the Liulaobei Formation of North China, Thule Supergroup of Greenland and Vychegda Formation of eastern Russia.

Material examined.—Forty-four specimens from Alinya Formation, Giles-1 drill core depths: 1237.74, 1242.84, 1244.17, 1248.91 and 1265.57 meters.

Genus SULCATISPHAERA new genus

Type species.—Sulcatisphaera simiipugnus n. sp., by monotypy.

Diagnosis.—As for type species.

Etymology.—From the Latin *sulcata*, meaning "furrowed" and *sphaera*; a furrowed sphere.

Remarks.—The genus *Sulcatisphaera* was erected for *S. simiipugnus* as no previously erected genus accommodated the diagnostic characters of this species. This species differs from other acritarchs bearing lineations such as *Valeria lophostriata* and *Karenagare alinyaensis* n. sp. The linear striae of *S. simiipugnus* are straight, deep grooves within the surface of the internal vesicle and typically measure ~1 μm in width. This contrasts with the striae of *V. lophostriata*, which are found upon the interior of the single vesicle (Javaux et al., 2004) and typically measure ~0.5 μm in width and form concentric circles about the poles– similar to lines of latitude on a globe or grooves on a vinyl record. The striae of *S. simiipugnus* are dissimilar from those of *K. alinyaensis* n. sp. in that *K. alinyaensis* bears wide, parallel, undulating ripple-like striations (Figs. 5.1–5.5) rather than ruts or gouges that incise the vesicle of *S. simiipugnus* (Figs. 5.8–5.13).

SULCATISPHAERA SIMIIPUGNUS new species

Figures 5.8–5.13

?1995 *Striasphaera radiata* GAO, XING AND LIU, pp. 14 and 20, figs. 2.10 and 2.11.

1999 ?*Leiosphaeridia* sp. COTTER, fig 8H.

?2000 Form 1 SIMONETTI AND FAIRCHILD, p. 25, fig 8S.

?2009 Unnamed form A NAGY, PORTER, DEHLER AND SHEN, fig 4D.

Diagnosis.—Optically dense, double-walled, sphaeroidal organic-walled microfossils typically ~27 µm in diameter, bearing ~1 µm wide linear striations on the surface of the inner vesicle. Groups of two to four striae are frequently oriented at opposing angles to each other. Outer vesicle unornamented.

Description.—Sphaeroidal organic-walled microfossils 20.1 to 35.4 µm in diameter ($\bar{x}$=26.2 µm, s=3.8 µm, N=15) bearing linear striations 0.9 to 1.8 µm wide ($\bar{x}$=1.2 µm, s=0.2 µm, N=15) as measured from crest to crest on vesicle surface. Vesicle optically dense. Groups of two to four striae frequently oriented at opposing angles to each other. Individual striae are typically visible for less than half the diameter of the vesicle surface. SEM specimens indicate the presence of unornamented outer envelope that may obscure the identity of this fossil, the additional layers serving to make some specimens opaque in light microscopy.

Etymology.—From the Latin *simia*, meaning "monkey" and *pugnus* meaning "fist", literally "monkey's fist" for the fossil's resemblance to the nautical knotted ball used to weight the end of a heaving line being thrown from ship to shore.

Holotype.—SAM collection number P49511, (Fig. 5.12) from sample 1265.57 m, Giles-1 drillcore, Alinya Formation. Slide 1265.57-19A, coordinate M40-0.

Occurrence.—This form invites comparison with those reported from early Neoproterozoic units in the Chuar Group, USA (Nagy et al., 2009), Officer Basin, Australia (Cotter, 1999), a Mesoproterozoic unit of northeastern China and a poorly constrained unit considered an equivalent of the Mesoproterozoic Conselheiro Mata Group of Brazil (Simonetti and Fairchild, 2000).

Remarks.—An additional possible occurrence may be as *Striasphaera radiata* in the Neoproterozoic Qinggouzi Formation of northeastern China (Gao et al., 1995); the species description of *S. radiata* is permissive and the fossils figured are suggestive but not conclusively similar to *S. simiipugnus*. The species description of these Chinese forms indicates presence of only a single vesicle, inconsistent with the construction of *S. simiipugnus,* but also difficult to determine by light microscopy alone. In the specimens figured by Gao and colleagues (1995) the surface ridges appear to bulge outward from the vesicle, a feature inconsistent with forms reported here in which the lineations are ruts or gouges in the exterior of the internal vesicle. In order to consider *S. radiata* synonymous

(the senior synonym) with *S. simiipugnus*, further study of the types of the former would be required.

The possibility of a taphonomic origin of the distinguishing striae cannot be ruled out (cf. Grey and Willman, 2009), but the case for a taphonomic origin is no stronger than that of a primary origin. Measurements of vesicle diameter, striae width, spacing and orientation are all tightly distributed and in all specimens with a visible outer envelope, it was seen to be similar- albeit smooth, lacking distinguishing ornament.

Material examined.—Fifteen specimens from the Alinya Formation, Giles-1 drill core depths 1255.43, 1265.46, 1265.57 meters.

cf. "TAPPANIA" *sensu* Butterfield 2005.

Figures 7.7–7.9

?2005 *Tappania* sp. BUTTERFIELD, p. 167, figs. 1–7.

Description.—Three specimens of sphaeroidal, organic-walled acritarchs 30.6 to 47.9 µm diameter and bearing frequent but variable processes that are up to 3.0 µm in length and less than 0.5 µm in width, and that show occasional bifurcation (left-hand arrow in Fig. 7.7, 7.8a). In transmitted light microscopy bifurcation of the processes can be difficult to distinguish from overlap of adjacent processes (right-hand arrow in Fig. 7.7).

Remarks.—These specimens are tentatively allied with forms from the 750–850 Ma Wynniatt Formation of northwestern Canada. Butterfield (2005) identified those forms as *Tappania* sp., a fossil genus previously known only from Mesoproterozoic units. Javaux (2011) has cited uncertainty about the assignment of the Wynniatt fossils to *Tappania* as the Wynniatt fossils lack the diagnostic neck-like extension and possess distinctive distal fusing not seen in the type material (a feature Butterfield suggested may have been destroyed by laboratory processing of the older materials). The occurrence of occasional septae in the processes is a feature shared by the Mesoproterozoic and Wynniatt forms (not seen in the Alinya specimens).

The fossils recovered from the Alinya Formation do not conform well to the description of *Tappania* species from the type material (Yin, 1997) or from the somewhat older Roper Group (1.5 Ga; Javaux et al., 2001). Although the vesicles of the Alinya fossils are only slightly smaller, the processes of the Alinya forms are significantly narrower than those described for these Mesoproterozoic *Tappania* species. Additionally, the fossils described here do not possess the diagnostic neck-like protrusion.

The fossils described here are small but in keeping with the vesicle and process diameters of the Wynniatt material and demonstrate the irregularly furcating processes of both the Wynniatt "*Tappania"* and *Tappania* of Yin (1997) and Javaux and colleagues (2001). Additionally, the broad extension of the vesicle into a conical base of a process as

seen in the Wynniatt fossils is seen in one of the Alinya specimens (white arrow, Fig. 7.7). No fusing of the processes is seen in the Alinya material; it is possible some processes have been shortened by breakage, but at this point that is no more than conjecture. The ends of the processes of the SEM specimens are unbroken and lobe-shaped; a similar feature is seen in some specimens of "*Tappania*" (figs. 3A, B, 7B).

Material examined.—Three specimens from the Alinya Formation, Giles-1 drill core depth 1255.76, 1265.46 and 1265.57 meters

Genus VALERIA Jankauskas, 1982

Type Species.—*Valeria lophostriata* Jankauskas (1979) 1982.

VALERIA LOPHOSTRIATA Jankauskas (1979) 1982

Figure 7.1

1979 *Kildinella lophostriata* JANKAUSKAS, p. 53, figs. 1.13–1.15.

1982 *Valeria lophostriata* JANKAUSKAS, p.109, pl.39, fig. 2.

1989 *Valeria lophostriata* JANKAUSKAS *in* JANKAUSKAS, MIKHAILOVA AND HERMANN, p. 86, pl. 16, figs. 1-5.

1995 *Valeria lophostriata* ZANG, p. 170, fig. 28I.

1999 *Valeria lophostriata* SAMUELSSON, DAWES AND VIDAL, fig. 8E.

2001 *Valeria lophostriata* JAVAUX, KNOLL AND WALTER, fig 1D.

2009 *Valeria lophostriata* NAGY, PORTER, DEHLER AND SHEN, figs. 1a and b.

2009 *Valeria lophostriata* NAGOVITSIN, 144, fig 4E.

?2011 *Valeria lophostriata* COUËFFÉ AND VECOLI, fig 6.4.

?2012 dark walled megasphaeric coccoid BATTISON AND BRASIER, fig. 8B.

(For additional synonymy see Jankauskas et al., 1989 and Hofmann, 1999, Table 1)

Description.—Sphaeroidal organic-walled microfossils bearing distinctive sculpture of parallel ridges, similar to corduroy fabric. Vesicle diameters range from 50.4 to 119.0 µm ($\bar{x}$=79.3 µm, s=26.2 µm, N=13), ridges are ~0.5 µm apart.

Occurrence.—Widely distributed in late Paleoproterozoic through early (pre-Sturtian glacial) Neoproterozoic rocks.

Material examined.—Fourteen specimens from Alinya Formation, Giles-1 drill core depths: 1265.46, 1265.57 and 1265.71 meters.

Genus VIDALOPALLA new genus

Type species.—*Vidalopalla verrucata* by monotypy.

Diagnosis.—Sphaeroidal organic-walled microfossil bearing more or less regularly arranged, solid, small (typically 1 to 2 μm in diameter), hemisphaerical verrucate external ornament.

Etymology.—Named in honor of the Precambrian paleontologist Gonzalo Vidal with the addition of the Greek, *palla*, describing the sphaerical form of the fossils.

Remarks.—The genus *Vidalopalla* is erected here to accommodate the species *V. verrucata* (=*Kildinosphaera verrucata*). Originally erected in 1983 by Vidal (*in* Vidal and Siedlecka) as a species of the new genus, *Kildinosphaera*, *K. verrucata* was born into limbo. In erecting *Kildinosphaera* and naming one of its constituent species as *Kildinosphaera lophostriata* (transferring it from *Kildinella*), Vidal and Siedlecka unknowingly transferred the newly minted type species of the genus *Valeria* that Jankauskas (1982) had created less than a year previous. This caused the genus *Kildinosphaera* to instantaneously become a junior (homotypic) synonym of *Valeria*. The other species Vidal and Siedlecka named to *Kildinosphaera* (*K. chagrinata*, *K. granulata* and *K. verrucata*) were left homeless—validly published but belonging to an illegitimate genus. In 1990 Fensome and colleagues suggested

a new combination, placing "*K." verrucata* into the genus *Valeria* as *V. tschapomica*. This specific epithet was chosen in light of implications in the species remarks by Vidal and Siedlecka (1983) and the more formal recommendation by Amard (1984) that *Kildinosphaera verrucata* was synonymous with the earlier named form *Kildinella tschapomica* Timofeev 1966 (Amard also suggested synonymy with *Kildinella exsculpta* Timofeev, 1969, but *K. tschapomica* would have priority if these forms were truly synonymous). The recommendation of Fensome and colleagues (1990) (and suggested synonymies of Amard [1984]) are rejected here (as done tacitly by others such as Knoll [1994] and Butterfield and Rainbird [1998]). The ornament of *K. tschapomica* and *K. exsculpta* appear to be diagenetically introduced features on a smooth-walled acritarch belonging to the form genus, *Leiosphaeridia* (Knoll, 1996, p.70).

Samuelsson and colleagues (1999) informally suggested the transfer of "K". *verrucata* to the genus *Lophosphaeridium.* This suggestion is not taken here primarily because the descriptions of the genus and type species, although permissive, are so broad as to include a number of other genera and the illustration of the holotype material, a hand-drawn figure (Timofeev, 1959), is not instructive for purposes of determining similarity. Additionally, the genus has become worryingly speciose and almost certainly artificially long ranging with at least 70 validly published species ranging from the Precambrian into the Eocene (Fensome et al., 1990). Transfer of "K." verrucata to *Lophosphaeridium* would explicitly state close biological relationships with these 70 other species that is unfounded at

this time. However, should future study of Timofeev's *Lophosphaeridium rarum* type material indicate sufficient similarity, this species should be transferred and the other constituent species evaluated.

VIDALOPALLA VERRUCATA (Vidal) new comb.

Figures 6.3, 6.4

1981 *Kildinella* sp. B VIDAL, p. 26, figs. 13 A–D.

1983 *Kildinosphaera verrucata,* VIDAL AND SIEDLECKA, p. 62, fig. 5C.

?1984 *Kildinosphaera verrucata,* AMARD, p. 1406, fig. 3C.

?1985 *Kildinosphaera verrucata,* VIDAL AND FORD, p. 363, fig. 4A.

1990 *Leiosphaeridia exculpta* (sic), HERMANN, pl. 1, fig. 3.

?1992 *Leiosphaeridia verrucata* ZANG AND WALTER, p. 68, fig. 52I, *non* 50I.

Non 1994 *Kildinosphaera verrucata* YIN AND SUN, p. 100, figs. 5I, 5J, 7A.

1996 *Kildinosphaera verrucata,* KNOLL, p. 70, pl. 4, fig. 5.

1999 *Lophosphaeridium* sp. A, SAMUELSSON, DAWES AND VIDAL, figs. 4E and 4H.

?2005 *Kildinosphaera verrucata* PRASAD, UNIYAL AND ASHER, figs. 7.19, 8.12, 11.15.

non 2009 *?Kildinosphaera verrucata* NAGY, PORTER, DEHLER AND SHEN, fig.1F.

?2011 *Lophosphaeridium* sp. STROTHER, BATTISON, BRASIER AND WELLMAN , figs. 1C–D.

Description.—Sphaeroidal organic-walled microfossil with vesicle of moderate opacity, ~50 µm in diameter (range 25.8µm to 68.6 µm, $\bar{x}$=50.4 µm, s=17.8 µm, N=4) with circular to ellipsoidal verrucae ~1 µm in diameter (range 0.7 to 1.3 µm, $\bar{x}$= 0.9 µm, s=0.3 µm, N=4).

Basionym.—Kildinosphaera verrucata Vidal (*in* Vidal and Siedlecka, 1983. Norges geol. Unders. 382, p.62).

Holotype.—Specimen E74–02: V/47 from the Ekkerøy Formation; Vidal 1981, p. 26, figs. 13A–D; in keeping with the original designation by Vidal and Siedlecka (1983).

Occurrence.—Occurs as a common component of early Neoproterozoic organic-walled microfossil assemblages. Distribution includes: Gillen Member of the Bitter Springs Formation of Amadeus Basin, Australia, Vadsø and Barents Sea Groups of East Finnmark, Baffin Bay Group of Greenland and Miroyedikha Formation of eastern Russia. Occurrence of this species was reported from the Wynniatt Formation of arctic Canada but no fossils were figured.

Remarks.— The Alinya specimens are somewhat smaller than those of the Ekkerøy Formation (Vidal, 1981; 40–132 μm) and somewhat larger than those of the Atar Formation (Amard, 1984; 24– 40 μm) but are generally in accord with both.

Vidal (1976) reports *Stictosphaeridium verrucatum* from the upper Visingsö beds of southern Sweden, but the specimen figured does not conform to the concept of *V. verrucata* (=*K. verrucata*) that he and Anna Siedlecka described from the Båtsfjord Formation of the Barents Sea Group, Norway. Instead, the specimen appears to be a leiosphaerid that may bear sparse, possibly taphonomically induced spots or bumps. Vidal (1979) also reports *S. verrucatum* from the Eleonore Bay Group of East Greenland but no specimens were figured.

V. verrucata can be distinguished from *Coneosphaera arctica* by the fact that the former bears ~1 to 2 μm solid, hemisphaerical vesicular ornament, whereas the latter is distinguished by bearing loosely aggregated, irregularly distributed (?hollow) sphaeroids about one-eight to one-tenth the diameter of the main vesicle.

Material examined.—Four specimens from the Alinya Formation, Giles-1 drill core depths 1244.17, 1265.46 and 1265.57 meters.

Unnamed Acritarch species A

Figure 7.5

Description.—A single specimen of an optically-dense, sphaeroidal, organic-walled acritarch bearing frequent (2 to 3 per 10μm of vesicle periphery) tubular processes. Vesicle is 26.9 μm in diameter and processes are 2 μm in width and up to 3 μm in length, although they have probably been shortened by breakage.

Remarks.—This specimen is somewhat similar to two recovered from the upper Svanbergfjellet Formation (Butterfield et al., 1994) and left in open nomenclature as *Goniosphaeridium* sp. With only one specimen recovered from the Alinya material, we hesitate to formally assign a taxonomic home.

Material examined.—Single specimen from the Alinya Formation, Giles-1 drill core depth 1242.84 meters.

Unnamed Acritarch species B

Figure 7.6

Description.—A single specimen of an optically-dense, ellipsoidal, organic-walled acritarch measuring 24.9 μm by 34.6 μm and bearing a single neck-like structure that extends from the main vesicle; structure is 7.0 μm wide at base and extends 3.0 μm, tapering to 3.8 μm at what may be a broken tip.

Material examined.—Single specimen from the Alinya Formation, Giles-1 drill core depth 1255.43 meters.

Unnamed Acritarch species C

Figure 7.10

Description.—A single specimen of an organic-walled, probably originally sphaeroidal acritarch measuring 31.6 μm across and bearing frequent, irregularly distributed hemisphaerical bodies (0.6 to 1.0 μm in diameter) as well as processes up to 1.5 μm in length and 0.6 to 0.8 μm in width. Processes may originate as hemisphaerical bodies. In addition to these features, this specimen also bears a number of what appear to be ruptured blisters; these have centers of about 0.7 μm diameter and a flaring collar that extends 1.5 to 3.0 μm away from the center (Fig. 7.10a). It is currently unclear if this feature is primary or is a result of heterotrophic degradation.

Material examined.—Single specimen from the Alinya Formation, Giles-1 drill core depth 1265.57 meters.

COLONIAL AGGREGATES

Genus SYNSPHAERIDIUM Eisenack, 1965

SYNSPHAERIDIUM spp.

Figures 12.6–12.8, 12.10, 12.12–12.16

Description.—Colonial aggregates of organic-walled, sphaeroidal cells; tight-packing habit may lead to compression and polygonal cell outline. Cell diameters range from 7.5 to 33.7 µm ($\bar{x}$=14.8 µm, s= 4.6 µm, N= 450 measured cells from 221 colonies) across a varied population including forms that show loose association, tight-packing, optically dense and not dense vesicles and forms with dark spots upon the vesicle surface (those with dark bodies *within* the interior of the vesicle rather than a part of the vesicle were not counted separately).

Remarks.—Initially, variations in cell-packing, vesicle opacity and presence of dark spots were thought to indicate separate taxa but over the course of the study, these characters were seen to grade into each other, particularly the more objective classifications such as "optically dense" and "loose or tight" packing, indeed variation was found to occur within single colonies (Fig. 12.10). Although these forms are placed here together, the specimens exhibiting the characters mentioned above were coded separately in anticipation of an emergent pattern (that never materialized). Those data are: forms exhibiting tight-packing resulting in polygonal cell shape (left side of Fig. 12.10) range from 7.5 to 23.0 µm ($\bar{x}$= 12.5

μm, s= 3.2 μm, N=115 measured cells from 57 colonies), forms with optically-dense spots upon the vesicle (Figs. 12.6, 12.7, 12.13, 12.14; see also discussion of *Leiosphaeridia* sp. B) range from 8.3 to 33.7 μm in diameter ($\bar{x}$= 17.8 μm, s= 6.1 μm, N=77 cells measured of 52 colonies) the spots range in diameter from 1.4 μm to 8.3 μm ($\bar{x}$= 3.8 μm, s= 1.5 μm).

A number of genera have been erected for smooth-walled colonial aggregates of cells (e.g. *Synsphaeridium* Eisenack, 1965; *Myxococcoides* Schopf, 1968; *Symplassosphaeridium* Timofeev, 1959 *ex* Timofeev, 1969; *Ostiana* Hermann, 1976 *in* Timofeev et al., 1976). Descriptions vary slightly but all generally describe aggregations of cells 3 to ~90 μm in diameter that may show tight or loose-packing habit and may or may not have optically dense vesicles and occasionally display optically dense or opaque spots upon or within the vesicle. The fossils recovered from the Alinya Formation that conform to such a description have been placed in open nomenclature with attribution to *Synsphaeridium*, the first erected of these genera.

This morphologically simple group is almost certainly polyphyletic but there is also no indication that the preponderance of available generic designations addresses this issue in a biologically relevant way. A major revision of fossil colonial aggregates is warranted and should be guided by neontology, including consideration of phenotypic plasticity as well as actualistic studies of taphonomic variation.

Occurrence.—Ubiquitous in Precambrian and Phanerozoic organic-walled microfossil assemblages.

Material examined.—Two hundred seventy-six colonies from the Alinya Formation, Giles-1 drill core depths 1237.74, 1242.84, 1244, 1244.17, 1248.91, 1255.43, 1255.76, 1257.73, 1265.36, 1265.46, 1265.57, 1265.71, 1266.03 and 1266.31 meters.

FILAMENTOUS MICROFOSSILS

Genus CYANONEMA (Schopf 1968), emend. Butterfield, Knoll and Swett, 1994

Type Species.—Cyanonema attenuata Schopf, 1968.

Remarks.—Members of the genus *Cyanonema* are unbranched, uniseriate cellular trichomes that are distinguished from those of *Oscillatoriopsis* on the basis of length to width ratios of the cells. Members of *Cyanonema* have cell lengths greater than cell widths and members of *Oscillatoriopsis* have cell lengths greater than, or equal to, cell widths.

CYANONEMA sp.

Figure 15.7

Description.—The single specimen recovered in the present study has cells of length ~6 µm and cell widths ~5 µm, thus falling into the genus *Cyanonema*. However, these dimensions are greater than those indicated for the type species, *C. attenutata* and the length to width ratio of 1.1 is less than the diagnosed 1.5 to 2.5 for the type.

Material examined.—One specimen from the Alinya Formation, Giles-1 drill core depth 1244.17 meters.

Genus OBRUCHEVELLA Reitlinger, 1948, emend. Yakshchin and Luchinina, 1981

OBRUCHEVELLA PARVA Reitlinger, 1959

Figures 15.1, 15.2

1959 *Obruchevella parva* REITLINGER, p. 21, pl. 6, figs. 1 and 2.

1992 *Obruchevella parva* KNOLL, p756, pl. 1, figs. 2 and 5.

Description.—Helically coiled, organic-walled filaments measuring ~5 µm in filament diameter (range 3.4 to 6.0 µm, $\bar{x}$= 4.7 µm, s= 1.2 µm, N=5). These fossils have the appearance of concentric circles due to the long-axis view provided by macerates.

Remarks.—Reitlinger erected three species of *Obruchevella,* differentiated chiefly by filament width: *O. delicata* (12–18 µm; Reitlinger, 1948), *O. parva* (6.8–8.5 µm; Reitlinger, 1959) and *O. sibirica* (14–17 µm; Reitlinger, 1959). The difference between *O. delicata* and *O. sibirica* is the total width of the specimen, effectively the number of whorls preserved of the filament. This character is taphonomically controlled, thus *O. sibirica* is a junior synonym of *O. delicata*.

The Alinya Formation specimens are somewhat smaller in diameter than the dimensions of 6.8 to 8.5 µm, given in the original description of *O. parva* (Reitlinger, 1959; p. 20–21). However, the size of the Alinya forms is in keeping with those from the Baklia Formation of the Scotia Group (Knoll, 1992), which measured 4 to 5 µm in diameter. This is also consistent with specimens of the Bylot Group (3 to 10 µm in filament diameter); however, those specimens were assigned to *O. valdaica* rather than *O. parva* without mention of the latter. We place the Alinya specimens into *O. parva* rather than the also comparable *O. valdaica* (erected as *Volyniella valdaica* by Shepeleva in an unpublished dissertation (validly published by Aseeva, 1974) and moved to *Obruchevella* by Jankauskas et al., 1989) due to its nomenclatural priority.

Mankiewicz (1992) gives a careful analysis of the genus and lists seventeen validly named species of *Obruchevella*, suggesting many may be synonyms, but stops short of a major revision.

Occurrence.—Widely distributed in Proterozoic through Paleozoic units.

Material examined.—Five specimens from the Alinya Formation, Giles-1 drill core depth 1265.57 meters.

Genus POLYTHRICHOIDES (Hermann, 1974),

emend. Hermann (*in* Timofeev et al., 1976)

POLYTHRICHOIDES LINEATUS (Hermann, 1974),

emend. Knoll et al., 1991

Figures 15.4, 15.5, 15.9

1976 *Polythrichoides lineatus* TIMOFEEV, HERMANN AND MIKHAILOVA, p. 37.

1989 *Polytrichoides* (*sic*) *lineatus* JANKAUSKAS, MIKHAILOVA AND HERMANN, p. 119, pl. 30, figs. 5A, B, 6, 7.

1991 *Polytrichoides* (*sic*) *lineatus* KNOLL, SWETT AND MARK, p. 563, figs. 4.3, 4.5.

1992 *Polytrichoides* (*sic*) *lineatus* KNOLL, p. 760, pl. 2, fig. 6.

1994 *Polythrichoides lineatus* HOFMANN AND JACKSON, p. 12, FIGS. 11.13–11.17.

1995 *Quaestiosignum filum* ZANG, p. 171, figs. 32A–C.

2009 *Polytrichoides* (*sic*) *lineatus* VOROB'EVA, SERGEEV AND KNOLL, p. 188, figs. 15.13, 15.14.

Description.—Tightly grouped bundles of parallel, smooth-walled, apparently aseptate trichomes ranging in width from 0.9 to 2.5 µm ($\bar{x}$=1.4 µm, s=0.5 µm, N=10). Filament bundles range in width from 8 to 24 µm ($\bar{x}$=14.1 µm, s=5.6 µm, N=11).

Remarks.—The *P. lineatus* specimens recovered from the Alinya Formation are slightly smaller than the 3.9 µm indicated in the diagnosis by Hermann (1974) and the range of 3 to 5 µm given in her later emendation (*in* Timofeev et al., 1976) but are very similar in range to those described from the Bylot Supergroup (1 to 3 µm) by Hofmann and Jackson (1994). Similarly, the widths of the bundles of filaments found in the Alinya Formation (8 to 24 µm) are somewhat smaller than those of the type material (19.5 to 39 µm), but are consistent with findings from Bylot Supergroup specimens (5 to 30µm). This form is often compared with members of the extant cyanobacterial genus *Microcoleus* in which the widths of filaments is typically 2 to 10µm and the number of filaments within a sheath varies from 2–3 to more than 100, resulting in a wide range of bundle widths.

Occurrence.—Widely distributed in Proterozoic organic-walled microfossil assemblages.

Material examined.—Eleven specimens from the Alinya Formation, Giles-1 drill core depths 1265.46, 1265.57, 1265.71 and 1266.31 meters.

Genus RUGOSOOPIS (Timofeev and Hermann, 1979), emend. Butterfield, Knoll and Swett, 1994

Type species.—*Rugosoopsis tenuis* Timofeev and Hermann, 1979.

Remarks.—In the emended diagnosis of Butterfield et al., 1994 (followed here) this genus is indicated to be bi-layered, consisting of a smooth-walled or pseudoseptate inner sheath surrounded by a diagnostic outer sheath bearing a transverse fabric. In the material recovered from the Alinya Formation, this form is most frequently found to be missing the inner smooth-walled filament.

Butterfield and colleagues (1994) suggest a cyanobacterial affinity for *Rugosoopsis* based on observations of *Rugosoopsis*-like transverse fabric developed during cyanobacterial response to desiccation in modern lagoonal systems (Horodyski et al., 1977).

RUGOSOOPSIS TENUIS (Timofeev and Hermann, 1979), emend. Butterfield, Knoll and Swett, 1994

Figures 15.10, 15.13, 15.14

1979 *Rugosoopsis tenuis* TIMOFEEV AND HERMANN, p. 139, pl. 29, figs. 5, 7.

1994 *Rugosoopsis tenuis* BUTTERFIELD, KNOLL AND SWETT, p. 62, figs. 25A-D, 27B.

2001 *Rugosoopsis tenuis* SAMUELSSON AND BUTTERFIELD, fig. 3.

(For additional synonymy, see Butterfield et al., 1994.)

Description.—Alinya Formation *R. tenuis* vary in diameter from 6.2 to 29.5 µm ($\bar{x}$=11.7 µm, s=4.9 µm, N=23), consistent with the forms described from the Svanbergfjellet Formation (7 to 57 µm in diameter) described by Butterfield and colleagues (1994) and from which the emended diagnosis was made. In two specimens cellular contents are retained (Fig. 15.10).

Occurrence.—This form has been reported from early Neoproterozoic units such as the Svanbergfjellet, Lone land and Lakhanda formations.

Material examined.—Twenty-three specimens from the Alinya Formation, Giles-1 drill core depths 1265.46, 1265.57, 1265.71 and 1266.31 meters.

Genus SIPHONOPHYCUS (Schopf, 1968),

emend. Knoll, Swett and Mark, 1991

Type species.—*Siphonophycus kestron* Schopf, 1968.

Remarks.—Siphonophycus is a form genus of unbranched, smooth-walled originally tubular filamentous sheaths that are differentiated based on width groupings; in this way *Siphonophycus* is the filamentous equivalent of *Leiosphaeridia*.

SIPHONOPHYCUS SEPTATUM (Schopf, 1968),

Knoll, Swett and Mark, 1991

Figure 15.6

1968 *Tenuofilum septatum* SCHOPF, p. 679, pl. 86, figs. 10–12.

1991 *Siphonophycus septatum* KNOLL, SWETT AND MARK, p. 565, fig. 10.2.

1994 *Siphonophycus septatum* BUTTERFIELD, KNOLL AND SWETT, p. 64, figs. 10H, 22 G–H.

1994 *Siphonophycus septatum* HOFMANN AND JACKSON, p. 10, figs. 11.1–11.4.

(For additional synonymy, see Butterfield et al., 1994.)

Diagnosis.—Unbranched, nonseptate, smooth-walled filamentous microfossil 1 to 2 μm in diameter.

Description.—The Alinya population consists of only two specimens, both of which are 1.6 μm in diameter.

Occurrence.—Widely distributed; found in Mesoproterozoic through Paleozoic units.

Material examined.—Five specimens, one measuring ~ 235 μm in length, were recovered from the Neoproterozoic Alinya Formation, 1265.36, 1265.57 and 1265.71meters depth in Giles-1 drill core, Officer Basin, South Australia.

SIPHONOPHYCUS ROBUSTUM (Schopf, 1968),

Knoll, Swett and Mark, 1991

Figure 15.11

1968 *Eomycetopsis robusta* SCHOPF, p. 685, pl. 82, figs. 2–3 and pl. 83, figs. 1–4.

1994 *Siphonophycus robustum* BUTTERFIELD, KNOLL AND SWETT, p. 64, figs. 26A, G.

1994 *Siphonophycus robustum* HOFMANN AND JACKSON, p. 10, figs. 11.5.

1998 *Siphonophycus robustum* YUAN AND HOFMANN, p. 209, fig 13I.

2001 *Siphonophycus robustum* SAMUELSSON AND BUTTERFIELD, figs. 2B, 9F–H.

2009 *Siphonophycus robustum* DONG, XIAO, SHEN, ZHOU, LI AND YAO, p. 39, fig. 6.12.

2010 *Siphonophycus robustum* SERGEEV AND SCHOPF, p. 387, fig. 6.4.

(For additional synonymy, see Butterfield et al., 1994.)

Diagnosis.—Unbranched, nonseptate, smooth-walled filamentous microfossil 2 to 3 μm in diameter.

Description.—The Alinya population ranges in diameter from 2.1 to 3.8 μm ($\bar{x}$=3.2 μm, s=0.6 μm, N=7).

Occurrence.—Widely distributed; found in Mesoproterozoic through Paleozoic units.

Material examined.—Twelve specimens from the Alinya Formation, Giles-1 drill core depths 1244.17, 1255.43, 1265.36, 1265.57 and 1266.21 meters.

SIPHONOPHYCUS TYPICUM (Hermann, 1974),

Butterfield (*in* Butterfield et al., 1994)

Figures 15.4, 15.8

1974 *Leiothricoides typicum* HERMANN, p. 7, pl. 6, figs. 1–2.

1994 *Siphonophycus typicum* BUTTERFIELD, p. 66, figs. 23 B–D, 26B, H, I.

1995 *Siphonophycus robustum* ZANG, figs. 32L, M.

2001 *Siphonophycus typicum* SAMUELSSON AND BUTTERFIELD, figs. 2A, 8F.

2008 *Siphonophycus typicum* MOCZYDŁOWSKA, p. 83, fig. 5E.

2010 *Siphonophycus typicum* SERGEEV AND SCHOPF, p. 387, fig. 6.4.

(For additional synonymy, see Butterfield et al., 1994.)

Diagnosis.—Unbranched, nonseptate, smooth-walled filamentous microfossil 4 to 8 µm in diameter.

Description.—The Alinya population ranges in diameter from 4.0 to 8.0 µm ($\bar{x}$=5.8 µm, s=1.2 µm, N=35).

Occurrence.—Widely distributed; found in Mesoproterozoic through late Ediacaran units.

Material examined.—Forty-seven specimens from the Alinya Formation, Giles-1 drill core depths 1244.17, 1255.43, 1255.76, 1265.36, 1265.46, 1265.57, 1265.71 and 1266.31 meters.

SIPHONOPHYCUS KESTRON Schopf, 1968

Figure 15.12

1994 *Siphonophycus kestron* BUTTERFIELD, KNOLL AND SWETT, p. 67, fig. 21D.

1994 *Siphonophycus kestron* HOFMANN AND JACKSON, p. 12, figs. 11.8–11.9.

1995 *Siphonophycus* sp. cf. *S. kestron* ZANG, p. 171, fig. 32G *non* 32F.

1998 *Siphonophycus rugosum* YUAN AND HOFMANN, fig 13H.

2001 *Siphonophycus kestron* SAMUELSSON AND BUTTERFIELD, fig. 8F.

2008 *Siphonophycus kestron* MOCZYDŁOWSKA, p. 82, fig. ?4G, 5F, 7F.

2010 *Siphonophycus kestron* SERGEEV AND SCHOPF, p. 385, fig. 8.5.

(For additional synonymy, see Butterfield et al., 1994.)

Diagnosis.—Unbranched, nonseptate, smooth-walled filamentous microfossil 8 to 16 µm in diameter.

Description.—The Alinya population ranges in diameter from 8.3 to 15.2 µm ($\bar{x}$=10.9 µm, s=2.1 µm, N=22).

Occurrence.—Widely distributed; found in Mesoproterozoic through early Cambrian units.

Material examined.—Twenty-six specimens from the Alinya Formation, Giles-1 drill core depths 1255.43, 1265.36, 1265.46, 1265.57 and 1266.31 meters.

SIPHONOPHYCUS SOLIDUM (Golub, 1979),

Butterfield (*in* Butterfield et al., 1994)

Figure 15.15

1994 *Siphonophycus solidum* BUTTERFIELD, KNOLL AND SWETT, p. 67, fig. 25H–I, 27D.

?1995 *Siphonphycus* sp. cf. *S. kestron* ZANG, p. 171, fig. 32F.

2001 *Siphonophycus solidum* SAMUELSSON AND BUTTERFIELD, figs. 8A, C, ?D, E.

2002 *Siphonophycus solidum* XIAO, YUAN, STEINER AND KNOLL, p. 371, figs. 10.1–10.3.

2010 *Siphonophycus solidum* SERGEEV AND SCHOPF, p. 387, fig. 7.6–7.8, 8.1, 8.2.

(For additional synonymy, see Butterfield et al., 1994.)

Diagnosis.—Unbranched, nonseptate, smooth-walled filamentous microfossil 16 to 32 μm in diameter.

Description.—The Alinya population ranges in diameter from 16.9 to 32.6 μm ($\bar{x}$=24.3 μm, s=6.4 μm, N=6).

Occurrence.—Widely distributed in Proterozoic and Paleozoic organic-walled microfossil assemblages.

Material examined.—Seven specimens from the Alinya Formation, Giles-1 drill core depths 1265.36, 1265.46 and 1266.31 meters.

CONCLUSIONS

Study of micro- and nano-scale morphology by SEM has proven to be of great use in the description of the Alinya assemblage. Happily, it appears that the apparent lack of morphological detail in early to mid-Neoproterozoic acritarchs is partly a methodological limitation; the traditional use of transmitted light microscopy does not permit appreciation of the very subtle diagnostic detail found in some of these taxa. More widespread use of SEM in study of mid- Neoproterozoic taxa may illustrate that fine detail is common in acritarchs of this age. Such a finding could have a significant impact upon Neoproterozoic biostratigraphy and, in turn, our understanding of early eukaryotic diversity trends. Routine use of SEM in acritarch studies would also reduce taxonomic inflation and depression caused by taphonomic variation— results valuable not only for within-assemblage diversity

assessment, but also important for identification of taxa from units of poor preservational quality.

The high taxonomic richness of the mid-Neoproterozoic Alinya Formation is consistent with the elevated levels of eukaryotic diversity seen from other pre-glacial Cryogenian units. However, the Alinya assemblage is more similar to that of the 770-742 Ma Chuar Group than to the somewhat older Svanbergfjellet and Wynniatt formations. Indeed, the Alinya and Chuar assemblages may be two of the youngest records of high organic-walled microfossil diversity before the onset of the Cryogenian glaciations.

ACKNOWLEDGMENTS

This work was supported by National Science Foundation grant EAR-0922305 to S. M. P. Authors thank managers and staff of core facilities at Glenside Core Library, Adelaide, SA for aid in sampling, G. Waanders for sample preparations, and J. L. Moore for manuscript feedback and a generally insightful nature.

REFERENCES

ALLISON, C. W. AND S. M. AWRAMIK. 1989. Organic-walled microfossils form the earliest Cambrian or latest Proterozoic Tindir Group Rocks, northwest Canada. Precambrian Research, 43:253–294.

ANDERSON, R. P., I. J. FAIRCHILD, N. J. TOSCA AND A. H. KNOLL. 2013. Microstructures in metasedimentary rocks from the Neoproterozoic Bonahaven Formation, Scotland: microconcretions, impact spherules, or microfossils? Precambrian Research, 233:59–72.

AMARD, B. 1984. Nouveaux éléments de datation de la couverture Protérozoïque du craton ouest-africain: un assemblage de microfossiles (Acritarches) caractéristique du Riphéen supérieur dans la formation d'Atar (Mauritanie). Comptes rendus des séances de l'Academie des sciences. Série 2, Mécanique-physique, Chimie, Sciences de l'univers, Sciences de la Terre, 299:1405–1410.

ASSEVA, E. A. 1974. O spirale-i kol'tsevidnykh obrazovaniiakh v verkhnedkembriiskikh otlozheniiakh Podolii. Paleontologicheskii Sbornik, 11:95–98, 1 plate.

BATTISON, L. AND M. D. BRASIER. 2012. Remarkably preserved prokaryote and eukaryote microfossils within 1 Ga-old lake phosphates of the Torridon Group, NW Scotland. Precambrian Research, 196–197:204–217.

BERNEY, C. AND J. PAWLOWSKI. 2006. A molecular time-scale for eukaryote evolution recalibrated with the continuous microfossil record. Proceedings of the Royal Society, B. 273:1867–1872.

BUICK, R. AND A. H. KNOLL. 1999. Acritarchs and microfossils from the Mesoproterozoic Bangemall Group, northwestern Australia. Journal of Paleontology, 73:744–764.

BUTTERFIELD, N. J. 2004. A vaucheriacean alga from the middle Neoproterozoic of Spitsbergen: implications for the evolution of Proterozoic eukaryotes and the Cambrian explosion. Paleobiology, 30:231–252.

BUTTERFIELD, N. J. 2005. Probable Proterozoic fungi. Paleobiology, 31:165–182.

BUTTERFIELD, N. J. 2007. Macroevolution and macroecology through deep time. Palaeontology, 50:41–55.

BUTTERFIELD, N. J., A. H. KNOLL AND K. SWETT. 1994. Paleobiology of the Neoproterozoic Svanbergfjellet Formation, Spitsbergen. Fossils and Strata, 34:1–84.

CANFIELD, D. E. 2014. Oxygen: a four billion year history. Princeton University Press, 224 p.

COMBAZ, A., F. W. LANG AND J. PANSART. 1967. Les "Leiofusidae" Eisenack, 1938. Review of Palaeobotany and Palynology, 1:291–307.

COUËFFÉ, R. AND M. VECOLI. 2011. New sedimentological and biostratigraphic data in the Kwahu Group (Meso- to Neo-Proterozoic), southern margin of the Volta Basin, Ghana: stratigraphic constraints and implications on regional lithostratigraphic correlations. Precambrian Research, 189:155–175.

COTTER, K. L. 1997. Neoproterozoic microfossils from the Officer Basin, Western Australia. Alcheringa, 21:247–270.

COTTER, K. L. 1999. Microfossils from Neoproterozoic Supersequence 1 of the Officer Basin, Western Australia. Alcheringa, 23:63–86.

DONG, L., S. XIAO, B. SHEN, C. ZHOU, G. LI AND J. YAO. 2009. Basal Cambrian microfossils from the Yangtze Gorges area (South China) and the Aksu area (Tarim Block, northwestern China). Journal of Paleontology, 83:30–44.

DOWNIE, C. 1963. 'Hystrichospheres' (acritarchs) and spores of the Wenlock Shales (Silurian) of Wenlock, England. Palaeontology, 6:625–652.

DOWNIE, C AND W. A. S. SARJEANT. 1963. On the interpretation and status of some hystrichosphere genera. Palaeontology, 6:83–96.

DOWNIE, C., W. R. EVITT AND W. A. S. SARJEANT. 1963. Dinoflagellates, hystrichospheres, and the classification of the acritarchs. Stanford University Publications: Geological Sciences, Vol. 7, No. 3, 16 p.

EISENACK, A. 1958a. *Tasmanites* Newton 1875 und *Leiosphaeridia* n. g. als Gattungen der Hystrichosphaeridea. Palaeontographica, Abteilung A. v. 110, no.1–3:1–19, pl. 1–2.

EISENACK, A. 1958b. Mikrofossilien aus dem Ordovizium des Baltikums. 1. Markasitschicht, *Dictyonema*-Schiefer, Glaukonitsand, Glaukonitkalk. Senckenbergiana Lethaea. v.39, no. 5/6:389–405.

EISENACK, A. 1965. Mikrofossilien aus dem Silur Gotlands Hystrichosphären, Problematika. Neues Jarbuch für Geologie und Paläontologie Abhandlungen, 122:257–274.

EISENACK, A. 1976. Mikrofossilien aus dem Vaginatenkalk von Hälludden, Öland. Palaeontographica, Abteilung A. vol. 154, no. 4–6, p. 181–203, pl. 1–7.

FENSOME, R. A., G. L. WILLIAMS, M. S. BARSS, J. M. FREEMAN AND J. M. HILL. 1990. Acritarchs and fossil prasinophytes: and index to genera, species and infraspecific taxa. American Association of Stratigraphic Palynologists Foundation, AASP Contributions Series Number 25, 771 p.

GAO, L., Y. XING AND G. LIU. 1995. Neoproterozoic micropalaeoflora from Hunjiang area, Jilin province and its sedimentary environment. Professional Papers of Stratigraphy and Palaeontology, 26:1–23, and 4 plates.

GRAY, J. AND A. J. BOUCOT. 1989. Is *Moyeria* a euglenoid? Lethaia, 22:447–456.

GREY, K. 1999. A modified palynological preparation technique for the extraction of large Neoproterozoic acanthomorph acritarchs and other acid-insoluble microfossils. Western Australia Geological Survey, Record 1999/10, 23 p.

GREY, K. 2005. Ediacaran palynology of Australia. Memoirs of The Association of Australiasian Palaeontologists, 31. 439 p.

GREY, K., A. C. HILL AND C. CALVER. 2011. Biostratigraphy and stratigraphic subdivision of Cryogenian successions of Australia in global context, p113-134. *In* E. Arnaud, G. P. Halverson and G. Shields-Zhou (eds.), The Geological Record of Neoproterozoic Glaciations. Geological Society, London, Memoirs, 36.

GREY, K. AND S. WILLMAN. 2009. Taphonomy of Ediacaran acritarchs from Australia: significance for taxonomy and biostratigraphy. Palaios, 24: 239–256.

GOLUB, I. N. 1979. Novaya gruppa problematichnykh mikroobrazovanij v vendskikh otlozheniyakh Orshanskoj vpadiny (Russkaya platform), p. 147–155. *In* B. S. Sokolov (ed.), Paleontologiya Dokembriya i Rannego Kembriya. Nauka. Leningrad.

HALVERSON, G. P., P. F. HOFFMAN, D. P. SCHRAG, A. C. MALOOF AND A. H. N. RICE, 2005. Toward a Neoproterozoic composite carbon-isotope record. Geological Society of America Bulletin, 117:1181–1207.

HERMANN, T. N. 1974. Nakhodki massovykhs kopleniy trikhomov v rifee, p. 6-10. *In* B. V. Timofeev (ed.), Mikrofitofossilii proterozoya i rannego paleozoya SSSR. Nauka, Leningrad.

HERMANN, T. N. 1990. Organic world one billion years ago. Nauka, Leningrad, 51 p.

HILL, A. C. 2005. Stable Isotope stratigraphy, GSWA Lancer 1, Officer Basin, western Australia, p. 1–11. *In* A. J. Mory and P. W. Haines (eds.), GSWA Lancer 1 well completion report (interpretive papers), Officer and Gunbarrel Basins, western Australia. Western Australia Geological Survey, Record 2005/4.

HILL, A. C., K. L. COTTER AND K. GREY. 2000. Mid-Neoproterozoic biostratigraphy and isotope stratigraphy in Australia. Precambrian Research, 100:281–298.

HILL, A. C., K. GREY, V. A. GOSTIN AND L. J. WEBSTER, 2004. New records of Late Neoproterozoic Acraman ejecta in the Officer Basin. Australian Journal of Earth Sciences, 51:47–51.

HILL, A. C. AND M. R. WALTER. 2000. Mid-Neoproterozoic (~830–750 Ma) isotope stratigraphy of Australia and global correlation. Precambrian Research, 100:181–211.

HOFMANN, H. J. 1999. Global distribution of the Proterozoic sphaeromorph acritarch *Valeria lophostriata* (Jankauskas). Acta Micropalaeontologica Sinica, 16:215–224.

HOFMANN, H. J. AND G. D. JACKSON. 1994. Shale-facies microfossils from the Proterozoic Bylot Supergroup, Baffin Island, Canada. Memoir, The Paleontological Society, 37:1–39.

HORODYSKI, R. J., B. BLOESER AND S. VONDER HAAR. 1977. Laminated algal mats from a coastal lagoon, Laguna Mormona, Baja California, Mexico. Journal of Sedimentary Petrology, 47:680-696.

HUNTLEY, J. W., S. XIAO AND M. KOWALEWSKI. 2006. 1.3 Billion years of acritarch history: An empirical morphospace approach. Precambrian Research, 144:52–68.

JANKAUSKAS, T. V. 1979. Srednerifeyski microbiota Yuzhnogo Urala I Bashkirskogo Priural'ya. Akademiya Nauk SSSR, Doklady, 248:190-193 (1981, 248:51–54 in English version).

JANKAUSKAS, T. V. 1982. Mikrofossilii rifeya Yuzhnogo Urala. *In* B. M. Keller (ed.) Stratotype Rifeya-Paleontologiya paleomagnetizm. Akademiya Nauk SSSR Transactions, 368:84–120, plates. 31–48.

JANKAUSKAS, T. V., N. S. MIKHAILOVA AND T. N. HERMANN (GERMAN) (eds.) 1989. Mikrofossilii Dokembria SSSR. Nauka. Leningrad. 191 p.

JAVAUX, E. J. 2011. Early Eukaryotes in Precambrian oceans, p.414–449 *In* M. Gargaud, P. Lopez-Garcia and H. Martin (eds.), Origins and Evolution of Life: An Astrobiological Perspective: Cambridge University Press.

JAVAUX, E. J., A. H. KNOLL AND M. R. WALTER. 2001. Morphological and ecological complexity in early eukaryotic ecosystems. Nature, 412: 66–69.

JAVAUX, E. J., A. H. KNOLL AND M. R. WALTER. 2004. TEM evidence for eukaryotic diversity in mid-Proterozoic oceans. Geobiology, 2:121–132.

KAUFMAN, A. J., A. H. KNOLL AND S. M. AWRAMIK. 1992. Biostratigraphic and chemostratigraphic correlation of Neoproterozoic sedimentary successions: Upper Tindir Group, northwestern Canada, as a test case. Geology, 20:181–185.

KNOLL, A. H., 1992. Vendian microfossils in metasedimentary cherts of the Scotia Group, Prins Karls Forland, Svalbard. Palaeontology, 35:715–774.

KNOLL, A. H. 1994. Proterozoic and early Cambrian protists: evidence for accelerating evolutionary tempo. Proceedings of the National Academy of Sciences, 91:6743–6750.

KNOLL, A. H. 1996. Chapter 4: Archean and Proterozoic paleontology, p. 51–80. *In* J. Jansonius and D. C. McGregor (eds.), Palynology: principles and applications. American Association of Stratigraphic Palynologists Foundation, Vol 1.

KNOLL, A. H. 2011. The Multiple Origins of Complex Multicellularity. Annual Reviews in Earth and Planetary Sciences, 39:217–239.

KNOLL, A. H. AND E. S. BARGHOORN. 1975. Precambrian eukaryotic organisms: a reassessment of the evidence. Science, 190:52–54.

KNOLL A. H., E. J. JAVAUX, D. HEWITT AND P. COHEN. 2006. Eukaryotic organisms in Proterozoic oceans. Philosophical Transactions of the Royal Society, B, 361:1023–1038.

KNOLL, A. H., K. SWETT AND J. MARK. 1991. Paleobiology of a Neoproterozoic tidal flat/lagoonal complex: The Draken Conglomerate. Journal of Paleontology, 65:531–570.

LI, Z. X., S. V. BOGDANOVA, A. S. COLLINS, A. DAVIDSON, B. DE WAELE, R. E. ERNST, I. C. W. FITZSIMONS, R. A. FUCK, D. P. GLADKOCHUB, J. JACOBS, K. E. KARLSTROM, S. LU, L. M. NATAPOV, V. PEASE, S. A. PISAREVSKY, K. THRANE AND V. VERNIKOVSKY. 2008. Assembly, configuration, and break-up history of Rodinia: a synthesis. Precambrian Research, 160:179–210.

LINDSAY, J. F. AND J. H. LEVEN. 1996. Evolution of a Neoproterozoic to Palaeozoic intracratonic setting, Officer Basin, South Australia. Basin Research, 8:403–424.

LÜCKING, R., S. HUHNDORF, D. H. PFISTER, E. R., PLATA AND H. T. LUMBSCH. 2009. Fungi evolved on the right track. Mycologica, 101:810–822.

LUO, Q-L. 1991. New data on the microplants from Changlongshan Formation of Upper Precambrian in western Yanshan Range. Tianjin Institute of Geology and Mineral Resources, Bulletin, 25:107–118 (in Chinese with English abstract).

MACDONALD, F. A., M. D. SCHMITZ, J. L. CROWLEY, C. F. ROOTS, D. S. JONES, A. C. MALOOF, J. V. STRAUSS, P. A. COHEN, D. T. JOHNSTON AND D. P. SCHRAG. 2010a. Calibrating the Cryogenian. Science, 327:1241–1243.

MACDONALD, F. A., P. A. COHEN, F. Ö. DUDÁS AND D. P. SCHRAG. 2010b. Early Neoproterozoic scale microfossils in the Lower Tindir Group of Alaska and the Yukon Territory. Geology, 38:143–146.

MANKIEWICZ, C. 1992. *Obruchevella* and other microfossils in the Burgess Shale: preservation and affinity. Journal of Paleontology, 66:717–729.

MEYER, K. M. AND L. R. KUMP. 2008. Oceanic euxinia in Earth history: Causes and Consequences. Annual Review of Earth and Planetary Sciences, 36:251–288.

MOCZYDŁOWSKA, M. 2008. New records of late Ediacaran microbiota from Poland. Precambrian Research, 167:71–92.

MORTON, J. G. G. 1997. Lithology and environments of deposition, p. 47–86. *In* J. G. G. Morton and J. F. Drexel (eds.), The Petroleum Geology of South Australia. Vol 3: Officer Basin. South Australia. Department of Mines and Energy Resources. Report Book, 97/19

NAGOVITSIN, K. 2009. *Tappania*-Bearing association of the Siberian platform: biodiversity, stratigraphic position and geochronological constraints. Precambrian Research, 173:137–145.

NAGY, R. M., S. M. PORTER, C. M. DEHLER AND Y. SHEN. 2009. Biotic turnover driven by eutrophication before the Sturtian low-latitude glaciation. Nature Geoscience, 2:415–418.

NAUMOVA, S. N. 1949. Spory nizhnego kembriya. Izvestiya Akademiy Nauk, 4:49–56.

PARFREY, L. W., D. J. G. LAHR, A. H. KNOLL AND L. A. KATZ. 2011. Estimating the timing of early eukaryotic diversification with multigene molecular clocks. Proceedings of the National Academy of Sciences, 108:13624–13629.

PEAT, C. J., M. D. MUIR, K. A. PLUMB, D. M. MCKIRDY AND M. S. NORVICK. 1978. Proterozoic microfossils from the Roper Group, Northern Territory, Australia. BMR Journal of Australian Geology and Geophysics, 3:1–17.

PIERREHUMBERT, R. T., D. S. ABBOT, A. VOIGT AND D. KOLL. 2011. Climate of the Neoproterozoic. Annual Review of Earth and Planetary Sciences, 39:417–460.

PISAREVSKY, S. A., Z. X. LI, K. GREY AND M. K. STEVENS. 2001. A paleomagnetic study of Empress 1A, a stratigraphic drillhole in the Officer Basin: evidence for a low-latitude position of Australia in the Neoproterozoic. Precambrian Research, 110:93–108.

PISAREVSKY, S. A., M. T. D. WINGATE, M. K. STEVENS AND P. W. HAINES, 2007. Palaeomagnetic results from the Lancer 1 stratigraphic drillhole, Officer Basin, Western Australia, and implications for Rodinia reconstructions. Australian Journal of Earth Sciences, 54:561–572.

PORTER, S. M., R. MEISTERFELD AND A. H. KNOLL. 2003. Vase-shaped microfossils from the Neoproterozoic Chuar Group, Grand Canyon: a classification guided by modern testate amoebae. Journal of Paleontology, 77:409–429.

PORTER, S. M. AND A. H. KNOLL. 2000. Testate amoebae in the Neoproterozoic Era: evidence from vase-shaped microfossils in the Chuar Group, Grand Canyon. Paleobiology, 26:360–385.

PRASAD, B., S. N. UNIYAL AND R. ASHER. 2005. Organic-walled microfossils from the Proterozoic Vindhyan Supergroup of Son Valley, Madhya Pradesh, India. The Palaeobotanist, 54:13–60.

PYATILETOV, G. 1980. O nakhodkakh mikrofossiliy roda *Navifusa*. Palaeontological Journal, 3:143–145.

REITLINGER, E. A. 1948. Kembriĭskie Foraminifery Yakutii. Biulleten Moskovskogo Obshchestva Ispytalelej Prirody, Otdlenie Geologii, 23:77–81.

REITLINGER, E. A. 1959. Atlas mikroskopicheskikh organicheskikh ostatkov i problematiki drevnikh tolshch Sibiri. Trudy Geologicheskogo Instituta. Akademiia Nauka SSSR. Moscow. 63 p., 22 plates.

ROTHMANN, D. H., J. M. HAYES AND R. E. SUMMONS. 2003. Dynamics of the Neoproterozoic carbon cycle. Proceedings of the National Academy of Sciences, USA. 100:8124–8129.

SAMUELSSON, J. 1997. Biostratigraphy and palaeobiology of early Neoproterozoic strata of the Kola Peninsula, northwest Russia. Norsk Geologisk Tidsskrift, 77:165–192.

SAMUELSSON, J., P. R. DAWES AND G. VIDAL. 1999. Organic-walled microfossils from the Proterozoic Thule Supergroup, northwest Greenland. Precambrian Research, 96:1–23.

SAMUELSSON, J. AND N. J. BUTTERFIELD. 2001. Neoproterozoic fossils from the Franklin Mountains, northwestern Canada: stratigraphic and palaeobiological implications. Precambrian Research, 107:235–251.

SCHIFFBAUER, J. D. AND S. XIAO. 2009. Novel application of Focused Ion Beam Electron Microscopy (FIB-EM) in preparation and analysis of microfossil ultrastructures: a new view of complexity in early eukaryotic organisms. Palaios, 24:616–626.

SCHOPF, J. W. 1968. Microflora of the Bitter Springs Formation, late Precambrian, central Australia. Journal of Paleontology, 42:651–688.

SCHOPF, J. W. 1992. Chapter 24: Atlas of representative Proterozoic microfossils, p.1055–1117. *In* J. W. Schopf (ed.), The Proterozoic Biosphere. Cambridge University Press, Cambridge.

SERGEEV, V. N. AND J. W. SCHOPF. 2010. Taxonomy, paleoecology and biostratigraphy of the late Neoproterozoic Chichkan microbiota of south Kazakhstan: the marine biosphere on the eve of the metazoan radiation. Journal of Paleontology, 84:363–401.

SINGH, V. K. AND R. BABU. 2013. Neoproterozoic chert permineralized silicified microbiota form the carbonate facies of Raipur Group, Chhattisgarh Basin, India: their biostratigraphic significance. Geological Society of India Special Publication, 1: 1–15.

SIMONETTI, C. AND T. R. FAIRCHILD. 2000. Proterozoic microfossils from subsurface siliciclastic rocks of the São Francisco Craton, south-central Brazil. Precambrian Research, 103:1–29.

STAPLIN, F. L., J. JANSONIUS AND S. A. J. POCOCK. 1965. Evaluation of some acritarchous hystrichosphere genera. Neues Jarbuch für Geologie und Paläontologie Abhandlungen, 123:167–201.

STROTHER, P. K, L. BATTISON, M. D. BRASIER AND C. H. WELLMAN. 2011. Earth's earliest non-marine eukaryotes. Nature, 473:505–509.

SWANSON-HYSELL, N., C. V. ROSE, C. C., CALMET, G. P. HALVERSON, M. T. HURTGEN AND A. C. MALOOF. 2010. Cryogenian glaciations and the onset of carbon-isotope decoupling. Science, 328:608–611.

TALYZINA, N. M. AND M. MOCZYDŁOWSKA. 2000. Morphological and ultrastructural studies of some acritarchs for the lower Cambrian Lükati Formation, Estonia. Review of Palaeobotany and Palynology, 112:1–21.

TANG, Q., K. PANG, S. XIAO, X. YUAN, Z. OU AND B. WAN. 2013. Organic-walled microfossils from the early Neoproterozoic Liulaobei Formation in the Huainan region of North China and their biostratigraphic significance. Precambrian Research, 236:157–181.

TIMOFEEV, B. V. 1959. Drevneishaya flora Pribaltiki i ee stratigraficheskoe znachenie. Vseoyuznyi Neftyanoi Naucho-Issledovatelskii Geologorazvedochnyi Institut, Leningrad Trudy VNIGRI, 129:1–136, pl. 1–24.

TIMOFEEV, B. V. 1966. Mikropaleofitologicheskoe Issledovanie Drevnikh Svit. Nauka, Moscow, 147 p., 89 plates.

TIMOFEEV, B. V. 1969. Sferomorfidy Proterozoia. Akademiia Nauk SSSR. Leningrad, 146 p.

TIMOFEEV, B. V. AND T. N. HERMANN, 1979. Dokembrijskaya mikrobiota Lakhandinskoj svity, p. 137-147. *In* B. S. Sokolov (ed.), Paleontologiya Dokembriya i Rannego Kembriya. Nauka. Leningrad.

TIMOFEEV, B. V., T. N. HERMANN AND N. S. MIKHAILOVA. 1976. Mikrofitofossilii Dokembriia, Kembriia I Ordovika. Akademiia Nauk SSSR. Leningrad. 107 p.

TYNNI, R. AND A. UUTELA, 1984. Microfossils from the Precambrian Muhos Formation in western Finland. Geological Survey of Finland, Bulletin 330, 38p. and 20 plates.

VEIS, A. F, P. U. PETROV AND N. G. VOROB'EVA, 1998. Miroedikhinskaya mikrobiota Verkhnego Rifeya Sibiri. Soobshchenie 1. Sostav i fatsial'no-ekologicheskoe raspredelenie organostennykh mikrofossilii. Stratigrafiya, Geologicheskaya Korreliatsiya, 6 (5):15–37.

VIDAL, G. 1976. Late Precambrian microfossils from the Visingsö beds in southern Sweden: Fossils and Strata, no. 9, 37 p.

VIDAL, G. 1979. Acritarchs form the upper Proterozoic and lower Cambrian of East Greenland. Grønlands Geologiske Undersøgelse, Bulletin 134, 40 p., 7 plates.

VIDAL, G. 1981. Micropalaeontology and biostratigraphy of the upper Proterozoic and lower Cambrian sequence in East Finnmark, northern Norway. Norges Geologiske Undersøkelse Bulletin, 362:1–53.

VIDAL, G. AND T. D. FORD. 1985. Microbiotas from the Late Proterozoic Chuar Group (Northern Arizona) and Uinta Mountain Group (Utah) and their chronostratigraphic implications. Precambrian Research, 28:349–389.

VIDAL, G. AND A. SIEDLECKA. 1983. Planktonic, acid-resistant microfossils from the upper Proterozoic strata of the Barents Sea Region of Varanger Peninsula, East Finnmark, Northern Norway. Norges Geologiske Undersøkelse Bulletin, 382:45–79.

VOROB'EVA, N. G., V. N. SERGEEV AND A. H. KNOLL. 2009. Neoproterozoic microfossils from the northeastern margin of the East European Platform. Journal of Paleontology, 83:161–196.

WALTER, M. R., J. J. VEEVERS, C. R. CALVER AND K. GREY. 1995. Neoproterozoic stratigraphy of the Centralian Superbasin. Precambrian Research, 73:173–195.

WILLMAN, S. AND M. MOCZYDŁOWSKA. 2008. Ediacaran acritarch biota form the Giles 1 drillhole, Officer Basin, Australia, and its potential for biostratigraphic correlation. Precambrian Research, 162:498–530.

WILLMAN, S. 2009. Morphology and wall ultrastructure of leiosphaeric and acanthomorphic acritarchs from the Ediacaran of Australia. Geobiology, 7:8–20.

XIAO, S., A. H. KNOLL, A. J. KAUFMAN, L. YIN AND Y. ZHANG. 1997. Neoproterozoic fossils in Mesoproterozoic rocks? Chemostratigraphic resolution of a biostratigraphic conundrum from the North China Platform. Precambrian Research, 84:197–220.

XIAO, S., X. YUAN, M. STEINER AND A. H. KNOLL. 2002. Macroscopic carbonaceous compressions in a terminal Proterozoic shale: a systematic reassessment of the Miaohe biota, South China. Journal of Paleontology, 76:347–376.

YAKSHCHIN, M. S. AND V. A. LUCHININA. 1981. Novye Dannye po iskopaemym vodorosliam semeistva Oscillatoriaceae (Kirchn.) Elenkin. p. 28–34 *In* Meshkova and Nikolaeva (eds.), Pogranichnye otlozhenyia Dokembryia i Kembryia Cibirskoi platformi (biostratigrafiya, paleontologia, usloviya obrazovaniya, Nauka. Novosibirsk.

YAN, Y-Z. AND Z-L. LIU. 1993. Significane of eucaryotic organisms in the microfossil flora of Changcheng System. Acta Micropalaeontologica Sinica, 10:167–180.

YIN, L-M. 1997. Acanthomorohic acritarchs form the Meso-Neoproterozoic shales of the Ruyang Group, Shanxi, China. Review of Palaeobotany and Palynology.

YIN, L-M. AND SUN, W-G. 1994. Microbiota from the Neoproterozoic Liulaobei Formation in the Huainan region, northern Anhui, China. Precambrian Research, 65:95–114.

YUAN, X. AND H. J. HOFMANN. 1998. New microfossils from the Neoproterozoic (Sinian) Doushantuo Formation, Wengan, Guizhou Province, southwestern China. Alcheringa, 22:189–222.

ZANG, W-L. 1995. Early Neoproterozoic sequence stratigraphy and acritarch biostratigraphy, eastern Officer Basin, South Australia. Precambrian Research, 74:119–175.

ZANG, W-L. AND D. M. MCKIRDY. 1994. Microfossils and molecular fossils from the Neoproterozoic Alinya Formation– a possible new source rock in the eastern Officer Basin. PESA Journal, 22:89–90.

ZANG, W-L. AND M. R. WALTER. 1992. Late Proterozoic and early Cambrian microfossils and biostratigraphy, northern Anhui and Jiangsu, central-eastern China. Precambrian Research, 57:243–323.

ZIMMER, A., D. LANG, S. RICHARDT, W. FRANK, R. RESKI AND S. RENSING. 2007. Dating the early evolution of plants: detection and molecular clock analyses of orthologs. Molecular Genetics and Genomics, 278:393–402.

FIGURE CAPTIONS

FIGURE 1.—Stratigraphic column of Alinya Fm. from Giles-1 drillcore and fossil occurrences by sample depth; dot on map indicates location of drillcore within Officer Basin. Amadeus Basin is seen to the North and Adelaide Rift Complex (ARC) to the East.

FIGURE 2.—Abundance, taxonomic diversity and standardized diversity of upper Alinya Formation of Giles-1. Y-axis sample depth; lower X-axis number of taxa (sample diversity and standardized diversity); upper X-axis number of specimens recorded

(abundance). Standardized diversity reflects taxonomic diversity of subsamples consisting of the first twenty specimens recorded in light microscopy of strewn slides.

FIGURE 3.—Sequence of taphonomic degradation of *Culcitulisphaera revelata (1-5).* Note pillow-like elements of *C. revelata* (*1*) become progressively sunken (*2-4*), in parts of *5* the top layer of the pillow element is sheared away. Scale bar is 10 μm. Sample depths: *1, 3, 4*—1265.57 m*; 5*—1265.46 m. Slide/stub and coordinates: *1*–1265.57-1_17BigStubA (P49534); *2*–1265.46-Feb6/on top of other fossils, unavailable (P49497); *3*–1265.57-1_17BigStubA (P49535); *4*–1265.57-4_15/N45-2 (P49549); *5*–1265.46-2_28B/O50-2 (P49502).

FIGURE 4.— Transmitted light and scanning electron microscope images of *L. laufeldii* and *C. revelata* specimens; *1–3* are same specimen of *L. laufeldii*, *4–6* are same specimen of *C. revelata.* Images *1*, *4*– transmitted light microscope images; *2, 3, 5, 6*– SEM images. Samples from 1265.46 m. Scale bar below *1* is 50 μm for *1, 2*, *4* and *5*. Scale bars associated with *3* and *6* are 10 μm. Slide and coordinates: *1–3*—1265.46-Feb6/E29-0 (P49498); *4–6*—1265.46-2_28B/AA55-4 (P49503).

FIGURE 5.— *1–5 Karenagare alinyaensis*, *4* is holotype; 6–*7 Caelatimurus foveolatus*, *6* is holotype; *8–13 Sulcatisphaera simiipugnus, 12* is holotype. Note that on *2* and *3*,

striations are visible on only a portion of vesicle; possible outer vesicle visible on *1*; ridges suggestive of external ornamentation visible on the lower-most portions of 4*;* images *1–7* and *11–13* are from transmitted light microscopy and *8–10* are SEM; scale bar below *3* is 50 µm for *1-6* and *7*; and is 25 µm for *6a* and *8–13*. Sample depths: *1, 3, 4, 8*—1265.46m; *2, 5–7, 9–13*—1265.57m. Slide and coordinates: *1*–1265.46-18B/M28-2 (P49491); *2*–1265.57-19A/N38-1 (P49506); *3*–1265.46-18B/W31-0 (P49492); *4*–1265.46-18B/H18-3 (P49493); *5*–1265.57-19A/Y40-2 (P49507); *6*–1265.57-19A/G27-2 (P49508); *7*–1265.57-19A/L16-4 (P49509); *8*–1265.46-2_28B (P49504); *9*–1265.57-March8StubA (P49545); *10*–1265.57-March20_epoxyA (P49546); *11*–1265.57-19A/H38-2 (P49510); *12*–1265.57-19A/M40-0 (P49511); *13*–1265.57-19A/M15-4 (P49512).

FIGURE 6.— *1*, *2* ?*Coneosphaera arctica*; *3*, *4 Vidalopalla verrucata*; *5 Leiosphaeridia crassa*; *6 Leiosphaeridia minutissima*; *7 Leiosphaeridia jacutica*; *8, 9 Navifusa majensis; 10 Leiosphaeridia tenuissima. 4a* shows detail of *4. 8a* shows transverse annulations of *8.* Scale bar is 50 µm for *1-10*, 10 µm for *4a* and 25 µm for *8a*. Sample depths: *1*, *2*–1255.43 m; *3–5* and *7*, *8*–1265.57 m; *6*–1237.74 m; *9*–1266.31 m; *10*–1265.46 m. Slide and coordinates: *1*–1255.43-15A/E25-1 (P49477); *2*–1255.43-15B/L30-4 (P49479); *3*–1265.57-19A/H32-1 (P49513); *4*–1265.57- LittleStubB (P49540); *5*–1265.57-19A/T40-2 (P49514); *6*–1237.74-12/J34-1(P49464); *7*–1265.57- 19A/M43-0 (P49515); *8*–1265.57-19A/T28-3 (P49516); *9*–1266.31-20/P35-0 (P49556); *10*–1265.46-18A/N17-0 (P49486).

FIGURE 7.—*1 Valeria lophostriata; 2–4* "*C*" *tonium; 5* Unnamed Acritarch sp. A; *6* Unnamed Acritarch sp. B; *7–9* cf. "*Tappania*"; *10* Unnamed Acritarch sp. C. Black scale bar below *1* is 50 µm for *1–7* and is 25µm for *8, 9* and *10*. White bar is 10µm for *8a, 8b, 10a.* Sample depths: *1, 3, 9, 10*—1265.57m, *2, 4, 7*—1255.76m, *5*—1242.84m, *6*—1255.43m, *8*—1265.46m. Slide and coordinates: *1*–1265.57-19A/L38-0 (P49517); *2*–1255.76-16B/G22-1 (P49484); *3*–1265.57-19A/L18-3 (P49518); *4*–1255.76-16B/M34-3 (P49485); *5*–1242.84-13A/L16-1 (P49467); *6*–1255.43-15A/Q20-1 (P49478); *7*–1255.76-16A/T13-0 (P49482); *8*–1265.46-Feb6/on top of other fossils, unavailable (P49499); *9*–1265.57-1_29BigStubB (P49538)*, 10*–1265.57-1_29BigStubB (P49539).

FIGURE 8.— *C. revelata; 1–5* transmitted light images, *6–8* Scanning electron microscope images; 1 is holotype; black scale bar is 50µm for all except *6a, 7a, 8a.* White scale bar is 5 µm for *6a* and 10 µm for *7a, 8a* and *8b.* Sample depths: *1, 6, 7* —1265.57m; *2–5, 8*—1265.46m. Slide and coordinates: *1*–1265.57-19A/N24-1 (P49519); *2*–1265.26-18B/S34-2 (P49494); *3*–1265.46-18A/L38-3 (P49487); *4*–1265.46-18B/G30-3 (P49495); *5*–1265.46-18A/L26-2 (P49488); *6*–1265.57- LittleStubB (P49541); *7*–1265.57-1_17BigStubA (P49534); *8*–1265.46-Feb6/Z34-0 (P49500).

FIGURE 9.—FIB-EM sectioning of *C. revelata.* All images of same specimen. *2*–platinum coating and nearby fiducial marker applied to fossil before FIB sectioning. *3*–fossil after sectioning complete. *4*, *5*–acritarch wall with nanopores. Scale bars 20 µm for *1* and *3*; 5 µm for *2*; 2 µm for *4* and *5*. Stub: 1265.57 March20_epoxyA (P49547).

FIGURE 10.—*1–6 M. officerensis, 1* is holotype; *7, 8 L. laufeldii; 7a* close-up on nano-scale mammillary ornament upon vesicle; *8a* close-up on anastomosing filaments beneath outer envelope (absent from this specimen)*;* The black bar beneath *1* is 50 µm for *1–4*; the white bar beneath *5a* is 20 µm for *5, 6, 7, 8;* it is 10 µm for *5a*; it is 5 µm for *6a, 7a, 8a;* Sample depths: *1, 3, 5, 6, 7*—1265.57m; *2, 8*—1265.46 m; *4*—1265.71 m. Slide and coordinates: *1*–1265.57-19A/V32-4 (P49520); *2*–1265.46-18B/N19-1 (P49496); *3*–1265.57-19A/S38-0 (P49521); *4*–1265.71-105A/U27-2 (P49550); *5*–1265.57-LittleStubB (P49542)*, 7*–1265.57-LittleStubB (P49543); *6*–1265.57-LittleStubA (P49536); *8*–1265.46-Feb6/missing after epoxy (P49501).

FIGURE 11.—Vesicle detail of *L. laufeldii*; *1*–detail of inset in *3; 2*– detail of inset in *4;* Note nano-scale mammillary ornamentation. The black scale bar is 10 µm for *1* and *2*; the white bar is 20 µm for *3* and *4.* Sample depths: *1, 3*—1265.57m, *2, 4*—1265.46m. Slide/Stub and coordinates: *1, 3*–1265.57-1_29LittleStubA (P49537); *2, 4*–1265.46-Feb6/E29-0 (P49498).

FIGURE 12.—*1, 2, 3, 11 Leiosphaeridia* sp. B; note the darkened spot in *2* has a tear in the lower left quadrant, through which the back side of the sphaerical vesicle is visible; in *3* the cell has torn across the darkened spot; *4, 5* and *9 Leiosphaeridia* sp. A; *6–8, 10, 12–16 Synsphaeridium* spp. *6* and *7* are the same specimen imaged by SEM and transmitted light microscopy, respectively; note opaque spots in *7* are visible as raised knobs in *6; 10* illustrates variation of cell packing, ranging from a polygonal close-packing at the top-left to loose-pack habit at the right. Scale Bar 50µm. Sample depths: *1, 13, 14*—1265.71 m; *2*, *11*—1244.17 m; *3*—1237.74 m; *4, 5*, *9, 10, 15, 16*—1265.57 m; *6, 7*—1265.46 m; *8*—1266.31 m; 12—1255.43 m. Slide/Stub and coordinates: *1*–1265.71-105A/R16-3 (P49551); *2*–1244.17-14B/S30-3 (P49469); *3*–1237.74-12/E27-2 (P49465); *4*–1265.57-19A/M21-3 (P49522); *5*–1265.57-19A/L17-3 (P49523); *6, 7*–1265.46-2_28B/W53-0 (P49505); *8*–1266.31-20/U35-0(P49557); *9*–1265.57-19A/R23-1 (P49524); *10*–1265.57-19A/O19-4 (P49525); *11*–1244.17-14B/P17-3 (P49470); *12*–1255.43-15B/J19-4 (P49480); *13*–1265.71-105A/J26-2 (P49552); *14*–1265.71-105A/S34-2 (P49553); *15*–1265.57- March20_epoxyA (P49548); *16*–1265.57- LittleStubB (P49544).

FIGURE 13.—*Leiosphaeridia* sp. B vesicle diameter as compared with diameter of spot and histogram of vesicle diameters. Upper panel illustrates the linear relationship between diameters of vesicle and of spot upon vesicle.

FIGURE 14.— *1–5 Simia annulare*, note tears extending from equatorial flap into central portion in *3* and *5*; *6–9 Pterospermopsimorpha insolita*, note wrinkles and folds in outer vesicle in *6* and *9* and tears in outer vesicle in *7–9*. Scale Bar 50µm. Sample depths: *1–6* —1244.17 m; *7*— 1237.74 m; *8–9* —1265.71 m. Slide and coordinates: *1*–1244.17-14B/F16-1 (P49471); *2*–1244.17-14B/N36-2 (P49472); *3*–1244.17-14B/O34-0 (P49473); *4*–1244.17-14B/E31-0 (P49474); *5*–1244.17-14A/H22-0 (P49468); *6*–1244.17-14B/N36-2 (P49475); *7*–1237.74-12/O25-3 (P49466); *8*–1265.71-105A/Q38-3 (P49554); *9*–1265.71-105A/P11-2 (P49555).

FIGURE 15.— Filamentous microfossils; *1, 2–Obruchevella parva; 3–Siphonophycus typicum; 4–S. typicum* and *Polythricoides lineatus; 5–P. lineatus; 6–S. septatum; 7–Cyanonema* sp.; *8–S. typicum; 9– P. lineatus; 10–Rugosoopsis tenuis; 11–S. robustum; 12–S. kestron; 13, 14–R. tenuis; 15–S. solidum*. Scale Bar 50µm. Sample depths: *1, 2, 4, 6, 9, 10, 13, 14*–1265.57 m, *3, 7*–1244.17 m; *5*–1266.31 m; *8*– 1255.76 m; *11*– 1255.43 m, *12, 15*–1265.46 m. Slide and coordinates: *1*–1265.57-19A/O30-2 (P49526); *2*–1265.57-19A/L24-3 (P49527); *3*–1244.17-14B/T35-3 (P49476); *4*–1265.57-19A/O35-3 (P49528); *5*–1266.31-20/V33-0 (P49558); *6*–1265.57-19A/M41-2 (P49529); *7*–1244.17-14B/T35-3 (P49476); *8*–1255.76-16A/J35-3 (P49483); *9*–1265.57-19A/H22-3 (P49530); *10*–1265.57-19A/O20-2 (P49531); *11*–1255.43-15B/S18-0 (P49481); *12*–1265.46-18A/M38-0 (P49489);

13–1265.57-19A/J37-2 (P49532); *14*–1265.57-19A/L42-3 (P49533); *15*–1265.46-18A/Q38-1 (P49490).

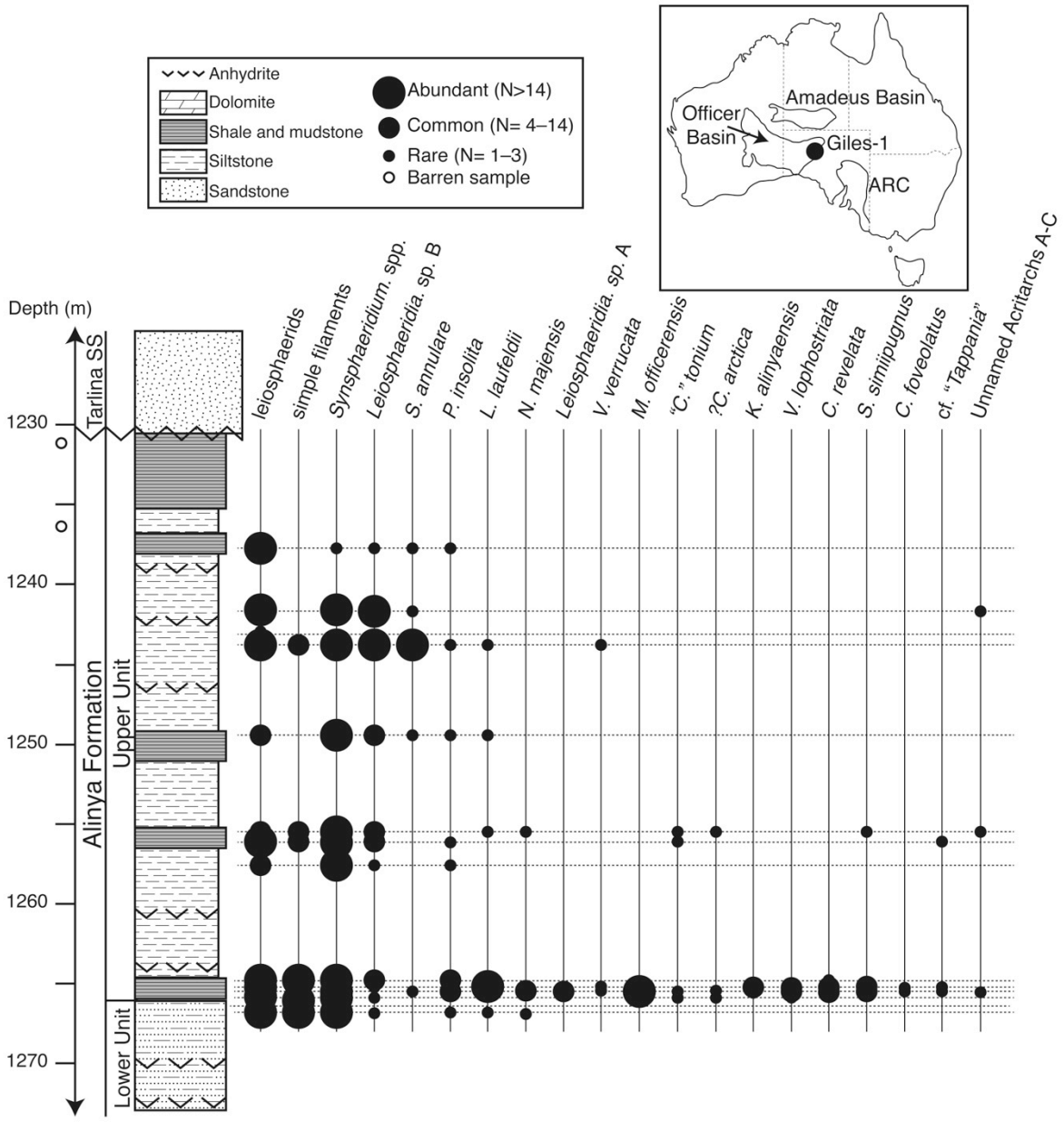

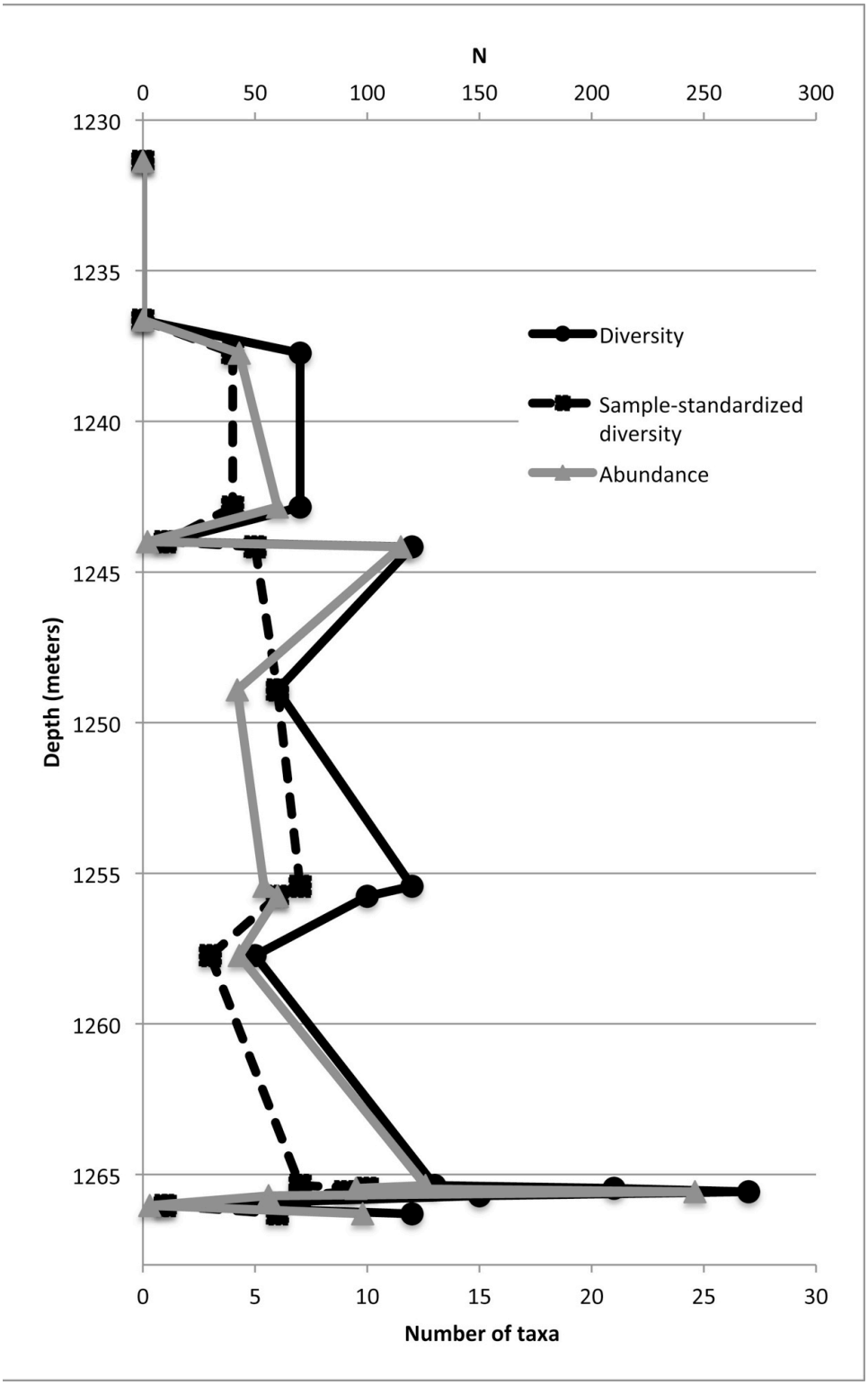
N
0
50
100
150
200
250
300
1230
1235
1240
1245
1250
1255
1260
1265
Depth (meters)
Diversity
Sample-standardized diversity
Abundance
0
5
10
15
20
25
30
Number of taxa

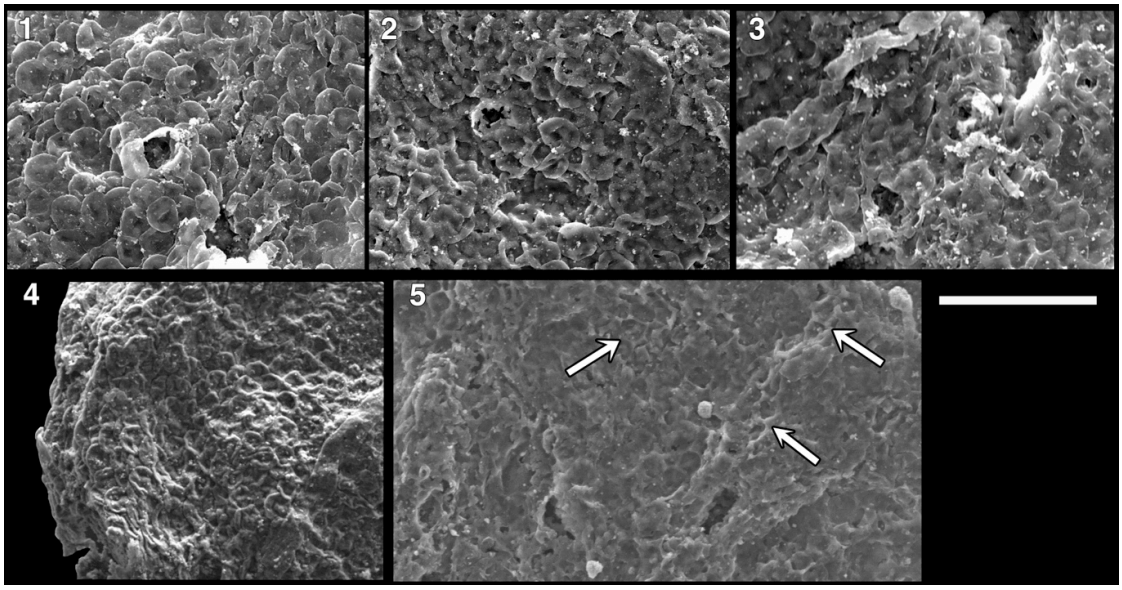
1
2
3
4
5

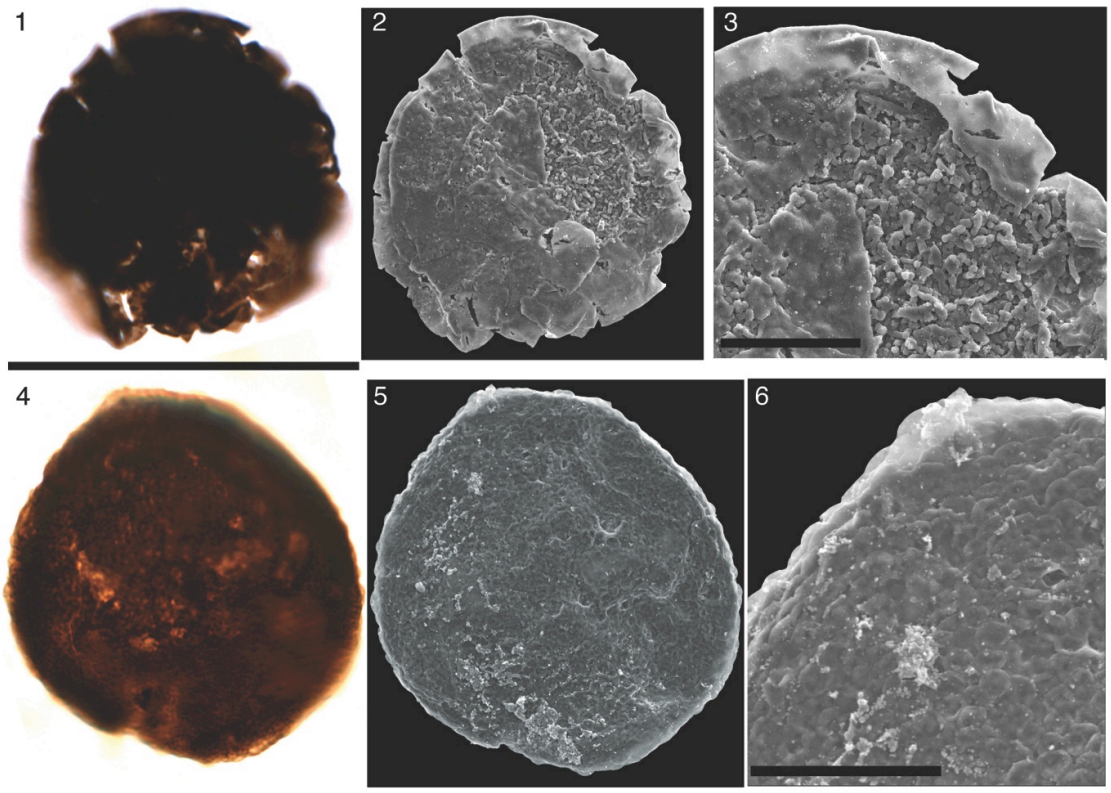
1
2
3
4
5
6

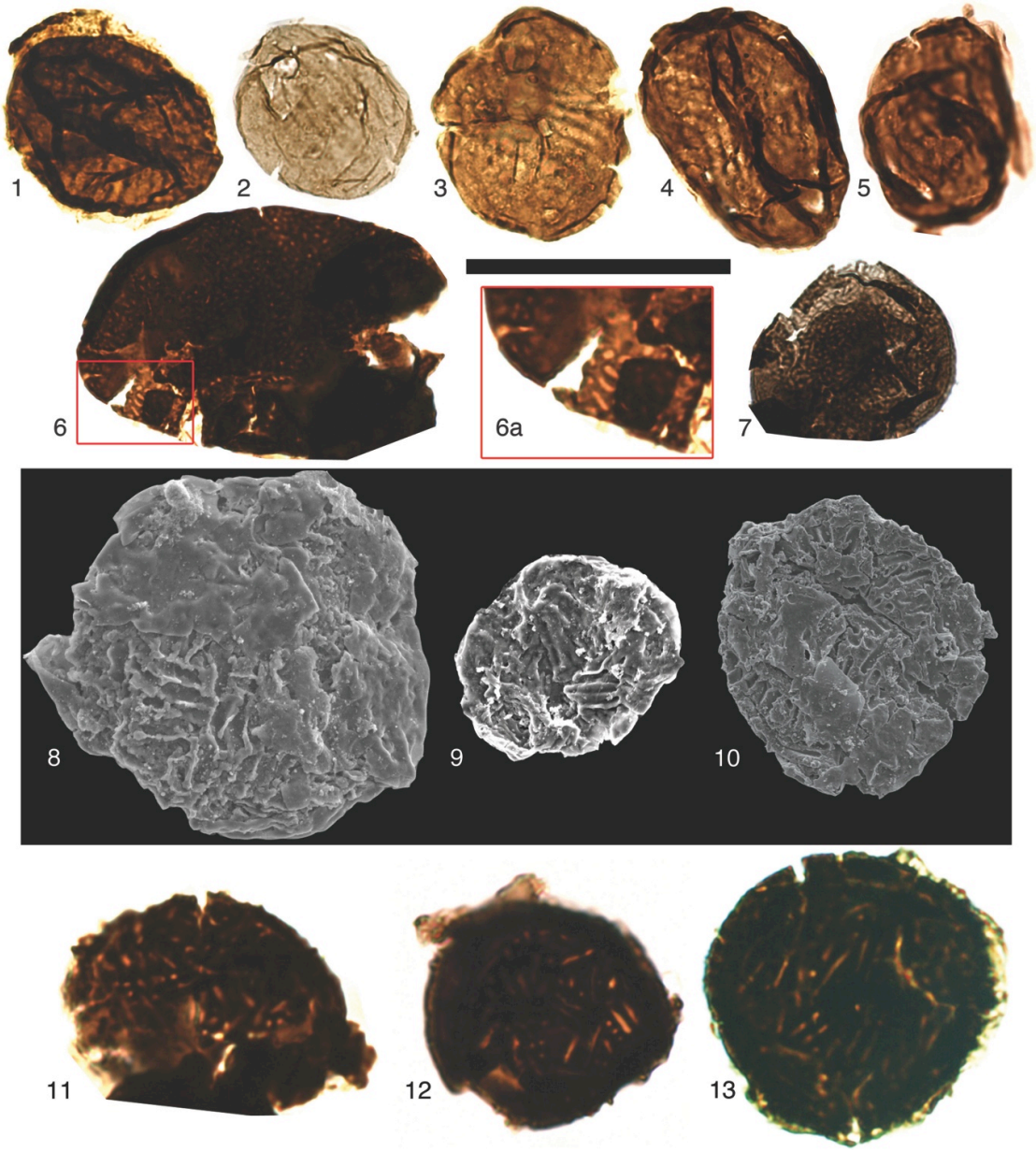
1
2
3
4
5
6
6a
7
8
9
10
11
12
13

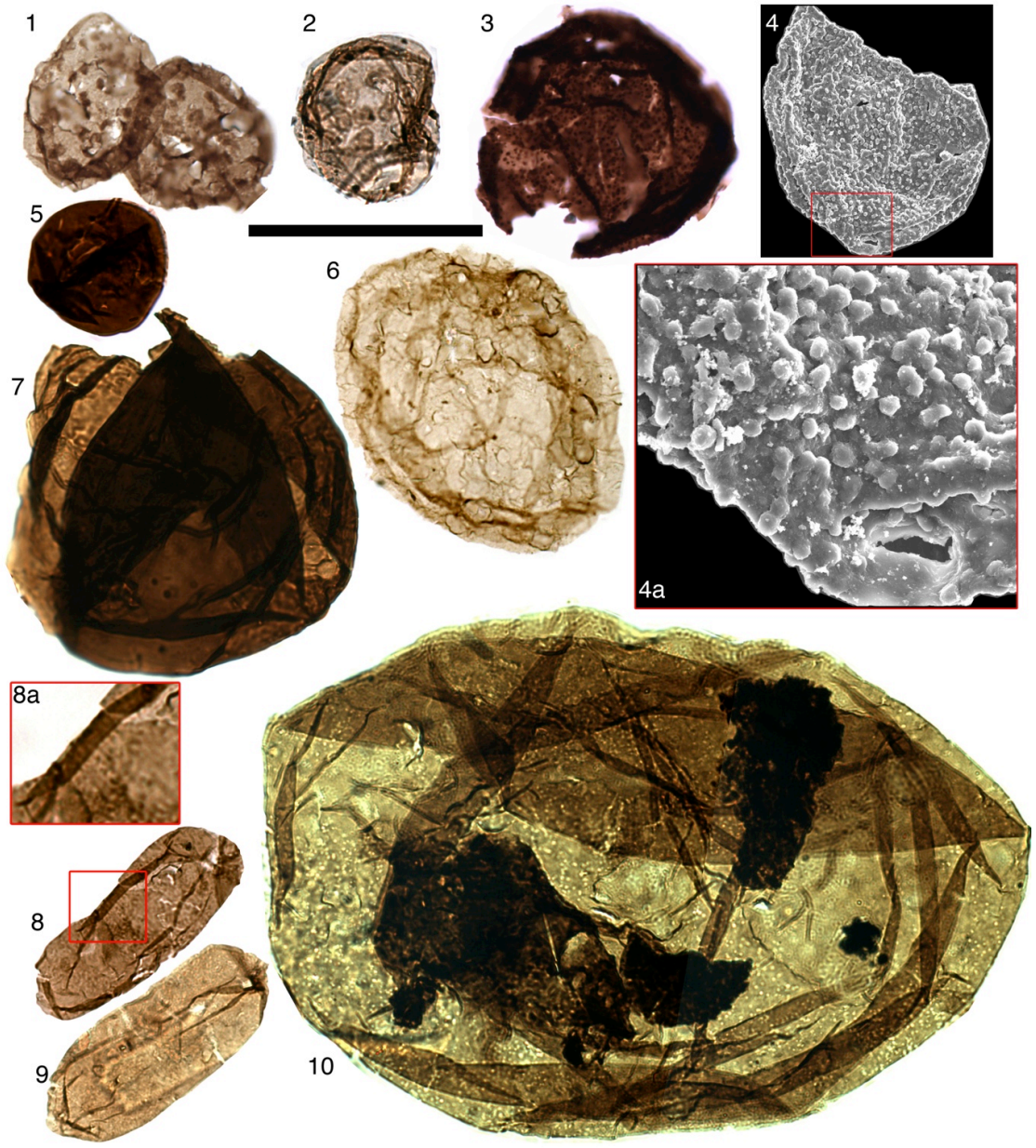
1
2
3
4
5
6
7
4a
8a
8
9
10

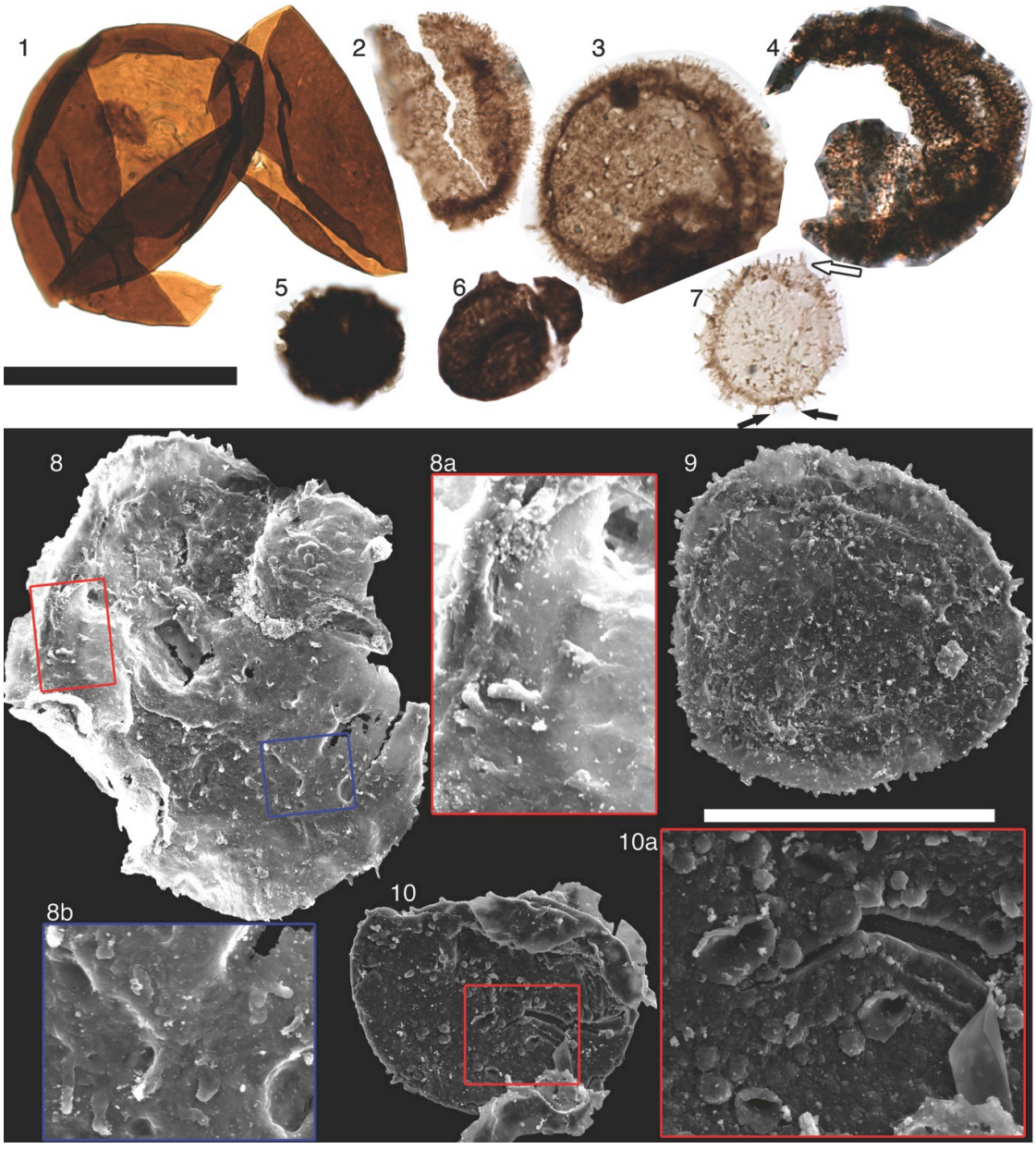
1
2
3
4
5
6
7
8
8a
9
10a
8b
10

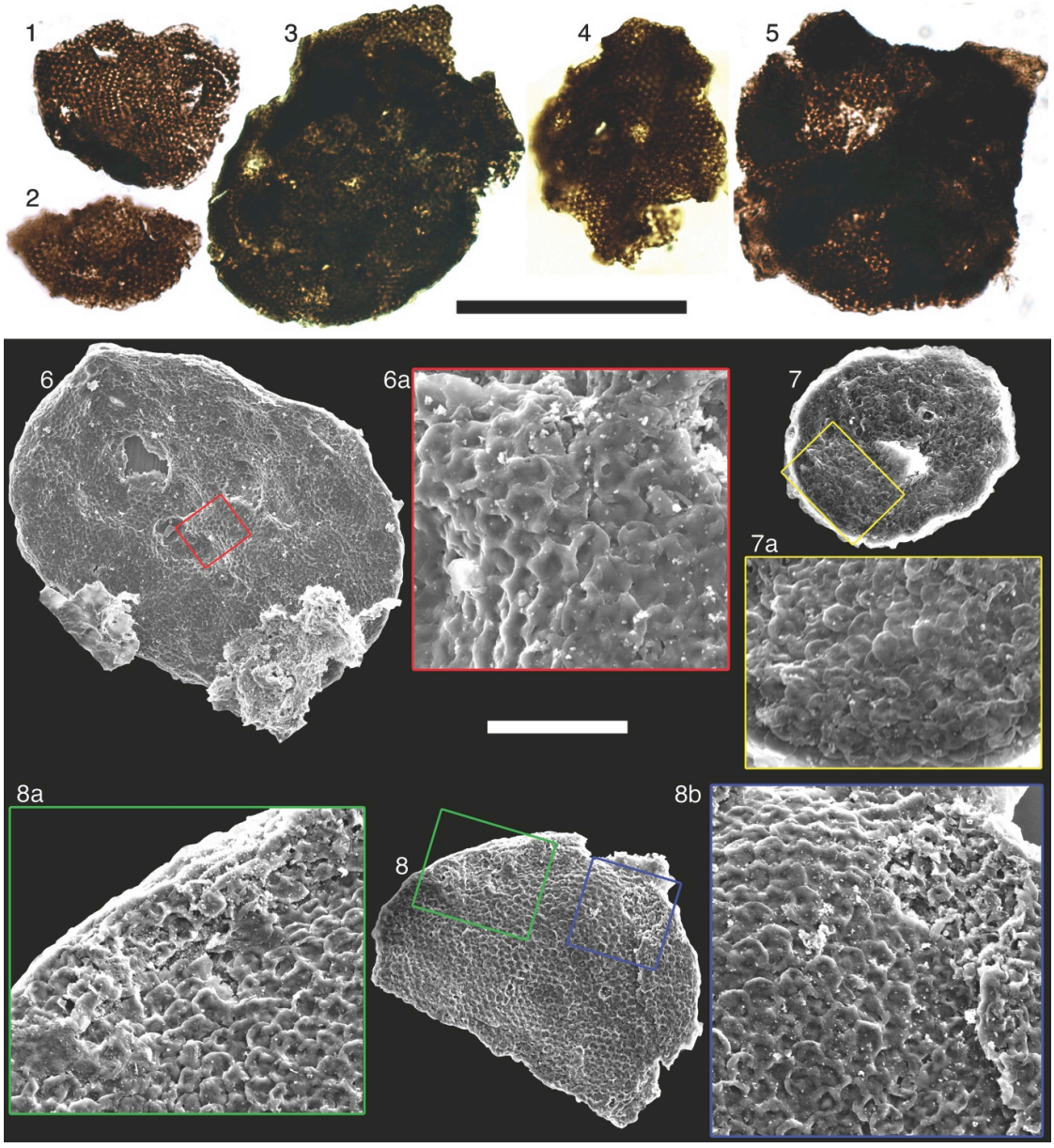
1
2
3
4
5
6
6a
7
7a
8a
8
8b

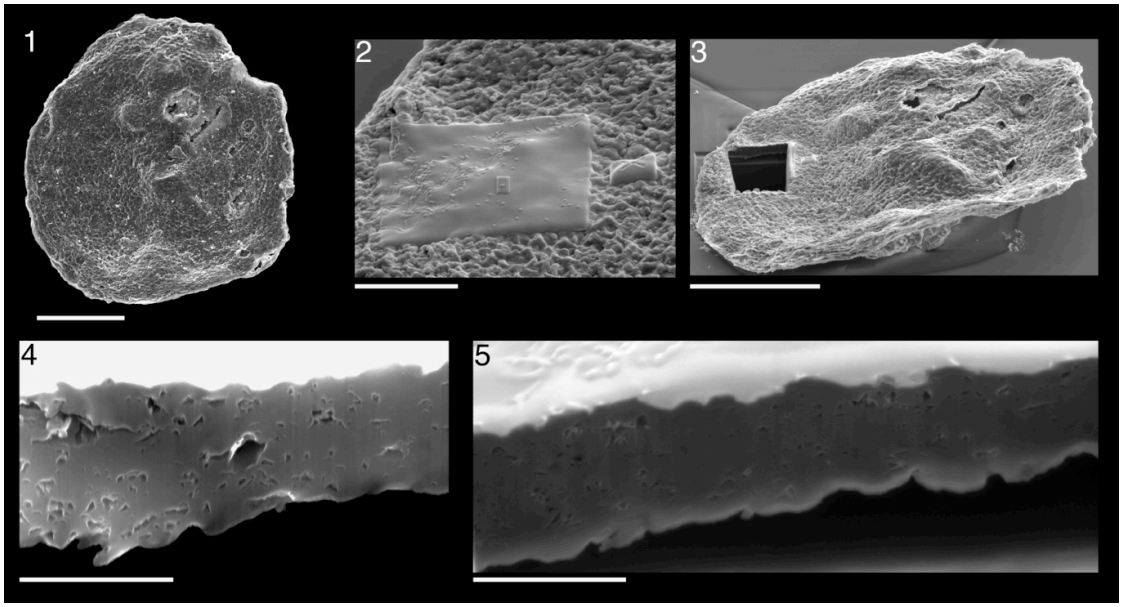
1
2
3
4
5

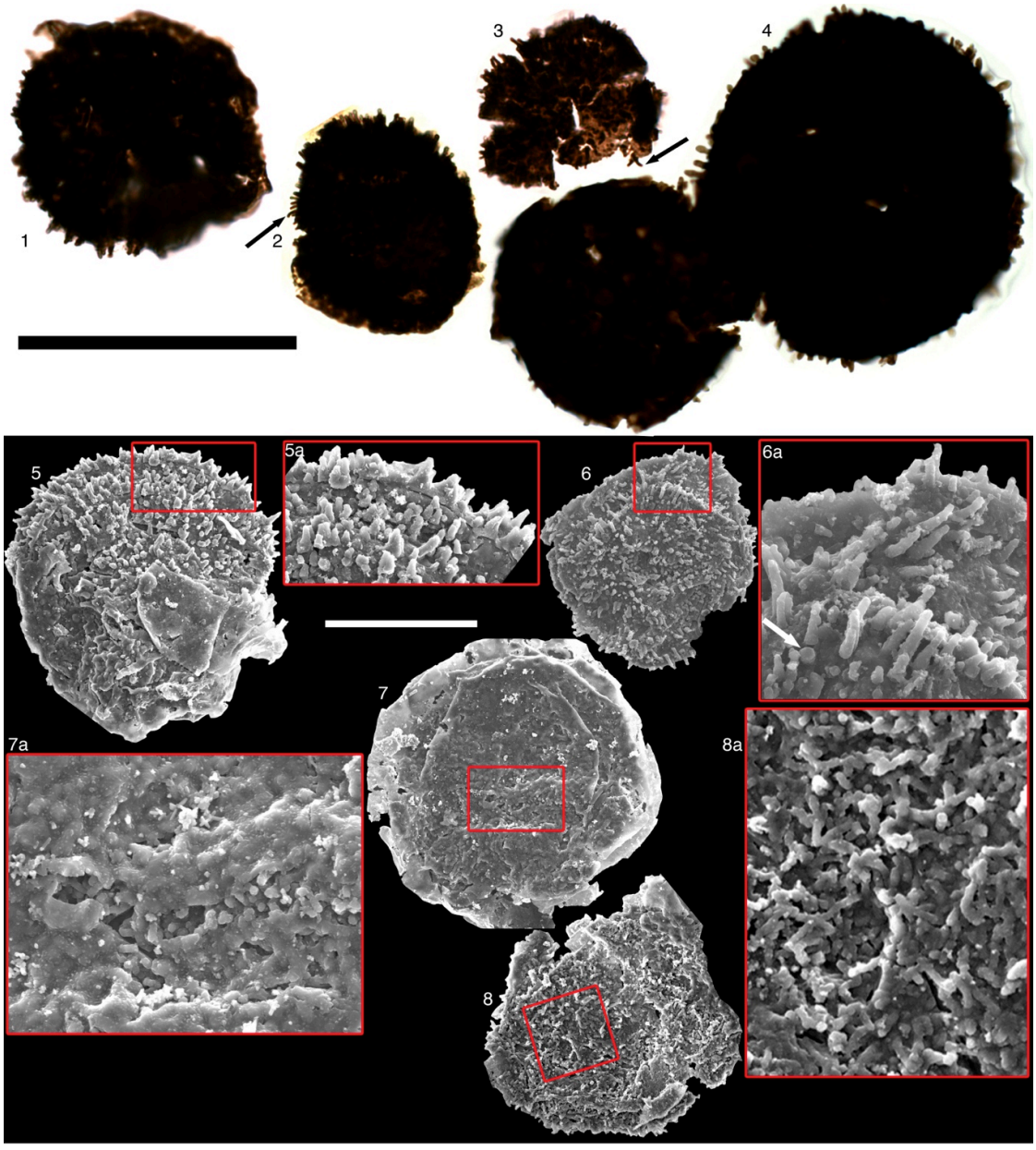
1
2
3
4
5
5a
6
6a
7
7a
8
8a

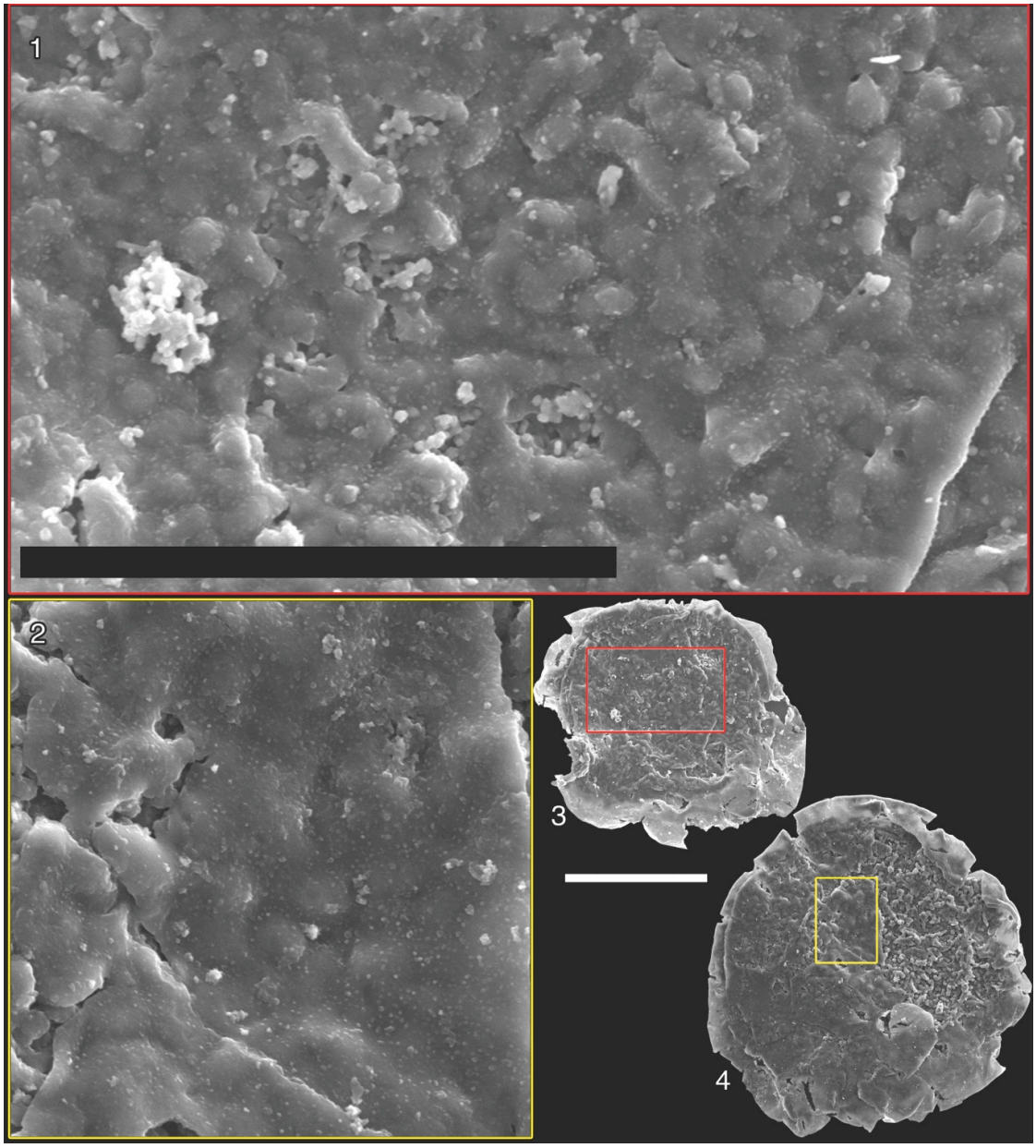
1
2
3
4

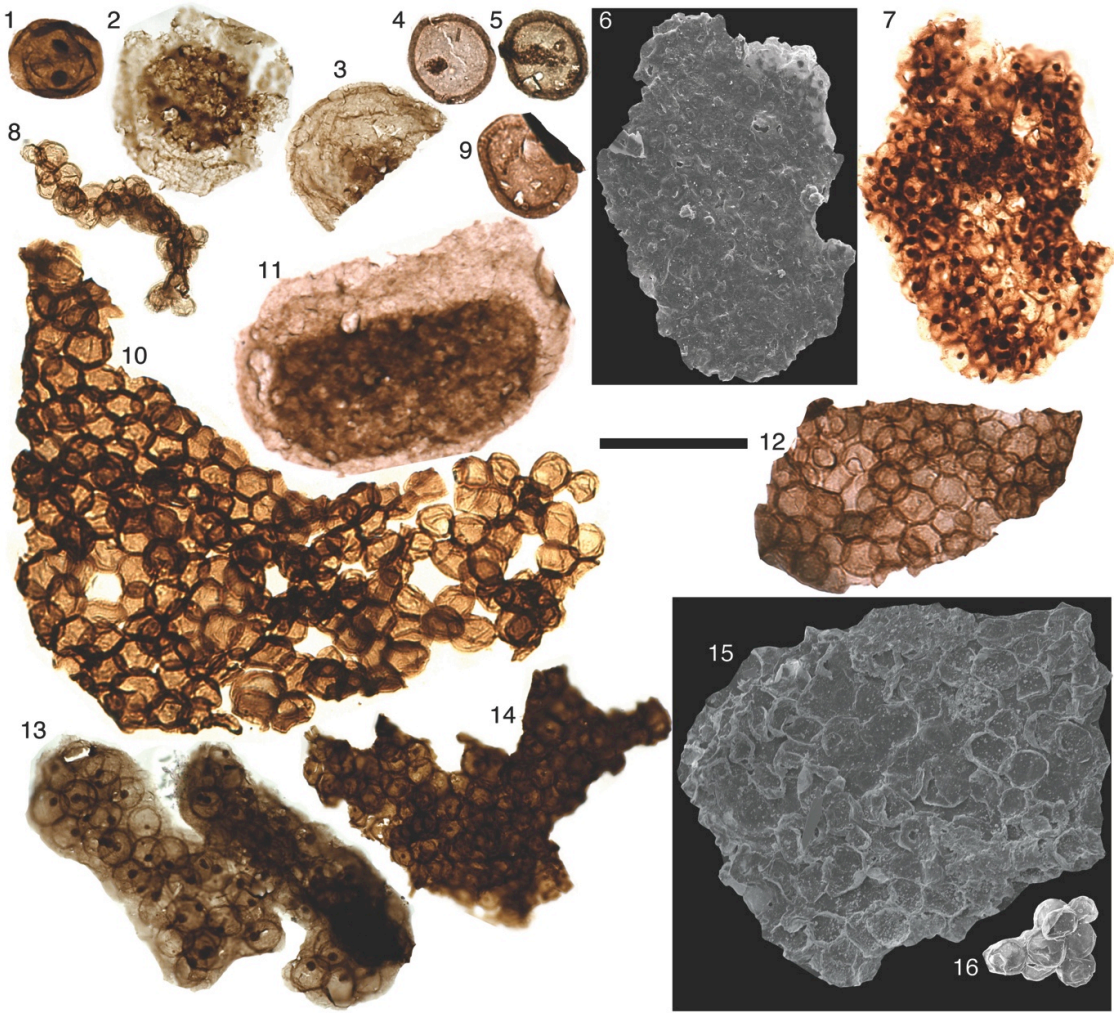
1
2
3
4
5
6
7
8
9
10
11
12
13
14
15
16

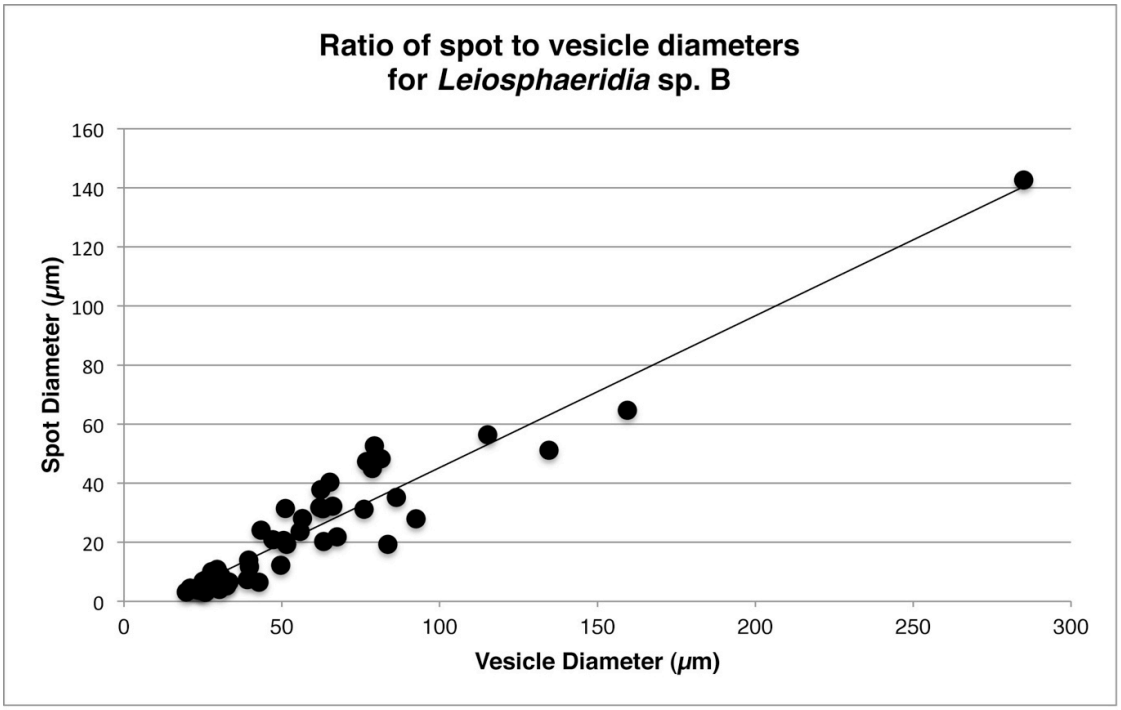
Ratio of spot to vesicle diameters
for Leiosphaeridia sp. B
Spot Diameter (μm)
Vesicle Diameter (μm)
0
20
40
60
80
100
120
140
160
0
50
100
150
200
250
300

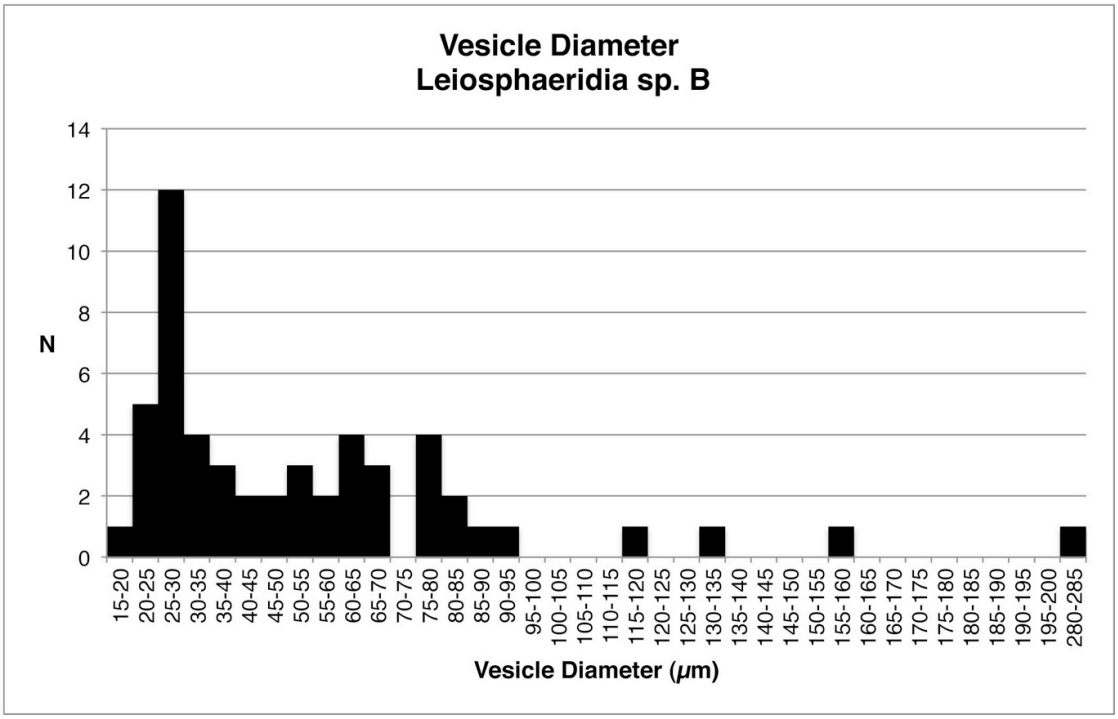
Vesicle Diameter
Leiosphaeridia sp. B
N
Vesicle Diameter (μm)
0
2
4
6
8
10
12
14
15-20
20-25
25-30
30-35
35-40
40-45
45-50
50-55
55-60
60-65
65-70
70-75
75-80
80-85
85-90
90-95
95-100
100-105
105-110
110-115
115-120
120-125
125-130
130-135
135-140
140-145
145-150
150-155
155-160
160-165
165-170
170-175
175-180
180-185
185-190
190-195
195-200
280-285

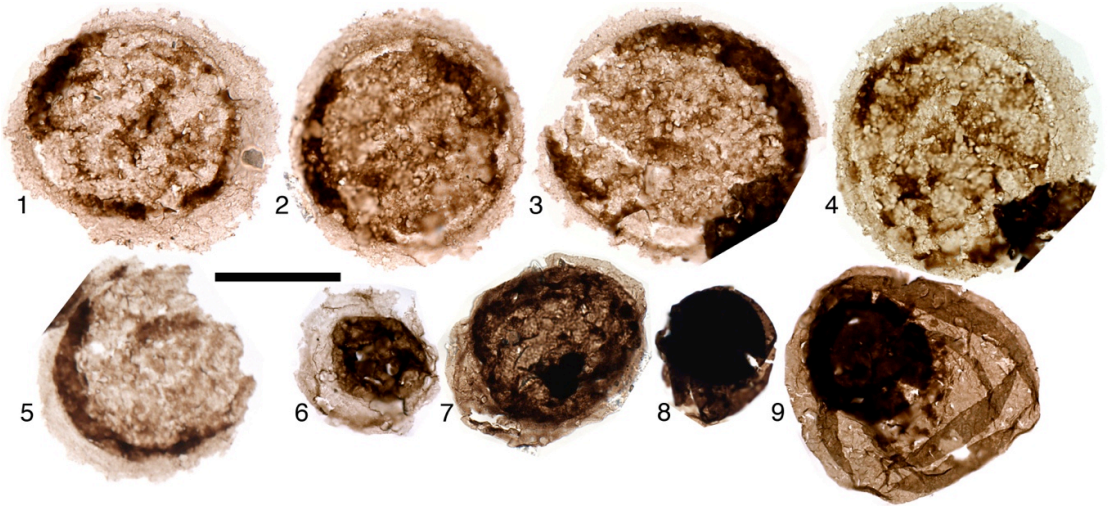
1
2
3
4
5
6
7
8
9


1
2
3
4
5
6
7
8
9
10
11
12
13
14
15

meterage*	lithological notes	barren	N	*Caelatimurus foveolatus*	*?Coneosphaera arctica*	*"Comasphaeridium" tonium*	*Culcitulisphaera revelata*	*Karenaggare alinyaensis*	*Lanulatisphaera laufeldii*	*Leiosphaeridia. sp.*	*L. crassa*	*L. jacutica*	*L. minutissima*	*L. tenuissima*	*Leiosphaeridia sp. A*	*Leiosphaeridia sp. B*	*Morgensternia officerensis*	*Nawfusa majensis*	*Pterospermopsimorpha insolita*	*Simia annulare*	*Sulcatisphaera similpugnus*	*cf. "Trappania"*	*Valeria lophostriata*	*Vidalopalla verrucata*	unnamed Acritarch sp. A	unnamed Acritarch sp. B	unnamed Acritarch sp. C	*Synsphaeridium* spp. (# of colonies)	*Cyanonema sp.*	*Obruchevella parva*	*Polythrichoides lineatus*	*Rugosoopsis tenuis*	*Siphonophycus spp.*
1231.37	green and red laminated claystone	x	**0**																														
1236.64	greenish interbedded with tan-white claystone layers	x	**0**																														
1237.74	Black-green to grey laminated		**43**								15		20	1		2			1	2								2					
1242.84	black, more massive mudstone		**60**								8	3	5			17				3					1			23					
1244	grey-black <1mm laminations; undulating/pinched out		**2**										1															1					
1244.17	grey-black <1mm laminations; undulating/pinched out		**115**								15	5	8	1		10			3	36				1				29	1				6
1248.91	fine, dark grey mm-scale laminations		**42**								6	3				5			2	1								25					
1255.43	greyish-black laminated		**54**		3	1				3	4	1				5		1			4					1		26					5
1255.76	grey siltstone		**60**			3					1	4	13	2		4			2			1						20					10
1257.73	Green-white laminated		**43**								5		8			1			1									28					
1265.36	black laminated; somewhat fissile		**126**				3				29	2	10	6		9			11									30					26
1265.46	black laminated; somewhat fissile		**95**	1			14	8	11		10	6	4	2	2	3	9				2	1	4	1				8			1	1	7
1265.57	black laminated		**246**	2	1	2	10	2	10		44	12	13	3	5		26	7	12	2	9	1	9	2			1	21		5	7	14	26
1265.71	black laminated		**56**		1	1					3		2	2		5	2		3				1					28			1	2	5
1266.03	green		**3**																									3					
1266.31	grey-green, laminated		**98**								27		16			1		1	2									32			2	6	11
	Totals		**1043**	**3**	**5**	**7**	**27**	**10**	**21**	**3**	**167**	**36**	**100**	**17**	**7**	**62**	**37**	**9**	**37**	**44**	**15**	**3**	**14**	**4**	**1**	**1**	**1**	**276**	**1**	**5**	**11**	**23**	**96**
*sample is 0.10 m up-core, beginning with noted depth																																	

Figure	SAM accession numbers	Taxon	depth	slide or stub	England finder coordinates
3.1, 8.7	P49534	*C. revelata*	1265.56	1_17 big stub A	stub
3.2	P49497	*C. revelata*	1265.46	Feb6-glass	on top of other fossils, unavailable in transmitted light
3.3	P49535	*C. revelata*	1265.56	1_17 big stub A	stub
3.4	P49549	*C. revelata*	1265.56	glass 4_15	N45-2
3.5	P49502	*C. revelata*	1265.46	glass 2_28B	O50-2
4.1-4.3, 11.2, 11.4	P49498	*L. laufeldii*	1265.46	Feb6-glass	E29-0
4.4-4.6	P49503	*C. revelata*	1265.46	glass 2_28B	AA55-4
5.1	P49491	*K. alinyaensis*	1265.46	18B	M28-2
5.2	P49506	*K. alinyaensis*	1265.56	19A	N38-1
5.3	P49492	*K. alinyaensis*	1265.46	18B	W31-0
*5.4	P49493	*K. alinyaensis*	1265.46	18B	H18-3
5.5	P49507	*K. alinyaensis*	1265.56	19A	Y40-2
*5.6	P49508	*C. foveolatus*	1265.56	19A	G27-2
5.7	P49509	*C. foveolatus*	1265.56	19A	L16-4
5.8	P49504	*S. simiipugnus*	1265.46	glass 2_28B	on top of other fossils, unavailable in transmitted light
5.9	P49545	*S. simiipugnus*	1265.56	march8stub A	stub
5.10	P49546	*S. simiipugnus*	1265.56	march20_epoxyA	stub
5.11	P49510	*S. simiipugnus*	1265.56	19A	H38-2
*5.12	P49511	*S. simiipugnus*	1265.56	19A	M40-0
5.13	P49512	*S. simiipugnus*	1265.56	19A	M15-4
6.1	P49477	*?C. arctica*	1255.43	15A	E25-1
6.2	P49479	*?C. arctica*	1255.43	15B	L30-4
6.3	P49513	*V. verrucata*	1265.57	19A	H32-1
6.4	P49540	*V. verrucata*	1265.57	Jan 28 little B	stub
6.5	P49514	*L. crassa*	1265.57	19A	T40-2
6.6	P49464	*L. minutissima*	1237.74	12	J34-1
6.7	P49515	*L. jacutica*	1265.57	19A	M43-0
6.8	P49516	*Navifusa majensis*	1265.57	19A	T28-3
6.9	P49556	*Navifusa majensis*	1266.31	20	P35-0
6.10	P49486	*L. tenuissima*	1265.46	18A	N17-0
7.1	P49517	*Valeria lophostriata*	1265.57	19A	L38-0
7.2	P49484	*"C" tonium*	1255.76	16B	G22-1
7.3	P49518	*"C" tonium*	1265.56	19A	L18-3
7.4	P49485	*"C" tonium*	1255.76	16B	M34-3
7.5	P49467	Unnamed A	1242.84	13A	L16-1
7.6	P49478	Unnamed B	1255.43	15A	Q20-1
7.7	P49482	cf. *"Tappania"*	1255.76	16A	T13-0
7.8	P49499	cf. *"Tappania"*	1265.46	Feb6-glass	on top of other fossils, unavailable in transmitted light
7.9	P49538	cf. *"Tappania"*	1265.56	1_29 big stub B	stub
7.10	P49539	*Unnamed C*	1265.56	1_29 big stub B	stub
*8.1	P49519	*C. revelata*	1265.56	19A	N24-1
8.2	P49494	*C. revelata*	1265.46	18B	S34-2
8.3	P49487	*C. revelata*	1265.46	18A	L38-3
8.4	P49495	*C. revelata*	1265.46	18B	G30-3
8.5	P49488	*C. revelata*	1265.46	18A	L26-2
8.6	P49541	*C. revelata*	1265.56	little stub B	stub
8.8	P49500	*C. revelata*	1265.46	Feb6-glass	Z34-0
9	P49547	*C. revelata*	1265.57	march20_epoxyA	stub
*10.1	P49520	*M. officerensis*	1265.56	19A	V32-4
10.2	P49496	*M. officerensis*	1265.46	18B	N19-1
10.3	P49521	*M. officerensis*	1265.56	19A	S38-0
10.4	P49550	*M. officerensis*	1265.71	105A	U27-2
10.5	P49542	*M. officerensis*	1265.56	Jan28 littleB	stub
10.6	P49536	*M. officerensis*	1265.56	little A	stub
10.7	P49543	*L. laufeldii*	1265.56	little stub B	stub
10.8	P49501	*L. laufeldii*	1265.46	Feb6-glass	cannot be relocated after epoxy, specimen moved
11.1, 11.3	P49537	*L. laufeldii*	1265.57	little A	stub
12.1	P49551	*L.* sp. B	1265.71	105A	R16-3
12.2	P49469	*L.* sp. B	1244.17	14B	S30-3
12.3	P49465	*L.* sp. B	1237.74	12	E27-2
12.4	P49522	*L.* sp. A	1265.57	19A	M21-3
12.5	P49523	*L.* sp. A	1265.57	19A	L17-3
12.6, 12.7	P49505	*Synsphaeridium* sp.	1265.46	glass 2_28B	W53-0
12.8	P49557	*Synsphaeridium* sp.	1266.31	20	U35-0
12.9	P49524	*L.* sp. A	1265.57	19A	R23-1
12.10	P49525	*Synsphaeridium* sp.	1265.57	19A	O19-4
12.11	P49470	*L.* sp. B	1244.17	14B	P17-3
12.12	P49480	*Synsphaeridium* sp.	1255.43	15B	J19-4
12.13	P49552	*Synsphaeridium* sp.	1265.71	105A	J26-2

Figure	SAM accession numbers	Taxon	depth	slide or stub	England finder coordinates
12.14	P49553	*Synsphaeridium* sp.	1265.71	105A	S34-2
12.15	P49548	*Synsphaeridium* sp.	1265.57	march20_epoxyA	stub
12.16	P49544	*Synsphaeridium* sp.	1265.57	Jan 28 little B	stub
14.1	P49471	*Simia annulare*	1244.17	14B	F16-1
14.2	P49472	*Simia annulare*	1244.17	14B	N36-2
14.3	P49473	*Simia annulare*	1244.17	14B	O34-0
14.4	P49474	*Simia annulare*	1244.17	14B	E31-0
14.5	P49468	*Simia annulare*	1244.17	14A	H22-0
14.6	P49475	*P. insolita*	1244.17	14B	N36-2
14.7	P49466	*P. insolita*	1237.74	12	O25-3
14.8	P49554	*P. insolita*	1265.71	105A	Q38-3
14.9	P49555	*P. insolita*	1265.71	105A	P11-2
15.1	P49526	*O. parva*	1265.57	19A	O30-2
15.2	P49527	*O. parva*	1265.57	19A	L24-3
15.3, 15.7	P49476	15.3-*S. typicum*, 15.7-*Cyanonema* sp.	1244.17	14B	T35-3
15.4	P49528	*S. typicum* and *P. lineatus*	1265.57	19A	O35-3
15.5	P49558	*P. lineatus*	1266.31	20	V33-0
15.6	P49529	*S. septatum*	1265.57	19A	M41-2
15.8	P49483	*S. typicum*	1255.76	16A	J35-3
15.9	P49530	*P. lineatus*	1265.57	19A	H22-3
15.10	P49531	*R. tenuis*	1265.57	19A	O20-2
15.11	P49481	*S. robustum*	1255.43	15B	S18-0
15.12	P49489	*S. kestron*	1265.46	18A	M38-0
15.13	P49532	*R. tenuis*	1265.57	19A	J37-2
15.14	P49533	*R. tenuis*	1265.57	19A	L42-3
15.15	P49490	*S. solidum*	1265.46	18A	Q38-1
*Holotypes					
England Coordinates for slides with labels to the left except for Slide 1265.46 Feb-6 glass and 1265.46 2_28B					
Coordinates unavailable for specimens upon stubs					

Chapter Two: **Organic-walled microfossil assemblages from glacial and interglacial Neoproterozoic units of Australia and Svalbard**[2]

ABSTRACT

A growing body of evidence suggests that during the Neoproterozoic Era Earth experienced at least two glaciations of global extent. Before the onset of these "snowball Earth" events eukaryotes had begun diversifying, and in their aftermath, macroscopic life (including animals and macroalgae) became abundant and widespread. Although glacially driven mass extinctions have been hypothesized, little is known about the biosphere during and between these glaciations. Here we present new data from organic-walled microfossil assemblages from five successions in Australia and Svalbard that collectively span the first ("Sturtian") glaciation and interglacial interval and integrate them with data derived from a critical evaluation of the literature to produce a new estimate of eukaryotic diversity from 850–650 Ma. These new glacial and interglacial assemblages consist of only smooth-walled sphaeroids (leiosphaerids), aggregates of sphaeroids, and filaments, in contrast to the much more diverse organic-walled microfossil assemblages found in early Neoproterozoic (>740

[2] This chapter has been published as: Riedman, L. A., Porter, S. M., Halverson, G. P., Hurtgen, M. T., Junium, C. K., Organic-walled microfossil assemblages from glacial and interglacial Neoproterozoic units of Australia and Svalbard. *Geology* v. 42, pp. 1011–1014.

Ma) rocks. This contrast is not attributed to biases in depositional environment or preservation, but instead is interpreted as reflecting an interval of lowered eukaryotic diversity that spanned the glaciations and that may have begun millions of years prior to their onset.

INTRODUCTION

The effect of low-latitude glaciation upon the biosphere has been a matter of speculation for more than 50 years (e.g. Harland and Rudwick, 1964) and interest has grown since Hoffman et al. (1998) hypothesized a glacially driven global biological collapse. Some authors suggest, in contrast, that the glaciations had a limited effect, citing a lack of change between pre-, syn- and postglacial fossil assemblages and range-through of certain taxa (Corsetti et al., 2006; Moczydłowska, 2008). Recent studies, however, have resulted in new age assignments for some of the units discussed in those works (e.g. Macdonald et al., 2013) and range-through arguments are based on genus-level assignments of species that are not obviously biologically related. Body fossil and biomarker evidence (reviewed in Javaux, 2011) indicate that several modern eukaryotic lineages, including red algae, green algae, alveolates and amoebozoans originated before the Sturtian glaciation and thus must have survived these events, and recent reports of microfossils and biomarkers from interglacial rocks (Love et al., 2009; Maloof et al., 2010; Bosak et al., 2011a, b, 2012) provide insight into the nature of the interglacial biosphere. However, this evidence does not imply the

biosphere was unaffected by glaciation; after all, Lower Triassic rocks also preserve fossils despite the decimation of the end-Permian extinctions.

Diversity compilations indicate a dramatic decline associated with the glaciations (Vidal and Knoll, 1982; Knoll, 1994; Vidal and Moczydłowska-Vidal, 1997; Knoll et al., 2006), and although early studies interpreted this as indicating widespread extinction of phytoplankton, more recent reviews suggest this pattern may simply reflect limited sampling of glacial and interglacial rocks (Knoll et al., 2006; Butterfield, 2007). Here we present new glacial and interglacial organic-walled microfossil data that support the hypothesis of significantly lowered eukaryotic diversity. When these new data are placed in context of all available body fossil data from the mid-Neoproterozoic Era, the glacial interval appears to be part of a period of reduced diversity that began well before glacial onset.

GEOLOGIC SETTING

Our paleobiological data come from Sturtian and Sturtian-correlative glacial diamictites and interbedded shales as well as interglacial shales from four drillcores of Amadeus Basin, Adelaide Rift Complex (ARC), and northwest Tasmania in Australia and from field samples of the Polarisbreen Group in Svalbard (Fig. 1).

The Sturtian Areyonga Formation of the Amadeus Basin (sampled from BR05DD01 and Wallara-1 drillcores) consists of diamictites and shales deposited during repeated cycles of shallow glaciomarine sedimentation (Lindsay, 1989). The overlying interglacial Aralka Formation (sampled from Wallara-1) consists of siltstones and shales deposited above storm

wave base (Walter and Veevers, 1997) during a widespread, post-glacial transgression (Preiss, 2000).

In the ARC the Sturtian glaciation is represented by the Appila Tillite and the interglacial interval by the Tapley Hill Formation and Brighton Limestone (sampled from SCYW-79-1a drillcore; Preiss, 2000). The basal Tapley Hill Formation records a maximum flooding interval that is followed by upward-shallowing and increasingly calcareous and silty sediments. Stromatolitic and oolitic facies of the conformably superjacent Brighton Limestone record the culmination of a post-glacial transgressive-regressive cycle (Preiss, 2000). Sturtian and interglacial rocks were also sampled from Blinman-2 drillcore of the ARC but all samples were barren and are excluded from discussion (Fig. DR1).

In the Togari Group of northwestern Tasmania (sampled from Forest-1 drillcore) the Julius River Member of the Black River Dolomite consists of two diamictite horizons with intercalated mudstones separated by a mixed limestone and shale interval (Calver, 2011). The overlying undifferentiated strata of the Black River Dolomite comprise black pyritic shales and minor limestones (Calver, 2011) and record interglacial sedimentation. Recently Rooney et al., (2014) implied the Julius River Member may be a Marinoan rather than Sturtian-equivalent unit, citing similarity in a Re-Os age from the overlying Black River Dolomite (640.7±4.7 Ma; Kendall et al., 2009) and a new U-Pb zircon age from the Marinoan-equivalent Cottons Breccia of King Island, Tasmania (636.41±0.45 Ma; Calver et al., 2013). However, the date from the upper Black River Dolomite (Fig. 1) can provide only

a minimum age for the Julius River Member, a unit associated with the Sturtian glaciation based not on this date, but on Sr and C chemostratigraphic correlations (Calver et al., 1998; Calver, 2011).

The Polarisbreen Group of Svalbard contains the Petrovbreen Member of the Elbobreen Formation, and the Wilsonbreen Formation, correlated with Sturtian and Marinoan glacial units, respectively (Hoffman et al., 2012). The interglacial MacDonaldryggen Member (sampled from northwestern Nordaustlandet (Fig. 1)) comprises ~200 meters of dark, finely laminated silty and locally calcareous mudstones deposited in an upward-shallowing sequence that initiated below storm wave base. It is conformably overlain by the marly ribbonites and subsequent oolitic, cross-bedded grainstones of the Slangen Member (Halverson et al., 2004).

Whereas no single sampled section or core spans the entirety of the Sturtian glaciation and interglacial period, this collection of samples from different basins and drill cores provides overlapping coverage from paleogeographically distant localities.

METHODS

Samples (~5 grams) were processed by standard hydrofluoric acid maceration by Waanders Palynology following protocol of Grey (1999). Resulting organic macerates were strewn upon coverslips, epoxied to microscopy slides and the entirety of each slide was studied in a grid-like pattern with 40X to 100X objectives using a transmitted light

microscope. Every fossil encountered was photographed and catalogued by species. (Raw data and additional methods available in online data repository.)

RESULTS

Seventy-four of the eighty-nine samples examined were fossiliferous; these were dominated by leiosphaerids and aggregates of small (<25μm) cells assigned to *Synsphaeridium* spp. (Figs. 1, 2 and Table DR3). Of the 21 glacial samples studied, 17 were fossiliferous, although two of these hosted only fragments of leiosphaerids. The most abundant component (~41% of specimens) of the glacial assemblage is *Leiosphaeridia crassa*, a small (<70μm), smooth-walled sphaeroid with an optically dense vesicle (Figs. 1, 2a). Also common in the glacial assemblage are *L. minutissima* (28%) (Figs. 2b,e,f,i), a smooth-walled sphaeroid distinguished from *L. crassa* by its more translucent vesicle; *Synsphaeridium* spp. (13%) (Figs. 2g,h); and simple filaments (4–23μm diameter) assigned to *Siphonophycus* spp. (Fig. 2d) and *Rugosoopsis tenuis* (Fig. 2j). Specimens of the stratigraphically long-ranging *Pterospermopsimorpha* sp. are rare. Eight ornamented specimens were found in glacial units; seven of these are fragments of *Cerebrosphaera buickii*, a robust and distinctively wrinkled form considered a pre-Sturtian biostratigraphic indicator (Grey et al., 2011). Due to their poor preservation and fragmentary nature (Fig. DR2), we interpret these *C. buickii* specimens to be reworked from pre-glacial sediments rather than indicative of an expanded age-range for this microfossil. The remaining ornamented specimen (Fig. 2c) is likely contemporaneous with glacial deposition due to its

high quality of preservation. It has an optically dense vesicle bearing short (<1μm), irregularly distributed processes and is comparable to, although smaller than, "*Kildinosphaera" verrucata*, a species associated with pre-Sturtian assemblages.

Of the 68 interglacial samples studied, 57 were fossiliferous; nine of these hosted only leiosphaerid fragments. As with the glacial assemblage, *L. crassa* (Figs. 2l,o) was very abundant (35%), as were *Synsphaeridium* spp. (35%; Figs. 2p,s,u). *L. minutissima* was also common (17%; Figs. 2m,v). Minor members of the assemblage include *Siphonophycus* spp. (Fig. 2k), *R. tenuis* (Fig. 2t), *Pterospermopsimorpha* sp. (Fig. 2n), and the leiosphaerids *L. jacutica* and *L. tenuissima*, which differ from *L. crassa* and *L. minutissima,* respectively, only by their larger size. Two ornamented specimens were recovered from interglacial sediments: a fragment of a vesicle bearing closely spaced, <1 μm-long, solid, conical spines (Fig. 2q); and a vesicle bearing short (1–1.5μm) tubular processes (Fig. 2r). These cannot confidently be assigned to any pre-Sturtian or post-Marinoan species. The glacial and interglacial assemblages are strikingly similar, differing only in the greater proportion of *Synsphaeridium* spp. in the latter (Figure DR3).

Particularly notable in our study is the absence of diverse, complexly ornamented forms confidently allied with the eukaryotes and characteristic of many early Neoproterozoic and late Ediacaran assemblages (Fig. 3, Table DR 2). Instead, both the glacial and interglacial assemblages are dominated by fossils of prokaryotes (i.e. *Synsphaeridium* spp. and simple filaments) and by fossils belonging to featureless form-taxa

(*Leiosphaeridia* species), that are known to be polyphyletic, likely comprising both prokaryotes and eukaryotes.

DISCUSSION

We have provided new organic-walled microfossil data from two Sturtian glacial and five interglacial units and have critically reviewed and compiled all body fossil data from this interval, including forms interpreted to be heterotrophic protists (Bosak et al., 2011a, b, 2012) and sponges (Maloof et al., 2010; Brain et al. 2012; Fig. 3; Table DR1). The biological affinities of these fossils are questionable, but at most they indicate the presence of an additional five taxa. All fossiliferous Sturtian glacial and interglacial units display diversity lower than what is seen in fossiliferous units of the early and late Neoproterozoic Era.

The difference between the diversity of this interval and that of the early and late Neoproterozoic could reflect biases in deposition (i.e. biostratinomic bias), preservation, or sampling or could indicate genuinely depressed diversity during the Cryogenian Period. In order for a biostratinomic bias to be responsible for this lack of diversity, a filter would be required to preferentially prevent burial of macroalgae and of ornamented and spiny acritarchs but allow burial of smooth-walled leiospheres, aggregates such as *Synsphaeridium* sp., and simple filaments, and would need to act upon shales and carbonates worldwide during the glacial and interglacial period but not during the early or late Neoproterozoic. Similarly, a diagenetic bias would have to preferentially degrade buried complex fossils

such as those mentioned above but leave the more delicate fossils such as *L. minutissima* and *L. tenuissima* (Fig. 2) unscathed. We consider both of these unlikely.

This pattern is also unlikely to reflect facies bias: low-diversity Sturtian glacial and interglacial assemblages are reported from units that span broad paleogeographic and depositional ranges (Fig. 3, Tables DR 1, DR 2). Indeed, two of the units of this study (Tapley Hill Formation and MacDonaldryggen Member) record shallowing upward sequences that being with deep-water facies and culminate in the deposition of conformably overlying oolitic grainstones (Preiss, 2000; Halverson et al., 2004). Low diversity fossil assemblages are found throughout these sequences.

The present work has added appreciably to the number of fossiliferous units of this interval and although still low in Phanerozoic terms, it is comparable to the number of units from similar length intervals of the early Neoproterozoic (Fig. 3, Tables DR 1, DR 2). Whereas the possibility that preservational, facies or sampling biases are responsible for low estimates of diversity cannot be ruled out, such a possibility is increasingly unlikely in the face of these new data. A more parsimonious hypothesis is that there was low eukaryotic diversity during this time. This hypothesis has the further value of being easily testable; it would be falsified by a single discovery of a high-diversity fossil assemblage from Cryogenian-aged rocks.

One explanation for this lowered diversity is a glacially driven extinction (cf. Vidal and Knoll, 1982; Hoffman et al., 1998). Indeed, early and late Neoproterozoic assemblages

have limited taxonomic overlap (Vidal and Knoll, 1982; Vidal and Moczydłowska-Vidal, 1997; Knoll et al., 2006), implying intervening extinction (although the relative timing of extinctions is unclear, i.e. mass extinction event or accumulated background extinctions with reduced speciation rate). We see no increase in diversity from the Sturtian to interglacial assemblages. This lack of biotic recovery could indicate that the interglacial fossil record captures only a portion of the interval between glacial events, that the interglacial period itself was short (Rooney et al., 2014), or that unfavorable conditions continued through the interglacial period. This last possibility would suggest that the glaciations *per se* were not the sole drivers of extinction.

Intriguingly, our diversity compilation suggests that the initial shift to a low-diversity biota may have occurred ~30 million years prior to the onset of Sturtian glaciation; strata that immediately underlie Sturtian-age glaciogenic rocks are characterized by low diversity assemblages (Fig. 3; cf. Nagy et al., 2009). Read literally, this pattern suggests a protracted (~ 95 Ma) interval of limited diversity with an onset broadly correlated with, but decoupled from, the onset of low-latitude glaciations.

CONCLUSIONS

At least two global glaciations are hypothesized to have occurred during the mid-Neoproterozoic Era, and compilations of fossil data suggest a coincident lull in diversity. However, those compilations included few data from the glacial interval, prompting concerns that the pattern of lowered diversity reflects sampling bias. We have provided new

fossil data from this interval and have compiled body fossil reports from carbonate and siliciclastic rocks from both the pre-glacial and glacial interval. These data indicate both that fossils are widespread and reasonably abundant in glacial and interglacial rocks and that those assemblages are of much lower diversity than those found in similar early Neoproterozoic rocks. Depositional, preservational and sampling biases are unlikely to be responsible for this pattern; instead the most parsimonious hypothesis is that biotic diversity was indeed lower during the mid-Neoproterozoic Era. It is clear that several lineages survived the mid-Neoproterozoic glaciations, however, the fossil record indicates that the Cryogenian Earth was characterized by significantly lower eukaryotic diversity than that of the early Neoproterozoic in which eukaryotes diversified or the late Neoproterozoic Era in which multicellular life flourished.

ACKNOWLEDGEMENTS

Authors thank C. Calver and E. Domack for sampling aid, J. Moore for manuscript feedback and G. Waanders for sample preparation. Thanks to personnel of core facilities in Darwin and Alice Springs, NT, Adelaide, SA and Hobart, Tas. Financial support by National Science Foundation: grants EAR-0922305 to S.M.P. and EAR-0921913 to M.T.H. and Palaeontological Association grant to S.M.P.

REFERENCES CITED

Ambrose, G. et al., 2010, Well completion report for NTGS stratigraphic drillholes LA05DD01 and BR05DD01, southwestern Amadeus Basin: NT Geological Survey, Record 2010-015.

Bosak, T. et al., 2011a, Agglutinated tests in post-Sturtian cap carbonates of Namibia and Mongolia: Earth and Planetary Science Letters v. 308, p. 29–40.

Bosak, T. et al., 2011b, Putative Cryogenian ciliates from Mongolia: Geology, v. 39, p. 1123–1126.

Bosak, T. et al., 2012, Possible early foraminiferans in post-Sturtian (716–635 Ma) cap carbonates: Geology, v. 40, p. 67–70.

Brain, C. K. et al., 2012, The first animals: ca. 760-million-year-old sponge-like fossils form Namibia: South African Journal of Science, v. 108 (1/2), 8 p.

Butterfield, N., 2007, Macroevolution and macroecology through deep time: Palaeontology, v. 50, p. 41–55.

Calver, C., 1998, Isotope Stratigraphy of the Neoproterozoic Togari Group, Tasmania: Australian Journal of Earth Sciences, v. 45, p. 865–874.

Calver, C., 2011, Neoproterozoic glacial deposits of Tasmania, *in* Arnaud, E., Halverson, G. P., Shields-Zhou, G., eds., The Geological Record of Neoproterozoic Glaciations: Geological Society of London Memoirs, no. 36, p. 649–657.

Calver, C. et al., 2013, Globally synchronous Marinoan deglaciation indicated by U-Pb geochronology of the Cottons Breccia, Tasmania, Australia: Geology, v. 41, p. 1127–1130.

Corsetti, F., Olcott, A. & Bakermans, C., 2006, The biotic response to Neoproterozoic snowball Earth: Palaeogeography, Palaeoclimatology, Palaeoecology, v. 232, p. 114–130.

Grey, K., 1999, A modified palynological preparation technique for the extraction of large Neoproterozoic acanthomorph acritarchs and other acid-insoluble microfossils: Western Australia Geological Survey, record 1999/10, 23p.

Grey, K., Hill, A. & Calver, C., 2011, Biostratigraphy and stratigraphic subdivision of Cryogenian successions of Australia in a global context, *in* Arnaud, E., Halverson, G., Shields-Zhou, G., eds., The Geological Record of Neoproterozoic Glaciations: Geological Society of London Memoirs, no. 36, p. 113–134.

Halverson, G., Maloof, A. & Hoffman, P., 2004, The Marinoan glaciation (Neoproterozoic) in northeast Svalbard: Basin Research, v. 16, p. 297–324.

Halverson, G., et al., 2005, Toward a Neoproterozoic composite carbon-isotope record: GSA Bulletin, v. 117, 1181–1207.

Halverson, G. et al., 2010, Neoproterozoic chemostratigraphy: Precambrian Research, v. 182, p. 337–350.

Harland, B. & Rudwick, M., 1964, The great infra-Cambrian ice age: Scientific American, v. 211, p.28–36.

Hoffman, P. et al., 1998, A Neoproterozoic Snowball Earth: Science, v. 281, p. 1342–1346.

Hoffman, P. et al., 2012, Cryogenian glaciations on the southern tropical paleomargin of Laurentia (NE Svalbard and East Greenland), and a primary origin for the upper Russøya (Islay) carbon isotope excursion: Precambrian Research, v. 206–207, p. 137–158.

Javaux, E., 2011, Early eukaryotes in Precambrian oceans, *in* Gargaud, M., López-Garcìa, P. & Martin, H., eds., Origins and Evolution of Life: An Astrobiological Perspective: Cambridge University Press, p. 414–449.

Kendall, B., Creaser, R. & Selby, D., 2006, Re-Os geochronology of postglacial black shales in Australia: constraints on the timing of "Sturtian" glaciation: Geology, v. 34, p. 729–732.

Kendall, B. et al., 2009, Correlation of Sturtian diamictite successions in southern Australia and northwestern Tasmania by Re-Os black shale geochronology and the ambiguity of "Sturtian"-type diamictite-cap carbonate pairs as chronostratigraphic marker horizons: Precambrian Research, v. 172, p. 301–310.

Knoll, A., 1994, Proterozoic and early Cambrian protists: evidence for accelerating evolutionary tempo: Proceedings of the National Academy of Sciences, v. 91, p. 6743–6750.

Knoll A. et al., 2006, Eukaryotic organisms in Proterozoic oceans: Philosophical Transactions of the Royal Society B, v. 361, p. 1023–1038.

Lindsay, J. 1989, Depositional controls on glacial facies associations in a basinal setting, Late Proterozoic, Amadeus Basin, central Australia: Palaeogeography, Palaeoclimatology, Palaeoecology, v. 73, p. 205–232.

Love, G. et al., 2009, Fossil steroids record the appearance of Demospongiae during the Cryogenian period: Nature, v. 457, p. 718–722.

Macdonald, F. et al., 2010, Calibrating the Cryogenian: Science, v. 327, p. 1241–1243.

Macdonald, F. et al., 2013, The Laurentian record of Neoproterozoic glaciation, tectonism, and eukaryotic evolution in Death Valley, California. GSA Bulletin, v. 7–8, p. 1203–1223.

Maloof, A. et al., 2010, Possible animal-body fossils in pre-Marinoan limestones from South Australia: Nature Geoscience, v. 3, p. 653–659.

Moczydłowska, M., 2008, The Ediacaran microbiota and the survival of Snowball Earth conditions: Precambrian Research, v. 167, p. 1–15.

Nagy, R. et al., 2009, Biotic turnover driven by eutrophication before the Sturtian low-latitude glaciation: Nature Geoscience, v. 2, p. 415–418.

Preiss, W., 2000, The Adelaide Geosyncline of South Australia and its significance in Neoproterozoic continental reconstruction: Precambrian Research, v. 100, p. 21–63.

Rooney, A. et al., 2014, Re-Os geochronology and coupled Os-Sr isotope constraints on the Sturtian snowball Earth: Proceedings of the National Academy of Sciences, v. 111, p. 51–56.

Vidal, G. & Knoll, A., 1982, Radiations and extinctions of plankton in the late Proterozoic and early Cambrian: Nature, v. 297, p. 57–60.

Vidal, G. & Moczydłowska-Vidal, M., 1997, Biodiversity, speciation and extinction trends of Proterozoic and Cambrian phytoplankton: Paleobiology, v. 23, p. 230–246.

Walter, M. & Veevers, J., 1997, Australia Neoproterozoic palaeogeography, tectonic, and supercontinental connections. AGSO Journal of Australian Geology and Geophysics, v. 17, p. 73–92.

Zhou, C. et al., 2004, New constraints on the ages of Neoproterozoic glaciations in South China: Geology, v. 32, p. 437–440.

FIGURE CAPTIONS

Figure 1. Maps and stratigraphic columns with microfossil distribution. Map numbers correspond to position of stratigraphic columns left–right. Grey bars indicate correlations of Sturtian and Marinoan glacial units; note absence of Marinoan in Forest-1 and BR05DD01. Forest-1 modified from Calver, 2011; Re-Os date Kendall et al., 2009. BR05DD01 modified from Ambrose et al., 2010. Wallara-1 and SCYW-79-1a Re-Os dates and columns modified from Kendall et al., 2006. Polarisbreen Grp modified from Halverson

et al., 2004; Hoffman et al, 2012. “P. Ss.”= Pioneer Sandstone, “Pbreen”= Petrovbeen. All fossils indicated are from this study.

Figure 2. Glacial and interglacial microfossils. a-j from glacial assemblage, **k-v** from interglacial assemblage. Fossils **a**, **l** and **o** *L. crassa*; **o** may have been in process of cellular division; **b**, **e**, **f**, **i, m**, **v** *L. minutissima*; **c**, **q** and **r** ornamented (details in text); **g**, **h**, **s, p** and **u** *Synsphaeridium* spp.; **d** and **k** *Siphonophycus* sp.; **j** and **t** *Rugosoopsis tenuis*; **n** *Pterospermopsimorpha* sp. Scale bar 100 μm for **j** and **k**; 50 μm for others. Depths of specimens in DR.

Figure 3. Mid-Neoproterozoic eukaryotic diversity. Top panel, inferred stratigraphic ranges of major eukaryotic lineages; Below, eukaryotic diversity (Y-axes) 850–650 Ma; organic-walled eukaryotes includes macroalgae, spiny and ornamented acritarchs but not leiosphaerids, that column indicates number of taxa per assemblage, others indicated as present or absent; leiosphaerids separate due to poorly resolved taxonomy; column width indicates age constraints, not duration of deposition. Ages based on direct radiometric constraints where available and chemostratigraphic correlation to radiometrically dated successions elsewhere. Units constrained only by biostratigraphy were omitted (Table DR1). Composite carbon isotope record modified from Halverson et al. (2010), with new data and age calibrations (Zhou et al., 2004 (red triangle); Halverson et al., 2005 (black triangle); Macdonald et al., 2010 (yellow triangles); Rooney et al., 2014 (white triangle)). Far right blue line is Marinoan glaciation. Unit names and references in Table DR2.

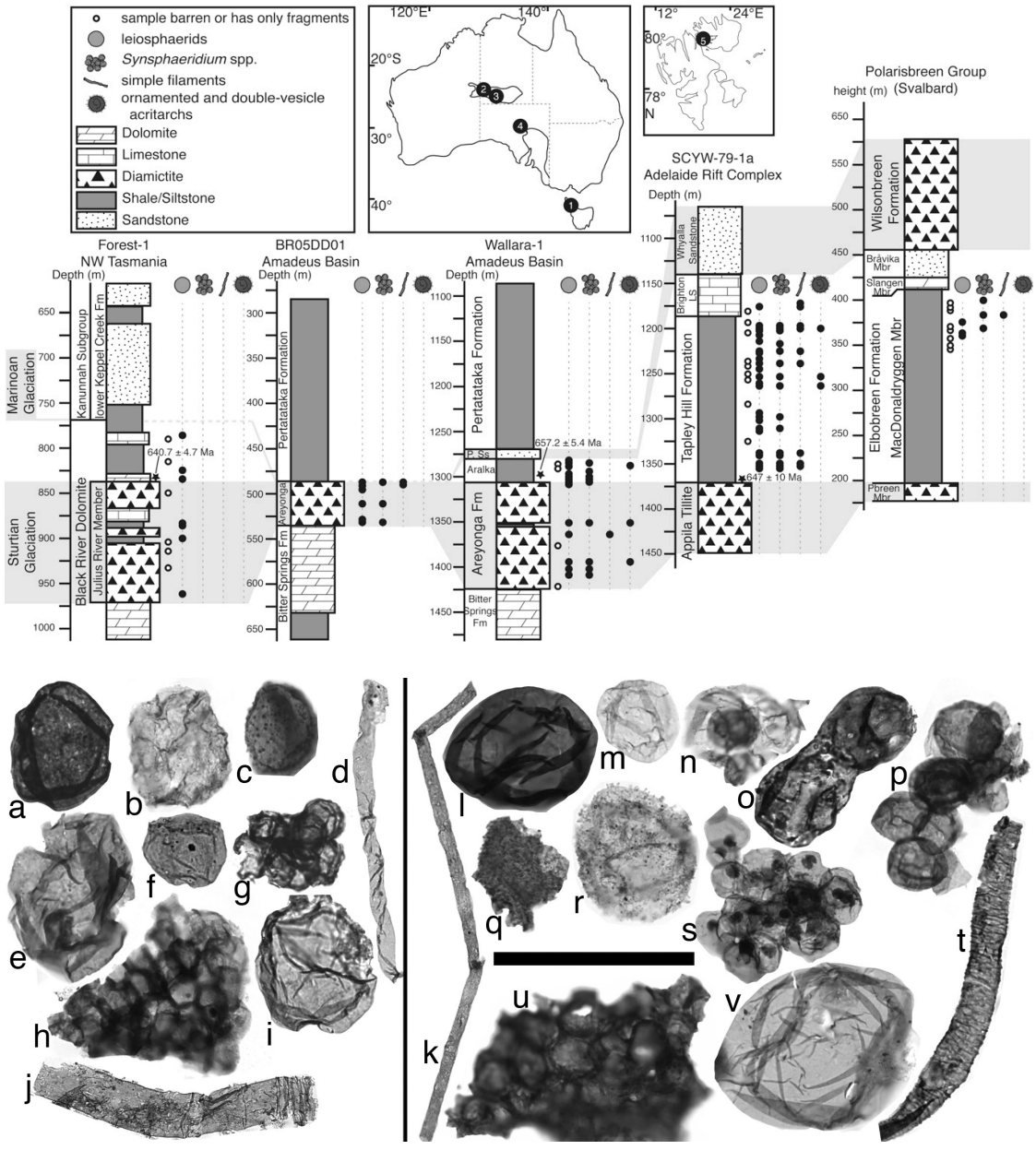
sample barren or has only fragments
leiosphaerids
Synsphaeridium spp.
simple filaments
ornamented and double-vesicle acritarchs
Dolomite
Limestone
Diamictite
Shale/Siltstone
Sandstone
120°E
140°
20°S
30°
40°
12°
24°E
60°
78° N
Forest-1
NW Tasmania
BR05DD01
Amadeus Basin
Wallara-1
Amadeus Basin
SCYW-79-1a
Adelaide Rift Complex
Polarisbreen Group
(Svalbard)
Depth (m)
height (m)
Marinoan Glaciation
Sturtian Glaciation
Kanunnah Subgroup
lower Keppel Creek Fm
Black River Dolomite
Julius River Member
Pertatataka Formation
Areyonga Fm
Bitter Springs Fm
P. Ss.
Aralka
Whyalla Sandstone
Brighton Ls
Tapley Hill Formation
Appila Tillite
Wilsonbreen Formation
Bråvika Mbr
Slangen Mbr
Elbobreen Formation
MacDonaldryggen Mbr
Fbreen Mbr
640.7 ±4.7 Ma
657.2 ±5.4 Ma
647 ±10 Ma
a
b
c
d
e
f
g
h
i
j
k
l
m
n
o
p
q
r
s
t
u
v

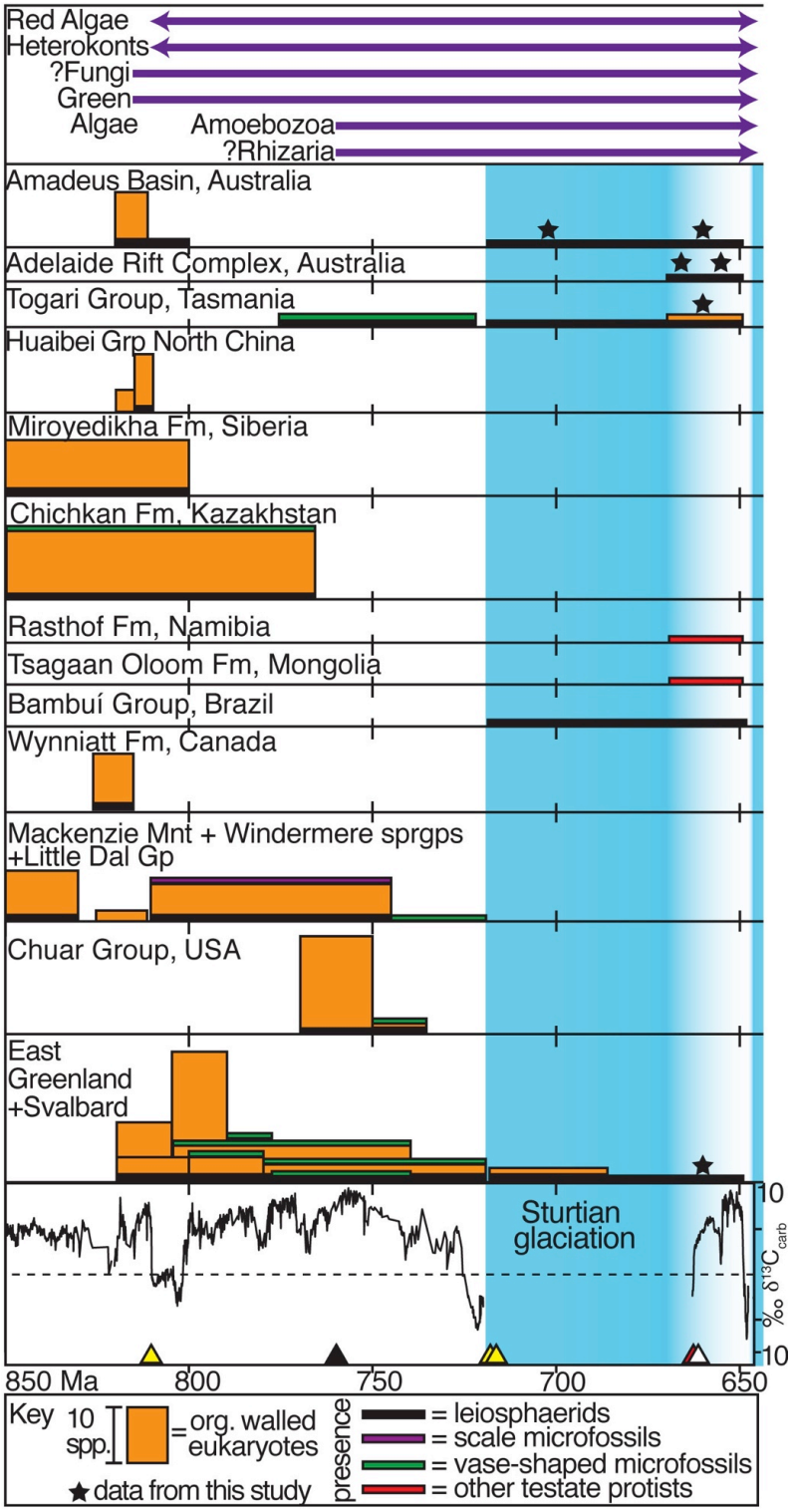
Red Algae
Heterokonts
?Fungi
Green Algae
Amoebozoa
?Rhizaria
Amadeus Basin, Australia
Adelaide Rift Complex, Australia
Togari Group, Tasmania
Huaibei Grp North China
Miroyedikha Fm, Siberia
Chichkan Fm, Kazakhstan
Rasthof Fm, Namibia
Tsagaan Oloom Fm, Mongolia
Bambuí Group, Brazil
Wynniatt Fm, Canada
Mackenzie Mnt + Windermere sprgps +Little Dal Gp
Chuar Group, USA
East Greenland +Svalbard
Sturtian glaciation
10
‰ δ13Ccarb
10
850 Ma
800
750
700
650
Key
10 spp.
= org. walled eukaryotes
data from this study
presence
= leiosphaerids
= scale microfossils
= vase-shaped microfossils
= other testate protists

Supplementary Information

Table DR1. Previous palaeontological studies of Sturtian-equivalent, interglacial and Marinoan-equivalent units.

Time Bin	Unit (Group or Basin- Country)	Biota	References
Marinoan Equivalent	Churochnaya Fm. (Laplandian Horizon- Russia)	simple filaments and coccoids	Sergeev et al., 2013
Marinoan Equivalent	Ghadir Manqil Fm (Abu Mahara Group- Oman)	simple filaments	Butterfield and Grotzinger, 2012
Marinoan Equivalent	Ghadir Manqil Fm (Abu Mahara Group- Oman)	24-Isopropylcholestane, biomarker interpreted as evidence of Demospongiae	Love et al., 2009
Interglacial	Ghadir Manqil Fm (Abu Mahara Group- Oman)	24-Isopropylcholestane, biomarker interpreted as evidence of Demospongiae	Love et al., 2009
Interglacial	Trezona Fm (Adelaide Rift Complex- Australia)	weakly calcified structures stromatolites	Maloof et al, 2010 Preiss, 1973
Interglacial	Rasthof Fm (Otavi Group- Namibia)	Agglutinated structures microbialaminites	Bosak et al, 2011a; Bosak et al., 2012 Pruss et al, 2010
Interglacial	Tsagaan Oloom Fm (Dzabkhan Basin -Mongolia)	Agglutinated structures Flask shaped structures	Bosak et al, 2011a Bosak et al., 2011b
Interglacial	Twitya Fm (Windermere Sprgrp- Canada)	Twitya disks- Ediacaran fauna-like macrofossils	Hofmann et al, 1990
Interglacial	Twitya/Keele Fm (Windermere Sprgrp- Canada)	Stromatolites	James et al., 2005
Interglacial	Cheikhia Group (Taoudeni Basin- W. Africa)	Disks- Ediacaran fauna-like macrofossils	Bertrand-Sarfati et al., 1995
Interglacial	Ombaatjie Fm and Auros Fm (Otavi Group- Namibia)	perforate globular structures	Brain et al., 2012
Interglacial	Ombaatjie Fm (Otavi Group- Namibia)	Stromatolites	Hoffman, 2011
Interglacial	Bonahaven Fm (Argyll Group- Scotland)	Stromatolites	Spencer and Spencer, 1972
Interglacial	Russøya Mbr (Polarisbreen Group- Svalbard)	Stromatolites	Hoffman et al., 2012
Interglacial	Etina Fm (Adelaide Rift Complex- Australia)	stromatolites	Preiss, 1973
Interglacial	Brighton Fm (Adelaide Rift Complex- Australia)	stromatolites	Preiss, 1973
Interglacial	Aralka Fm (Ringwood Mbr) (Amadeus Basin- Australia)	stromatolites	Glaessner et al, 1969
Interglacial	Aralka Fm (lower) (Amadeus Basin- Australia)	leiosphaerids, *Sphaerocongregus variabilis*, simple filaments, small fragment of ?process-bearing? Acritarch	Zang and Walter, 1992
Interglacial	Datangpo, Minle Fms (Yangtze Platform- China)	leiosphaerids, *Sphaerocongregus variabilis*, colonial aggregates	Yin, 1990
Interglacial	Serra da Saudade (Bambuí Group- Brazil)	leiosphaerids	Simonetti and Fairchild, 2000
Interglacial	Lagoa do Jacaré (Bambuí Group- Brazil)	leiosphaerids	Simonetti and Fairchild, 2000
Interglacial	Serra de Santa Helena Fm (Bambuí Group- Brazil)	leiosphaerids	Simonetti and Fairchild, 2000
Interglacial	Sete Lagoas Fm (Bambuí Group- Brazil)	columnar,digitate, domical, planar stromatolites leiosphaerids, colonial aggregates, simple filaments	Fairchild et al, 1996
Interglacial	Grasdal Formation (Tanafjord Group- Norway)	Columnar stromatolites leiosphaerids, *Sphaerocongregus variabilis*, rare, small, ?process-bearing? acritarchs, fragments of *Chuaria circularis,* abundant thin filaments	Bertrand-Sarfati and Siedlecka, 1980, Raaben et al., 1995 Vidal, 1981
Interglacial	Dakkovarre Formation (Tanafjord Group- Norway)	leiosphaerids, *Sphaerocongregus variabilis, Chuaria circularis,* small ?process-bearing? Acritarchs, colonial aggregates, thin filaments	Vidal, 1981
Interglacial	Stangenes Formation (Tanafjord Group- Norway)	leiosphaerids, *Sphaerocongregus variabilis*, small ?process-bearing? Acritarchs	Vidal, 1981
Interglacial	Arena Fm* (Tillite Group -Greenland)	leiosphaerids, *Sphaerocongregus variabilis*	Vidal, 1979 Vidal, 1976
Sturtian equivalent	Maikhan Ul Fm (Dzabkhan terrane- Mongolia)	problematic circular structures	Serezhnikova et al., 2014
Sturtian equivalent	Jequitaí Fm (Bambuí Group- Brazil)	planar microbialites leiosphaerids, colonial aggregates, simple filaments	Fairchild et al, 1996
Sturtian equivalent	Ulvesø Fm* (Tillite Group- Greenland)	leiosphaerids, *Sphaerocongregus variabilis*, *Octoedryxium truncatum*, *Chuaria circularis* (may be reworked)	Vidal, 1979 Vidal, 1976
Sturtian equivalent	Mineral Fork Fm (Wasatch Range-USA)	leiosphaerids, *Sphaerocongregus variabilis*	Knoll et al, 1981
Sturtian equivalent	Pirrilyunka Formation (Central Officer Basin- Australia)	fragments of *Cerebrosphaera buickii* (considered reworked)	Haines et al., 2008
Sturtian equivalent	Chambers Bluff Tillite (Eastern Officer Basin- Australia)	fragments of *Cerebrosphaera buickii* (considered reworked)	Eyles et al., 2007

*Vidal, 1976,1979 described fossils from the "Lower Tillite" and "Inter-tillite Beds", renamed "Ulvesø Fm" and "Arena Fm", respectively (Hambrey and Spencer, 1987).

The Pickelhaube Fm, Port Nolloth Group Namibia (Gaucher et al., 2005) hosts *Sphaerocongregus variabilis* but is not included here due to stratigraphic uncertainty (Macdonald et al., 2010b). Similarly, recent work has reinterpreted the Kingston Peak Fm, Death Valley, USA (Macdonald et al., 2013), thus that microbiota (Corsetti et al., 2003) is omitted here. Serezhnikova et al. (2014) report problematic circular structures from the glacial Maikhan Ul Fm of Monglia; they interpret this unit to be a Marinoan equivalent, but based upon the data presented by Macdonald (2011), this unit is placed here as a Sturtian equivalent.

Table DR2. Complement to text figure 3.

Paleocontinent	Basin/ Group	Unit	Age (nature of constraints)	leiosphaerids present?	# of eukaryote taxa including leiosphaerids	VSMs present?	other	References: paleo and age
Australia	Amadeus Basin	Bitter Springs Gillen Mbr	820-810 Ma ($\delta^{13}C$ correlation)	y	9	n		Zang and Walter, 1992
Australia	Amadeus Basin	Bitter Springs Loves Creek Mbr	810-800 Ma ($\delta^{13}C$ correlation)	y	1	n		Schopf, 1968
Australia	Amadeus Basin	Areyonga Fm	Sturtian glacial	y	1	n		this study; Kendall et al., 2006; Li et al., 2013
Australia	Amadeus Basin	Aralka Fm	Sturtian glacial	y	1	n		this study; Kendall et al., 2006; Li et al., 2013
Australia	Adelaide Rift Complex	Tapley Hill Fm	Sturtian-Marinoan interglacial	y	2	n		this study; Li et al., 2013
Australia	Adelaide Rift Complex	Brighton Limestone Fm	Sturtian-Marinoan interglacial	y	1	n		this study
Australia	Smithton Synclinorium Togari Group	lower Black River Dolomite	777-722 Ma (U-Pb zircon, $^{87}Sr/^{86}Sr$, $\delta^{13}C$)	y	1	y		Saito et al., 1988; LAR pers. obs.; Calver, 1998,
Australia	Smithton Synclinorium Togari Group	Black River Dolomite Julius River Mbr	Sturtian glacial-equivalent	y	1	n		this study; Calver, 1998; Li et al., 2013
Australia	Smithton Synclinorium Togari Group	upper Black River Dolomite	Sturtian-Marinoan interglacial	y	1	n		this study; Calver, 1998, Kendall et al., 2009
North China	southern North China Block Huainan Group	Liulaobei Fm	810-805 Ma ($\delta^{13}C$ correlation)	y	12	n		Yin and Sun, 1994; Tang et al., 2013
Siberia	Turukhansk region	Miroyedikha Fm	900-800 Ma ($\delta^{13}C$ correlation)	y	9	n		Jankauskas et al., 1989, Hermann, 1990; Knoll et al., 1995, Bartley et al., 2001
Kazakhstan	Lesser Karatau Malokaroy Series	Chichkan Fm	?-766±7 Ma (U-Pb zircon)	y	11	y		Sergeev and Schopf, 2010. Levashova et al., 2011
Congo	Otavi Group	Rasthof Fm	717-635.6± 0.5 Ma (U-Pb zircon, glacial correlation)	n	0	n	agglutinated forms	Bosak et al., 2011a, 2012
Tuva-Mongolia	Dzabkhan terrane	Tsagaan Oloom Fm	715-635 Ma (U-Pb zircon, $^{87}Sr/^{86}Sr$, $\delta^{13}C$)	n	0	n	putative ciliates	Bosak et al., 2011b
São Fancisco Craton	São Fancisco Block	Jequitaí Fm	Sturtian glacial-equivalent	y	1	n		Fairchild et al., 1996, Uhlein et al., 2011; but see Li et al., 2013
São Fancisco Craton	São Fancisco Block Bambuí Group	Sete Lagoas Fm	740±22 Ma (Pb-Pb isochron; $\delta^{13}C$, Sturtian-Marinoan interglacial correlation)	y	1	n		Fairchild et al., 1996; Babinski et al., 2007, Misi et al., 2007; but see Li et al., 2013
São Fancisco Craton	São Fancisco Block Bambuí Group	Serra de Santa Helena Fm	Sturtian-Marinoan interglacial	y	1	n		Simonetti and Fairchild, 2000, Misi et al., 2007
São Fancisco Craton	São Fancisco Block Bambuí Group	Lagoa do Jacaré Fm	Sturtian-Marinoan interglacial	y	1	n		Simonetti and Fairchild, 2000, Misi et al., 2007
São Fancisco Craton	São Fancisco Block Bambuí Group	Serra da Saudade Fm	Sturtian-Marinoan interglacial	y	1	n		Simonetti and Fairchild, 2000, Misi et al., 2007
Laurentia	Amundsen Basin Shaler Supergroup	Wynniatt Fm	825-815 Ma ($\delta^{13}C$, $\delta^{18}O$ correlations)	y	10	n		Hofmann and Rainbird, 1995; Butterfield and Rainbird, 1998; Butterfield 2005a,b; Jones et al., 2010
Laurentia	MacKenzie Mts Supergroup +Coates Lake Group	upper shale of Fifteenmile Group	810-745 Ma (U-Pb zircon)	y	6	n	scale microfossils	Allison and Awramik, 1989; Cohen and Knoll 2012, Macdonald et al., 2010
Laurentia	MacKenzie Mts Supergroup +Coates Lake Group	Callison Lake Dolostone	~745–716 Ma Re-Os	n	0	y		Strauss et al., 2012; Macdonald et al., 2010
Laurentia	Chuar Group	Galeros +lower Kwagunt	770-750 Ma (max:detrital zircon, min: interpolation	y	17	n		Vidal and Ford, 1985; Nagy et al. 2009; SMP pers.obs.; Dehler et al., 2012
Laurentia	Chuar Group	upper Awatubi +Walcott	750-742±6 Ma max: interpolation, min:U-Pb zircon)	y	2	y		Vidal and Ford, 1985; Nagy et al. 2009; SMP pers.obs.; Karlstrom et al., 2000
Laurentia	East Greenland+Svalbard Basin Roaldtoppen Group	Hunnberg Fm	820-805 Ma (lithological & $\delta^{13}C$ correlation)	y	10	n		Knoll, 1984
Laurentia	E.Greenland+Svalbard Basin Roaldtoppen	Ryssо Fm	805-740 Ma (lithological & $\delta^{13}C$ correlation)	y	6	y		Knoll and Calder, 1983
Laurentia	East Greenland+Svalbard Basin Academikerbreen Group	Svanbergfjellet Fm	~805-~790 Ma ($\delta^{13}C$ correlation)	y	22	n		Butterfield et al., 1994; Li et al., 2013
Laurentia	East Greenland+Svalbard Basin Academikerbreen Group	DrakenFm	~790-~778 Ma ($\delta^{13}C$ correlation)	y	8	y		Knoll et al., 1991
Laurentia	East Greenland+Svalbard Basin Academikerbreen Group	Backlundtoppen Fm	~778-~740 Ma ($\delta^{13}C$ correlation)	y	1	y		Knoll et al., 1989; Hoffman et al., 2012
Laurentia	East Greenland+Svalbard Basin Polarisbreen Group	Russoya Mbr	~740-~719 Ma ($\delta^{13}C$ correlation)	y	1	n		LAR pers obs.; Hoffman et al., 2012
Laurentia	East Greenland+Svalbard Basin Polarisbreen Group	Macdonaldryggen Mbr	Sturtian-Marinoan interglacial	y	1	n		this study; Hoffman et al., 2012; Li et al., 2013
Laurentia	E.Greenland+Svalbard Basin Eleonore Bay Supergroup	Eleonore Bay Grp Multicolor series	820-800 Ma (regional correlation with Svalbard)	y	4	n		Vidal, 1976b; Vidal, 1979; Hoffman et al., 2012
Laurentia	E.Greenland+Svalbard Basin Eleonore Bay Supergroup	Eleonore Bay Grp Lower Limestone	800-780 Ma (regional correlation with Svalbard)	y	4	y		Vidal, 1976b; Vidal, 1979; Hoffman et al., 2012
Laurentia	E.Greenland+Svalbard Basin Eleonore Bay Supergroup	Eleonore Bay Grp Upper Limestone	780-717 Ma (regional correlation with Svalbard)	y	3	y		Vidal 1976b; Vidal, 1979; Hoffman et al., 2012
Laurentia	E.Greenland+Svalbard Basin Tillite Group	Ulveso Fm	Sturtian glacial-equivalent	y	2	n		Vidal, 1979; Hoffman et al., 2012; Li et al., 2013
Laurentia	E.Greenland+Svalbard Basin Tillite Group	Arena Fm	Sturtian-Marinoan interglacial	y	1	n		Vidal, 1979; Hoffman et al., 2012; Li et al., 2013

Methods

Samples were processed by standard hydrofluoric maceration by Waanders Palynology Consulting and strewn slides were studied by transmitted light microscopy using Zeiss Axioskop 40. The abundance of organic-walled microfossils in these samples was low as compared to that of pre-Sturtian samples with similar lithology that have been processed in the same lab by the same methods (e.g. upper Chuar Group, Svanbergfjellet Formation, Bitter Springs Formation of BR05DD01 drillcore and Alinya Formation of Giles-1 drillcore).

Eukaryotic diversity assessments in text figure 3 are based on the first and second authors' estimates of within-assemblage taxonomic diversity based upon published synonymies and do not necessarily reflect the estimates given in the original works. As the genus concept is of dubious use in acritarch studies, these counts were based on occurrence of species. Forms considered by the present authors to be pseudofossils or taphonomic variants were not counted.

Text Figure 2 cores and depths: Wallara-1: **a** & **g**- 1411.2m, **c**-1395.9m, **j**-1367m, **q**-1293.9m **p**-1282.4m; BR05DD01: **b**, **h**, **d**-484.5m, **i**-531.5m, **e**-493.6m; Forest-1: **f**- 880.75m; SCYW-79-1a: **k**-1350.76m, **l**- 1238.7m, **m**- 1225.26m, **n** & **t**- 1201.32m, **o**-1266.74m, **v**, **r**, **s**-1254.9m, **u**-1298.81m.

Blinman-2 Discussion

In addition to samples discussed in the text, fourteen samples of Blinman-2 drill core (Fig DR1) of Adelaide Rift Complex were studied. All samples were found to be barren of fossils. Because a diagenetic cause of the absence of fossils cannot be ruled out, these data are not included in the main body of the study. These data are presented here in anticipation of future use and in the interest of publishing negative results to reduce duplication of efforts.

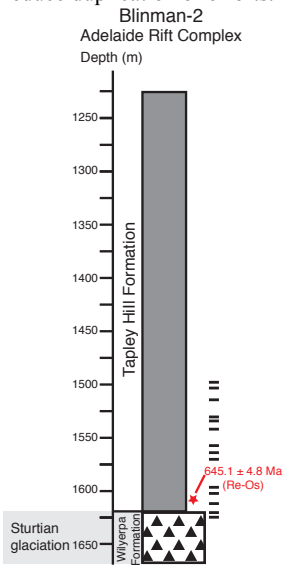

Figure DR1. Stratigraphic Column of Blinman- 2 drill core. Modified from Gorjan et al., 2000 and Kendall et al., 2006. Re-Os date from Kendall et al., 2006.

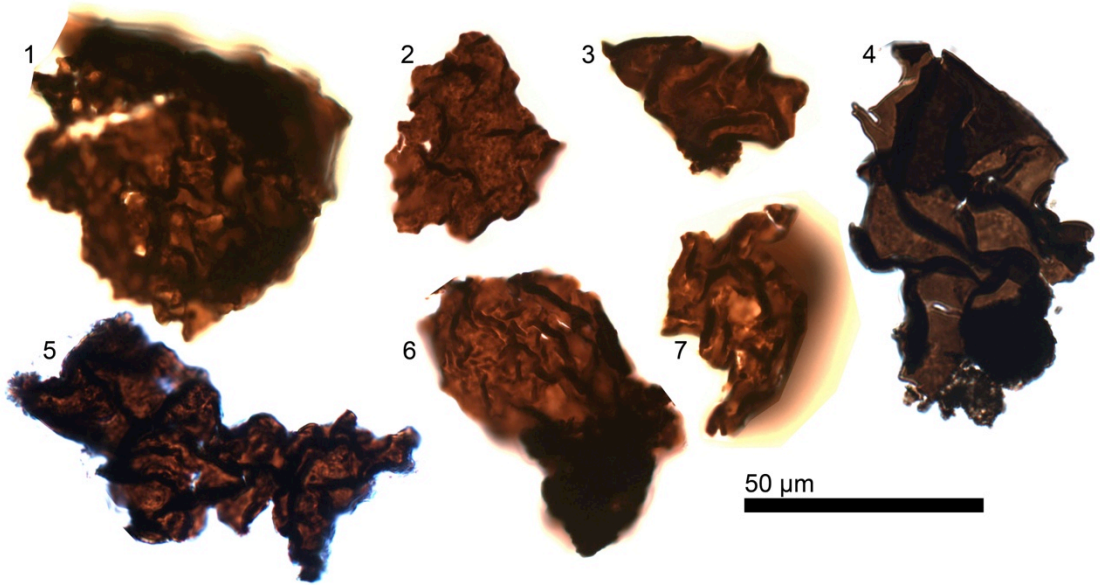

Figure DR2. Recovered fragments of *Cerebrosphaera buickii*. Due to poor quality, regarded as having been reworked. Cores and depths: **1**–**3**, **6**–**7** BR05DD01, 517.16 m, **4**–**5** Wallara-1, 1354.9 m.

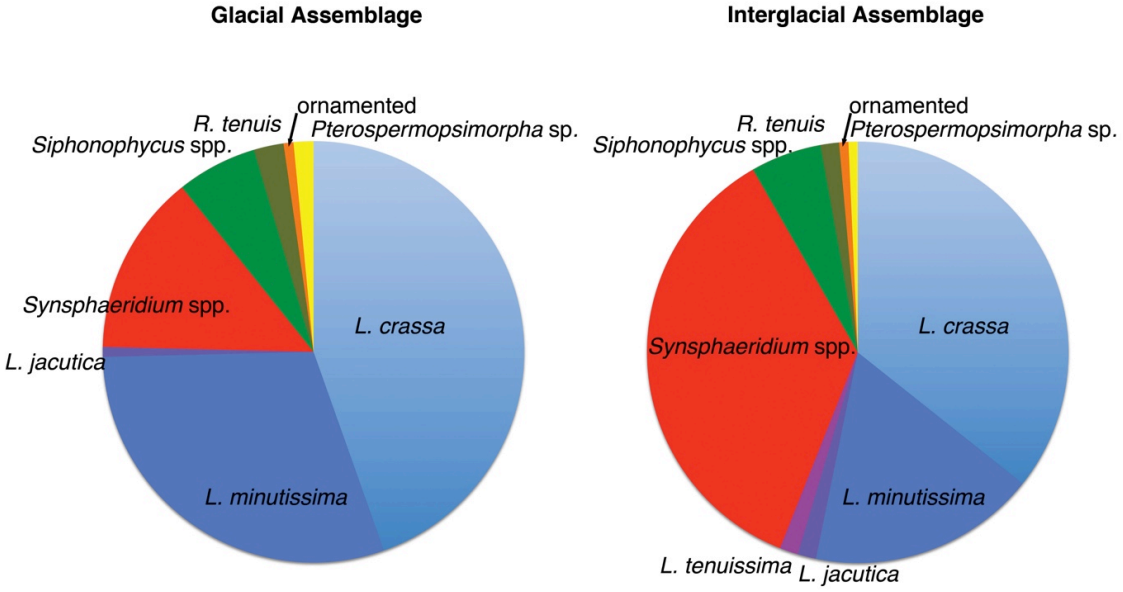

Figure DR3. Pie charts indicating relative contributions from various taxa.

Table DR3. Fossil counts for glacial and interglacial units discussed in text. Top-most table summarizes all samples from all units as divided by glacial or interglacial unit. Subsequent

						leiosphaerids						filaments				
			samples barren	fragments only	N	*Leiosphaeridia* sp.	*L. minutissima*	*L. crassa*	*L. jacutica*	*L. tenuissima*	*Synsphaeridium* spp.	*Siphophycus* sp.	*Rugosoopsis* sp.	ornamented acritarchs	*Pterospermopsimorpha* sp.	*C. buickii**
Total Interglacial (68 samples)			11	9	277	2	48	98	4	4	98	15	4	2	2	0
Total Synglacial (21 samples)			4	2	141	11	39	58	1	0	18	8	3	1	2	7

* *C. buickii* specimens occur as fragments and are interpreted to be reworked from pre-Sturtian sediments (see text). They are thus not included in total specimen counts (N)

Forest- 1 drill core

						leiosphaerids						filaments				
meterage	Unit Name	lithology	samples barren	fragments only	N	*Leiosphaeridia* sp.	*L. minutissima*	*L. crassa*	*L. jacutica*	*L. tenuissima*	*Synsphaeridium* spp.	*Siphophycus* sp.	*Rugosoopsis* sp.	ornamented acritarch	*Pterospermopsimorpha* sp.	*C. buickii**
816.4	Upper Black River Dolomite	black, fine-grained, pyritic	x													
827.1	Upper Black River Dolomite	black, fine-grained			5			3		2						
834.9	Upper Black River Dolomite	dark grey, fine-grained			4			3			1					
850.9	Julius River Member	black, fine-grained matrix mm to 1cm clasts	x													
880.75	Julius River Member	black, fine-grained			9			9								
886.3	Julius River Member	dark grey, fine-grained			1		1									
902.3	Julius River Member	dark grey, fine-grained matrix					1									
907.1	Julius River Member	dark grey, fine-grained matrix	x													
914.9	Julius River Member	dark grey, fine-grained matrix with ~3mm clasts		x												
933.9	Julius River Member	black matrix	x													
968.35	Julius River Member	black matrix			10		9								1	

BR05DD01 drill core

						leiosphaerids						filaments				
meterage	Unit Name	lithology	samples barren	fragments only	N	*Leiosphaeridia* sp.	*L. minutissima*	*L. crassa*	*L. jacutica*	*L. tenuissima*	*Synsphaeridium* spp.	*Siphophycus* sp.	*Rugosoopsis* sp.	ornamented acritarch	*Pterospermopsimorpha* sp.	*C. buickii**
484.5	Areyonga Formation	dark grey, fine-grained matrix			22			8	5		4	5				
489.4	Areyonga Formation	dark grey, fine-grained matrix			3			2				1				
493.6	Areyonga Formation	dark grey, fine-grained matrix			4				4							
517.16	Areyonga Formation	dark grey, fine-grained matrix			18			6	10	1	1					5
531.5	Areyonga Formation	dark grey-brown, fine-grained matrix			5			3	2							
532.25	Areyonga Formation	light grey-green, fine-grained matrix			6			3	2		1					

Wallara-1 drill core

						leiosphaerids						filaments				
meterage	Unit Name	lithology	samples barren	fragments only	N	*Leiosphaeridia* sp.	*L. minutissima*	*L. crassa*	*L. jacutica*	*L. tenuissima*	*Synsphaeridium* spp.	*Siphophycus* sp.	*Rugosoopsis* sp.	ornamented acritarch	*Pterospermopsimorpha* sp.	*C. buickii**
1281.2	Aralka Formation	dark grey, fine-grained, blocky			3			2	1							
1282.4	Aralka Formation	dark grey, fine-grained, shaley			9			1	2		6					
1283.8	Aralka Formation	medium to dark grey, blocky	x													
1284.4	Aralka Formation	dark grey, fine-grained, blocky			1				1							
1286.4	Aralka Formation	dark grey, fine-grained, blocky			4				2	2						
1287.9	Aralka Formation	dark grey, fine-grained, blocky			1				1							
1289.9	Aralka Formation	dark grey, fine-grained			1			1								
1292	Aralka Formation	dark grey, fine-grained			3			1	2							
1293.9	Aralka Formation	dark grey, fine-grained, blocky			3			2						1		
1294.5	Aralka Formation	dark grey, fine-grained	x													
1296.4	Aralka Formation	dark grey, fine-grained, blocky			1						1					
1298.5	Aralka Formation	dark grey, fine-grained, blocky			20			5	15							
1300.4	Aralka Formation	dark grey, fine-grained, blocky			3				1		2					
1301.9	Aralka Formation	dark grey, fine-grained			4			1	2		1					
1304.3	Aralka Formation	black, fine-grained, shaley			10			1	3		6					
1306.2	Aralka Formation	dark grey, fine-grained			2				1	1						
1354.9	Areyonga Formation	medium grey, silty matrix			18			1	10		4				1	2
1367	Areyonga Formation	medium grey, silty matrix			20			3	12			2	3			
1376.8	Areyonga Formation	light grey, fine-grained		x												
1395.9	Areyonga Formation	red-grey fine-grained matrix			6				2		3			1		
1407.5	Areyonga Formation	medium to dark grey, fine-grained matrix			3				2		1					
1411.2	Areyonga Formation	medium-grey, fine-grained matrix			17			4	9		4					
1422.6	Areyonga Formation	medium-grey, fine-grained matrix	x													

Macdonaldryggen Member outcrop samples

					leiosphaerids						filaments				
sample number	lithology	samples barren	fragments only	N	*Leiosphaeridia* sp.	*L. minutissima*	*L. crassa*	*L. jacutica*	*L. tenuissima*	*Synsphaeridium* spp.	*Siphophycus* sp.	*Rugosoopsis* sp.	ornamented acritarch	*Pterospermopsimorpha* sp.	*C. buickii**
G435.25	medium grey, fine-grained			1						1					
G435.35	dark grey, fine-grained	x													
G435.45	dark grey, fine-grained			2						1	1				
G435.56	dark grey, fine-grained, shaley			1						1					
G435.66	dark grey, fine-grained, shaley	x													
G435.76	dark grey, fine-grained	x													
G435.79.5	dark grey, fine-grained	x													
MacG 22-4-0.5m	medium grey, fine-grained, blocky			3	1	1	1								
MacG 22-4-2.15m	dark grey, fine-grained			1	1										
MacG 22-4-3m	medium grey, fine-grained		x												
MacG 22-4-10.2m	medium grey, fine-grained	x													
MacG 22-4-15.2m	dark grey, fine-grained, blocky			1		1									
MacG 22-4-22.5m	medium grey, fine-grained	x													
MacG 22-4-29m	medium grey, fine-grained, blocky	x													

SCYW-79-1a drill core

						leiosphaerids						filaments				
meterage	Unit Name	lithology	samples barren	fragments only	N	*Leiosphaeridia* sp.	*L. minutissima*	*L. crassa*	*L. jacutica*	*L. tenuissima*	*Synsphaeridium* spp.	*Siphophycus* sp.	*Rugosoopsis* sp.	ornamented acritarch	*Pterospermopsimorpha* sp.	*C. buickii**
1172.67	Brighton Limestone	light to medium grey, fine-grained			1							1				
1176.41	Brighton Limestone	medium grey fine-grained, shaley			1			1				1				
1182.24	Brighton Limestone	light to medium grey, fine-grained		x												
1191.42	Tapley Hill Fm	medium grey fine-grained, shaley		x												
1194.42	Tapley Hill Fm	medium grey fine-grained, shaley			12			1	2			8	1			
1201.32	Tapley Hill Fm	medium grey fine-grained, shaley			23			6	7			5	2	2		1
1202.68	Tapley Hill Fm	medium grey fine-grained, shaley			4				2			2				
1205.13	Tapley Hill Fm	medium grey fine-grained, shaley		x												
1207.16	Tapley Hill Fm	medium grey fine-grained, shaley			1						1					
1215.88	Tapley Hill Fm	dark grey, fine-grained, shaley			1				1							
1218.1	Tapley Hill Fm	dark grey, fine-grained, shaley			1							1				
1225.26	Tapley Hill Fm	dark grey, fine-grained, shaley			32			3	12			14	3			
1226.13	Tapley Hill Fm	dark grey, fine-grained			1				1							
1230.73	Tapley Hill Fm	dark grey, fine-grained, shaley			1				1							
1237.3	Tapley Hill Fm	medium grey fine-grained, shaley		x												
1238.7	Tapley Hill Fm	dark grey, fine-grained, shaley			28			8	4			12	2	2		
1239.4	Tapley Hill Fm	medium grey fine-grained, shaley		x												
1247.7	Tapley Hill Fm	medium grey fine-grained, shaley			1				1							
1249.86	Tapley Hill Fm	medium grey fine-grained, shaley		x												
1254.9	Tapley Hill Fm	medium to dark, fine-grained, shaley			13			2	3			7			1	
1256.9	Tapley Hill Fm	medium to dark, fine-grained, shaley		x												
1260.69	Tapley Hill Fm	dark grey, fine-grained, shaley			2			1	1							
1266.74	Tapley Hill Fm	dark grey, fine-grained, shaley			7				3			3			1	
1278.74	Tapley Hill Fm	medium grey fine-grained, shaley		x												
1289.73	Tapley Hill Fm	medium grey fine-grained, shaley			2				2							
1298.81	Tapley Hill Fm	dark grey, fine-grained, shaley			9				5	1		3				
1306.17	Tapley Hill Fm	dark grey, fine-grained, shaley			1			1								
1314.87	Tapley Hill Fm	dark grey, fine-grained, shaley			5				4			1				
1317.18	Tapley Hill Fm	dark grey, fine-grained, shaley			1				1							
1323.85	Tapley Hill Fm	dark grey, fine-grained, shaley	x													
1338.78	Tapley Hill Fm	dark grey, fine-grained			12			1	1	2		7	1			
1341.78	Tapley Hill Fm	dark grey, fine-grained, shaley			6				4			2				
1350.76	Tapley Hill Fm	dark grey, fine-grained, shaley			12				4			7	1			
1357.3	Tapley Hill Fm	dark grey, fine-grained, shaley			10			1	2			5	2			
1358.69	Tapley Hill Fm	dark grey, fine-grained, shaley			6			1	3			2				

Supplementary Information References:

Allison, C. and Awramik, S., 1989, Organic-walled microfossils from the earliest Cambrian or latest Proterozoic Tindir Group rocks, northwest Canada: Precambrian Research, v. 43, p. 253–294.

Babinski, M., Vieira, L. C. and Trindade, R. I. F., 2007, Direct dating of the Sete Lagoas cap carbonate (Bambuí Group, Brazil) and implications for the Neoproterozoic glacial events: Terra Nova, v. 19, p. 401–406.

Bartley, J. K., Semikhatov, M. A., Kaufman, A. J., Knoll., A. H., Pope, M. C. and Jacobsen, S. B., 2001, Global events across the Mesoproterozoic-Neoproterozoic boundary: C and Sr isotope evidence from Siberia: Precambrian Research, v. 111, p. 165–202.

Bertrand-Sarfati J. and Siedlecka, A., 1980, Columnar stromatolites of the terminal Precambrian Porsanger Dolomite and Grasdal Formation of Finnmark, north Norway: Norsk Geologisk Tidsskrift, v. 60, p. 1–27.

Bertrand-Sarfati, J., Moussine-Pouchkine, A., Amard, B. and Ahmed, A. Aït Kaci., 1995, Ediacaran fauna found in western Africa and evidence for an early Cambrian glaciation: Geology, v. 23, p. 133–136.

Bosak, T., Lahr, D. J. G., Pruss, S. B., Macdonald, F. A., Dalton, L. and Matys, E., 2011a, Agglutinated tests in post-Sturtian cap carbonates of Namibia and Mongolia: Earth and Planetary Science Letters, v. 308, p. 29–40.

Bosak, T., Macdonald, F., Lahr, D. and Matys, E., 2011b, Putative Cryogenian ciliates from Mongolia: Geology, v. 39, p. 1123–1126.

Bosak, T., Lahr, D. J. G., Pruss, S. B., Macdonald, F. A., Gooday, A. J. and Dalton, L., 2012, Possible early foraminiferans in post-Sturtian (716-635 Ma) cap carbonates: Geology, v. 40, p. 67–70.

Brain, C. K., Prave, A. R., Hoffmann, K.–H., Fallick, A. E., Botha, A., Herd, D., Sturrock, C., Young, I., Condon, D. and Allison, S., 2012, The first animals: ca. 760-million-year-old sponge-like fossils from Namibia: South African Journal of Science, v. 108 (1/2), article 658, 8 pages.

Butterfield, N., Knoll, A. and Swett, K., 1994, Paleobiology of the Neoproterozoic Svanbergfjellet Formation, Spitsbergen: Fossils and Strata, v. 34, 84p.

Butterfield, N., 2005a, Probable Proterozoic fungi: Paleobiology, v. 31, p. 165–182.

Butterfield, N., 2005b, Reconstructing a complex early Neoproterozoic eukaryote, Wynniatt Formation, arctic Canada: Lethaia, v. 38, p. 155–169.

Butterfield, N. J. and Grotzinger, J. P., 2012, Palynology of the Huqf Supergroup, Oman. In Bhat, G.M., Craig, J., Thurow, J. W., Thusu, B. & Cozzi, A., eds., Geology and Hydrocarbon Potential of Neoproterozoic-Cambrian Basins in Asia. Geological Society of London Special Publication, v. 366.

Butterfield, N. and Rainbird, R., 1998, Diverse organic-walled microfossils, including "possible dinoflagellates" from the early Neoproterozoic of arctic Canada: Geology, v. 26, p. 963–966.

Calver, C. R., 1998, Isotope stratigraphy of the Neoproterozoic Togari Groups, Tasmania: Australian Journal of Earth Sciences, v. 45, p. 865–874.

Cohen, P. and Knoll, A., 2012, Scale microfossils from the mid-Neoproterozoic Fifteenmile Groups, Yukon Territory: Journal of Paleontology, v. 86, p. 775–800.

Corsetti, F. A., Awramik, S. M. and Pierce, D., 2003, A complex microbiota from snowball Earth times: microfossils from the Neoproterozoic Kingston Peak Formation, Death Valley, USA: Proceedings of the National Academy of Sciences, USA, v. 100, p. 4399–4404.

Dehler, C. M., Karlstrom, K. E, Gehrels, G. E., Timmons, J. M. and Crossey, L. C., 2012, Stratigraphic revision, provenance and new age constraints of the Nankoweap Formation and Chuar Group, Grand Canyon Supergroup, Grand Canyon, Arizona:Geological Society of America Abstracts, v. 44, no. 6, p. 82.

Dong, L., Xiao, S., Shen, B., Yuan, X., Yan, X., Peng, Y., 2008. Restudy of the worm-like carbonaceous compression fossils *Protoarenicola, Pararenicola*, and *Sinosabellidites* from early Neoproterozoic successions in North China: Palaeogeography, Palaeoclimatology, Palaeoecology, v. 258, p. 138–161.

Eyles, C. H., Eyles, N. and Grey, K., 2007, Palaeoclimate implications form deep drilling of Neoproterozoic strata in the Officer Basin and Adelaide Rift Complex of Australia; a marine record of wet-based glaciers: Palaeogeography, Palaeoclimatology, Palaeoecology, v. 248, p. 291–312.

Fairchild T. R., Schopf, J. W., Shen-Miller, J., Guimarães, E. M., Edwards, M. D., Lagstein, A., Li, X., Pabst, M. and Soares de Melo-Filho, L., 1996, Recent discoveries of Proterozoic microfossils in south-central Brazil: Precambrian Research, v. 80, p. 125–152.

Gaucher, C., Frimmel, H. E. and Germs, G. J. B., 2005, Organic-walled microfossils and biostratigraphy of the upper Port Nolloth Group (Namibia): implications for the latest Neoproterozoic glaciations: Geological Magazine, v. 142, p. 539–559.

Glaessner, M. F., Preiss, W. V. and Walter, M. R., 1969, Precambrian columnar stromatolites in Australia: morphological and stratigraphic analysis: Science, v. 164, p. 1056–1058.

Gorjan, P., Veevers, J. J. and Walter, M. R., 2000, Neoproterozoic sulfur-isotope variation in Australia and global implications: Precambrian Research, v. 100, p. 151–179.

Haines, P. W., Hocking, R. M., Grey, K. and Stevens, M. K., 2008, Vines 1 revisted: are older Neoproterozoic glacial deposited preserved in Western Australia?: Australian Journal of Earth Sciences, v. 55, p. 397–406.

Hambrey M. J. and Spencer, A. M., 1987, Late Precambrian diamictites of northeastern Svalbard: Geological Magazine, v. 119, 527–551.

Hermann, T., 1990, Organic World One Billion years ago. Nauka, Leningrad, 51 p.

Hoffman, P., Halverson, G., Domack, E., Maloof, A., Swanson-Hysell, N. and Cox, G., 2012, Cryogenian glaciations on the southern tropical paleomargin of Laurentia (NE Svalbard and East Greenland), and a primary origin for the upper Russøya (Islay) carbon isotope excursion: Precambrian Research, v. 206-207, p. 137–158.

Hoffman, P. F., 2011, Strange bedfellows: glacial diamictite and cap carbonate from the Marinoan (635 Ma) glaciation in Namibia: Sedimentology, v. 58, p. 57–119.

Hofmann, H. J., 1985, The mid-Proterozoic Little Dal macrobiota, Mackenzie Mountains, North-west Canada: Palaeontology, v. 28, p. 331–354, pl. 35–39.

Hofmann, H. J. and Aitken, J. D., 1979, Precambrian biota from the Little Dal Group, Mackenzie Mountains, northwestern Canada: Canadian Journal of Earth Science, v. 16, 150–166.

Hofmann, H. J., Narbonne, G. M. and Aitken, J. D., 1990, Ediacaran remains from intertillite beds in northwestern Canada: Geology, v. 18, p. 1199–1202.

Hofmann, H. J. and Rainbird, R., 1995, Carbonaceous megafossils from the Neoproterozoic Shaler Supergroup of arctic Canada: Palaeontology, v. 37, p. 721–731.

James, N. P., Narbonne, G. M., Dalrymple, R. W. and Kyser, T. K., 2005, Glendonites in Neoproterozoic low-latitude, interglacial, sedimentary rocks, northwest Canada: Insights

into the Cryogenian ocean and Precambrian cold-water carbonates: Geology, v. 33, p. 9–12.

Jankauskas, T., Mikhailova, N. Hermann, T., 1989, Mikrofossilii Dokembria SSSR. Nauka, Leningrad, 191p.

Jones, D. S., Maloof, A. C., Hurtgen, M. T., Rainbird, R. H. and Schrag, D. P., 2010, Regional and global chemostratigraphic correlation of the early Neoproterozoic Shaler Supergroup, Victoria Island, northwestern Canada, v. 181, P. 43–63.

Karlstrom, K., Bowring, S., Dehler, C., Knoll, A., Porter, S., Des Marais, D., Weil, A., Sharp, Z., Geissman, J., Elrick, M., Timmons, J., Crossey, L., Davidek, 2000, v. 28, p. 619–622.

Kendall, B., Creaser, R. A. and Selby, D., 2006, Re-Os geochronology of postglacial black shales in Australia: constraints on the timing of "Sturtian" glaciation: Geology, v. 34, p. 729–732.

Kendall, B., Creaser, R. A., Calver, C. R., Raub, T. and Evans, D. A. D., 2009, Correlation of Sturtian diamictite successions in southern Australia and northwestern Tasmania by Re-Os black shale geochronology and the ambiguity of "Sturtian"-type diamictite-cap carbonate pairs as chronostratigraphic marker horizons: Precambrian Research, v. 172, p. 301–310.

Knoll, A., 1984, Microbiotas of the late Precambrian Hunnberg Formation, Nordaustlandet, Svalbard: Journal of Paleontology, v. 58, p. 131–162.

Knoll, A. H., Blick, N. and Awramik, S. M., 1981, Stratigraphic and ecologic implications of late Precambrian microfossils from Utah: American Journal of Science, v. 281, p. 247–263.

Knoll, A. and Calder, S., 1983, Microbiotas of the late Precambrian Ryssö Formation, Nordaustlandet, Svalbard: Palaeontology, v. 26, p. 57–61.

Knoll, A. H., Kaufmann, A. J. and Semikhatov, M. A., 1995, The carbon isotopic composition of Proterozoic carbonates: Riphean successions from northwestern Siberia (Anabar Massif, Turukhansk upfilt): American Journal of Science, v. 295, p. 823–850.

Knoll, A., Swett, K., Burkhardt, E., 1989, Paleoenvironmental distribution of microfossils and stromatolites in the upper Proterozoic Backlundtoppen Formation, Spitsbergen: Journal of Paleontology, v. 63, p. 129–145.

Knoll, A., Swett, K., Mark, J., 1991, Paleobiology of a Neoproterozoic tidal flat/lagoonal complex: the Draken Conglomerate Formation, Spitsbergen: Journal of Paleontology, v. 65, 531–570.

Levashova, N. M., Meert, J. G., Gibsher, A. S., Grice, W. C. and Bazhenov, M. L., 2011, The origin of microcontinents in the Central Asian Orogenic Belt: constraints from paleomagnetism and geochronology: Precambrian Research, v. 185, p. 37–54.

Li, Z.-X., Evans, D. A. D., Halverson, G., 2013, Neoproterozoic glaciations in a revised global palaeogeography from the breakup of Rodinia to the assembly of Gondwanaland: Sedimentary Geology, v. 294, p. 291–232.

Love, G., Grosjean, E., Stalvies, C., Fike, D. A., Grotzinger, J. P., Bradley, A. S., Kelly, A. E., Bhatia, M. Meredith, W., Snape, C. E., Bowring, S. A., Condon, D. J. and Summons, R. E., 2009, Fossil steroids record the appearance of Demospongiae during the Cryogenian period: Nature, v. 457, p. 718–722.

Macdonald, F. A., 2011, The Tsagaan Oloom Formation, southwestern Mongolia, *in* Arnaud, E., Halverson, G., Shields-Zhou, G., eds., The Geological Record of Neoproterozoic Glaciations: Geological Society of London Memoirs, no. 36, p. 331–337.

Macdonald, F. A., Halverson, G. P., Strauss, J. V., Smith, E. F., Cox, G., Sperling, E. A., Roots, C. F., 2012, Early Neoproterozoic Basin Formation in Yukon, Canada: Implications for the make-up and break-up of Rodinia: Geoscience Canada, v. 39, p. 77–99.

Macdonald, F. A., Schmitz, M. D., Crowley, J. L., Roots, C. F., Jones, D. S., Maloof, A. C., Strauss, J. V., Cohen, P. A., Johnston, D. T. and Schrag, D. P., 2010a, Calibrating the Cryogenian: Science, v. 327, p. 1241–1243.

Macdonald, F. A., Strauss, J. V., Rose, C. V., Dudás, F. Ö. and Schrag, D. P., 2010b, Stratigraphy of the Port Nolloth Group of Namibia and South Africa and implications for the age of Neoproterozoic iron formations: American Journal of Science, v. 310, p. 862–888.

Macdonald, F., Prave, A. R., Petterson, R., Smith, E., Pruss, S. B., Oates, K., Waechter, F., Trotzuk, D. and Fallick. A., 2013, The Laurentian record of Neoproterozoic glaciation, tectonism, and eukaryotic evolution in Death Valley, California. GSA Bulletin, v. 7–8, p. 1203–1223.

Maloof, A., Rose, C., Beach, R., Samuels, B., Calmet, C., Erwin, D., Poirier, G., Yao, N. and Simons, F., 2010, Possible animal-body fossils in pre-Marinoan limestones from South Australia: Nature Geoscience, v. 3, p. 653–659.

Misi, A., Kaufman, A. J., Veizer, J., Powis, K., Azmy, K., Boggiani, P. C., Gaucher, C., Batista, J., Teixeira, G., Sanches, A. L. and Iyer, S. S. S., 2007, Chemostratigraphic correlation of Neoproterozoic successions in South America: Chemical Geology, v. 237, P. 143–167.

Nagy, R. M., Porter, S. M., Dehler, C. M. and Shen, Y., 2009, Biotic turnover driven by eutrophication before the Sturtian low-latitude glaciation: Nature Geoscience, v. 2, p. 415–418.

Preiss, W. V., 1973, Palaeoecological interpretations of South Australia. Precambrian stromatolites. Journal of the Geological Society of Australia, v. 19, p. 501–532.

Preiss, W.V., 2000, The Adelaide Geosyncline of South Australia and its significance in Neoproterozoic continental reconstruction: Precambrian Research, v. 100, p. 21–63.

Pruss, S. B., Bosak, T., Macdonald, F. A., McLane, M. and Hoffman, P. F., 2010, Microbial facies in a Sturtian cap carbonate, the Rasthof Formation, Otavi Group, northern Namibia: Precambrian Research, v. 181, p. 187–198.

Qian, M-P., Jiang, Y., Yu, M-G., 2009, Neoproterozoic millimetric-centimetric carbonaceous fossils from Northern Anhui and Jiangsu, China: Acta Palaeontologica Sinica, v. 48, p. 73–88.

Raaben, M. E., Lyubtsov, V. V. and Predovsky, A. A., 1995, Correlation of stromatolitic formations of northern Norway (Finnmark) and northwestern Russian (Kildin Island and Kanin Peninsula): Norges Geologiske Undersøkelse Special Publication, no.7, p. 233–246.

Saito, Y., Tiba, T. and Matsubara, S., 1988, Precambrian and Cambrian cherts in northwestern Tasmania: Bulletin of the National Museum, Tokyo, Series C, v. 14, no. 2, p. 59–70.

Serezhnikova, E. A., Ragozina, A. L., Dorjnamjaa, D. and Zaitseva, L. V., 2014, Fossil microbial communities in Neoproterozoic interglacial rocks, Maikhanuul Formation, Zavkhan Basin, Western Mongolia: Precambrian Research, v. 245, p. 66–79.

Sergeev, V., Chumakov, N. M., Semikhatov, M. A. and Vorob'eva, N. G., 2013, Microfossils from the cap dolomites of the lower Vendian Churochnaya Formation in the Polyudov Range (North Urals): paleoecological approach to interpretation of late Proterozoic glaciations: Stratigraphy and Geological Correlation, v. 21, p. 1–7.

Sergeev, V. and Schopf, J. W., 2010, Taxonomy, paleoecology and biostratigraphy of the late Neoproterozoic Chichkan microbiota of south Kazakhstan: the marine biosphere on the eve of the metazoan radiation: Journal of Paleontology, v. 84, p. 363–401.

Simonetti, C. and Fairchild, T. R., 2000, Proterozoic microfossils from the subsurface siliciclastic rocks of the São Francisco Craton, south-central Brazil: Precambrian Research, v. 103, p. 1–29.

Schopf, J. W., 1968, Microflora of the Bitter Springs Formation, late Precambrian, central Australia: Journal of Paleontology, v. 42, p. 651–688.

Spencer, A. M. and Spencer, M. O., 1972, The late Precambrian/Lower Cambrian Bonahaven Dolomite of Islay and its stromatolites: Scottish Journal of Geology, v. 8, p. 269–282.

Strauss, J., Knoll, A., Cohen, P., Macdonald, F., 2012, Diverse vase-shaped microfossils in the Neoproterozoic Callison Lake Dolostone, Coal Creek Inlier, Yukon Territory, Canada: Geological Society of America Asbtracts with Programs, v. 44, no. 7, p. 603.

Tang, Q., Pang, K., Xiao, S., Yuan, X., Ou, Z. and Wan, B., 2013, Organic-walled microfossils from the early Neoproterozoic Liulaobei Formation in the Huainan region of North China and their biostratigraphic significance: Precambrian Research, 236:157–181.

Uhlein, A., Alvarenga, C. J. S., Dardenne, M. A. and Trompette, R. R., 2011, The glaciogenic Jequitaí Formation, southeastern Brazil, *in* Arnaud, E., Halverson, G. P.,

Shields-Zhou, G., eds., The Geological Record of Neoproterozoic Glaciations: Geological Society of London Memoirs, no. 36, p. 541–546.

Vidal, G., 1976, Late Precambrian acritarchs from the Eleonore Bay Group and Tillite Group in East Greenland: a preliminary report: Grønlands Geologiske Undersøgelse Rapport, no. 78.

Vidal, G., 1979, Acritarchs from the Upper Proterozoic and Lower Cambrian of East Greenland: Grønlands Geologiske Undersøgelse Bulletin, v. 134.

Vidal, G., 1981, Micropalaeontology and biostratigraphy of the Upper Proterozoic and Lower Cambrian sequence in East Finnmark, northern Norway: Norges Geologiske Undersøkelse, v. 362, p. 1–53.

Vidal, G. and Ford, T., 1985. Microbiotas from the Late Proterozoic Chuar Group (Northern Arizona) and Uinta Mountain Group (Utah) and their chronostratigraphic implications: Precambrian Research, v. 28, p. 349–389.

Walter, M and Veevers, J. J., 1997, Australia Neoproterozoic palaeogeography, tectonic, and supercontinental connections: AGSO Journal of Australian Geology and Geophysics, v. 17, p. 73–92.

Xiao, S., Shen, B., Tang, Q, Kaufman, A. J., Yuan, X., L, J. and Qian, M., 2014, Biostratigraphic and chemostratigraphic constraints on the age of early Neoproterozoic carbonate successions in North China: Precambrian Research, v. 246, p. 208–225.

Yin, L., 1990, Microbiota from middle and late Proterozoic iron and manganese ore deposits in China: Special Publication of International Association of Sedimentologists, v. 11, p. 109–118.

Yin, L. and Sun, W., 1994, Microbiota from the Neoproterozoic Liulaobei Formation in the Huainan region, northern Anhui, China: Precambrian Research, v. 65, p. 95–114.

Zang, W-L. and Walter, M. R., 1992, Late Proterozoic and Cambrian microfossils and biostratigraphy, Amadeus Basin, central Australia: Memoirs of the Association of Australasian Palaeontologists, v. 12, p. 1–132.

Chapter Three: Global species richness record and biostratigraphic potential of early to middle Neoproterozoic eukaryote fossils

Abstract

Over the past several decades, a number of studies have addressed the record of eukaryotic species richness in the Precambrian. However, the relative scarcity of radiometric age constraints during this time necessitated the use of coarse time bins (~100 Ma) as well as the omission of poorly dated units, resulting in low resolution. Here we describe a new dataset of paleontological, geochemical and radiometric data to which the CONOP correlation and seriation algorithm has been applied to produce an ordination of biotic, isotopic and age events. This ordinal sequence was calibrated to geologic time to produce a high-resolution eukaryotic species richness record for the early to middle Neoproterozoic Era. We find an increase in species richness at ~805 Ma, sustained high richness levels until a decrease ~770 Ma that resulted from a large number of acritarch extinctions, and then a sharp and short-lived increase at ~760 Ma reflecting first appearances of vase-shaped microfossil taxa, and finally a sharp decrease in richness and extended nadir through the Sturtian and Marinoan glacial periods.

Use of CONOP with this new dataset also permitted assessment of fossil taxa that had been previously suggested as Neoproterozoic biostratigraphic index taxa. Our results

provide support for biostratigraphic use of the acritarch *Cerebrosphaera buickii* and for vase-shaped microfossils as a group and individually.

The section correlation derived from this dataset reveals a reduction in the number of units described during the second half of the 1 Ga to 635 Ma interval of study and can be used to make testable predictions for potential sections recording specific fossil taxa and carbon isotopic excursions such as the Bitter Springs stage and Islay isotopic anomaly.

Introduction

Paleontological as well as molecular clock data indicate that the early to middle Neoproterozoic Era was one of major eukaryotic diversifications and extinctions (Knoll, 1994; Knoll et al., 2006; Huntley et al., 2006; Parfrey et al., 2011; Riedman et al., 2014). This interval was also marked by fluctuations in oceanic and atmospheric chemistry (Meyer and Kump, 2008; Canfield, 2014), formation and rifting of the supercontinent Rodinia (Li et al., 2008), and at least two global glaciations (Snowball Earth events; Hoffman and Li, 2009). Due to a general paucity of age constraints (Condon and Bowring, 2011), correlations of relevant stratigraphic successions have been problematic and the relative timings and relationships of these transformative events are still poorly constrained. By applying the CONOP ordination software to the early to middle Neoproterozoic (1 Ga to ~635 Ma) eukaryotic fossil record, we have resolved correlation and seriation of twenty-nine

fossiliferous sequences based upon biostratigraphy, radiometric age data and globally synchronous carbon isotopic negative excursions. With this new ordination of fossiliferous successions we were able to produce a high-resolution view of eukaryotic species richness for this time. This new estimate of eukaryote species richness trends in the first 80% of the Neoproterozoic is interesting in itself for purposes of understanding early eukaryotic evolution, but is also valuable as a context for understanding interactions of biological, geochemical and tectonic changes. In addition, the ordination of events used to establish the species richness record can also be used to answer questions about biostratigraphic potential of Neoproterozoic fossils.

Over the past few decades several estimates of Precambrian eukaryotic diversity and disparity have been published (Knoll, 1994; Vidal and Moczydłowska-Vidal, 1997; Huntley et al., 2006; Knoll et al., 2006), all of which indicate broad trends of increase in the Mesoproterozoic Era, leading to a peak and then decline by 750 to 600 Ma. However, the resolution of these studies is coarse because poor age constraints necessitated the use of broad (>100 Ma) time bins. Additionally, these estimates incorporate data from relatively few units, inviting worry over the effects of sampling bias. In order to include a larger number of fossiliferous units, however, new constraints on their ages are required. Here, this was accomplished by use of a combination of biostratigraphy, isotope chemostratigraphy and associated radiometric ages.

Neoproterozoic biostratigraphy has long been recognized as possibly useful but certainly problematic (Vidal, 1981a; Kaufman et al, 1992; Knoll, 1994; Butterfield and Rainbird, 1998). This is chiefly due to long or poorly constrained stratigraphic ranges or concerns of under-sampling of certain intervals (Butterfield and Grotzinger, 2012). Problematic taxonomy poses an additional difficulty. The dominant eukaryotic fossils of the Neoproterozoic are the acritarchs, originally sphaeroidal, organic-walled microfossils that are typically tens to hundreds of micrometers in diameter; smooth-walled, ornamented, or spine (processes)- bearing and are of unknown biological affinity. The question of the biological placements of these forms is not a hindrance to their use in biostratigraphy, but the lack of biological context is significant in that acritarch taxonomic hierarchy, although guided by morphology, is not necessarily guided by synapomorphies of coherent biological groups. This factor requires treatment of diversity of this group at the species level as the genus-concept for the acritarchs appears to be biologically meaningless.

Recent quantitative studies of Ediacaran-age acanthomorphic acritarchs of the Doushantuo Formation have resulted in recognition of two acritarch biozones applicable for regional correlation in North China with possible, but as yet untested, global applications (McFadden et al., 2009; Yin et al., 2011). Although no such studies have yet evaluated biostratigraphic potential of early to middle Neoproterozoic fossils, certain acritarch species have been suggested as possible index taxa due to their distinctive morphological features and seemingly relatively short durations. These include *Cerebrosphaera buickii* (Hill and

Walter, 2000; Grey et al., 2011) and *Trachyhystrichosphaera aimika* (Kaufman et al., 1992; Vidal et al., 1993; Butterfield et al., 1994; Knoll, 1996; Tang et al., 2013).

Fossils of the early to middle Neoproterozoic Era also include organic-walled fossil macroalgae (e.g. *Longfengshania*, *Tawuia*) and vase-shaped microfossils (VSMs), the originally organic-walled but frequently silicified or pyritized testate amoebae. VSMs have been found globally and in varying lithologies (Martí Mus and Moczydłowska, 2000;Porter and Knoll, 2000) and the biostratigraphic potential of VSMs as a broad group has long been suggested (Knoll and Vidal, 1980; Vidal et al., 1993; Porter and Knoll, 2000; Macdonald et al., 2013). Recently Strauss and colleagues (2014) reported a VSM assemblage and a Re-Os date from associated rocks in northwestern Canada, and discussed biostratigraphic potential, making the point that correlation should be based upon occurrences of species, not the group as a whole. Although the importance of this matter to the VSMs is as yet unclear (any diachronism within the VSM group has not yet been identified), the concern Strauss raises is one that must be extended to all fossil groups. Biostratigraphic correlations must be based upon unique taxa (either as individuals or designated combinations) rather than upon morphological grades (c.f. Xiao et al., 1997). Morphogroups such as “macroalgae”, “LOEM=large ornamented Ediacaran microfossils”, “ELP=Ediacaran leiospheres palynoflora” and “ECAP=Ediacaran complex acritarch palynoflora” are useful shorthand for broad-discussions of biotic changes but are of spurious use for biostratigraphic correlation.

In the past few decades increasingly high resolution geochemical analyses have permitted basin-wide and regional correlations and have resulted in global composite records of carbon and strontium isotopic values that permit global chemostratigraphic correlations. Additionally, new radiometric ages constrain major, globally recognizable features of the carbon isotopic record (Macdonald et al., 2010; Strauss et al., 2014), providing temporal context for chemostratigraphic correlations. These geochemical and radiometric data can be combined with biostratigraphic data to correlate units of variable lithological, depositional, and diagenetic histories. Indeed, Hill and colleagues (2000) and Hill and Walter (2000) used a combination of isotope chemostratigraphy, stromatolite stratigraphy and acritarch biostratigraphy (*C. buickii* first occurrences) to create five tie-lines for Australian interbasinal and global correlations and hypothesized an older age of the Svanbergfjellet Formation of Svalbard than had been previously suggested—an age subsequently corroborated by carbon and strontium isotopic data (Hoffman et al., 2012). The approach of combining paleontologic, geochemical and radiometric data for purposes of global correlation is extended here but with the ultimate goal of developing a species richness record. This required utilization of the whole of the eukaryotic fossil record for this interval rather than *a priori* determinations of index taxa. Management of all eukaryote fossil occurrences over 365 million years of Earth history quickly becomes computationally overwhelming and requires automation. The CONOP seriation and correlation program is

used here to establish best-fit hypotheses of ordinal timelines of isotopic, radiometric and biotic (species first and last occurrences) events.

Methods

Here we present analyses of paleontological data from eighty-one formations in twenty-nine paleogeographically distant successions (Fig. 1). These analyses required well-constrained taxonomic data (i.e. accurate identification and careful synonymy) and stratigraphic depth information for local first and last occurrences of each taxon. The inclusion of radiometric age data and negative carbon isotopic anomalies provided time calibration and further constraints on sequence.

Paleontological data

Although Precambrian paleontology is a rather young field, a staggering number of taxa have been named, several many times over. This problem is especially acute for the principal fossil group of this time, the acritarchs. Taphonomic and ontogenetic variations of a given species may be described under multiple names, resulting in inflation of species richness; alternatively, richness may be artificially depressed if morphological differences are lost during decay and diagenesis or are too subtle to be recognized during routine transmitted light microscopy (Riedman and Porter, *in press*).

During our collection of species first and last occurrence data from the literature the greatest of care was exercised in accepting, rejecting or synonymizing fossil identifications (see Table 1). Because of the importance of accurate and consistent identification for these biostratigraphic analyses, occurrences of fossil taxa were not accepted unless accompanied by convincing illustrations. Good-quality illustration was particularly important when an early find of a given species was left in open nomenclature and later discovered and named in a subsequent publication (e.g. fossils recorded as only VSMs or "tear-shaped fossils" in multiple units were later identified in Porter et al., 2003; *Kildinella* sp., pl. 4, C and D in Vidal 1979 recognized as a new species with occurrences in the Chuar Group and Alinya Formation, Riedman and Porter, *in press*).

Stratigraphic range data

Because the CONOP program operates upon local estimates of first and last appearance data (FAD and LAD) and is constrained to honor observed species co-occurrences, the stratigraphic positions of fossil occurrences were required of the primary paleontological literature. In some cases important and diversely fossiliferous assemblages could not be included here because those data were missing; in particular, the well-preserved fossil assemblage of the ~1 Ga Lakhanda Group of Siberia is omitted due to a lack of taxonomic range information.

When possible, occurrence data from multiple publications of the same unit were combined into a single section to simplify correlation (e.g. Butterfield et al. [1994] and Butterfield [2004] for the Svanbergfjellet Formation or Hofmann and Aitken [1979] and Hofmann [1985] for the Little Dal Group). Additionally, fossiliferous sections reported in separate publications but of known superpositional relationship were "stitched together" by creating fictitious marker beds within CONMAN, the CONOP data manager. In this way the program received as much relative depth information as possible for biostratigraphic correlation. The ability to insert fictitious marker beds was also useful where unfossiliferous units or hiatuses were known to occur within or between units. This allowed creation of fictitious intervening sections that could stretch or shrink to accommodate the best-fit correlation result. Taxon range-ends at the base or top of a measured section are automatically discounted as estimators of FADs or LADs. The same should apply to range ends at a significant hiatus; this is achieved most simply by replacing the hiatus with the fictitious section.

In the Phanerozoic case histories to which CONOP has been applied, taxon ranges typically have durations much briefer than the time spans of the sections in which they are preserved. The Neoproterozoic data reverse this relationship: taxon durations tend to exceed the time span of measured sections. Indeed, some "sections" are single samples, used to establish coexistences. Consequently, the task of sequencing Neoproterozoic events places a

higher premium on the ability of the CONOP algorithms to include other time-stratigraphic information.

Radiometric and Carbon Isotopic data

Biostratigraphic correlations were aided and calibrated by addition of radiometric ages and carbon isotopic data. Radiometric age data were applied conservatively, included if they were established from the fossiliferous sections or basinal correlations. Carbon isotopic events were included within fossiliferous sections only if those data were derived from the rocks of that stratigraphic succession. Because the two most significant carbon isotope anomalies recorded during this interval, the Bitter Springs carbon isotopic stage and the Islay negative carbon excursion, are thought to be globally synchronous and have recently been constrained in age (see below), the occurrences of these isotopic events in a fossiliferous unit served not only for chemostratigraphic correlation, but also acted, effectively, as an age constraint.

The Neoproterozoic carbon isotopic record is characterized by generally high values (~+5‰ $\delta^{13}C_{carb}$) and punctuated by high amplitude excursions into negative values (~-5‰; Halverson and Shields-Zhou, 2011). This is as opposed to the lower 0 to 1‰ $\delta^{13}C_{carb}$ and relatively more uniform values of the Mesoproterozoic and Phanerozoic Eras (Halverson et al., 2010). The first of these negative excursions in the Neoproterozoic Era is the Bitter Springs carbon isotopic stage, named for its initial discovery in the Bitter Springs Formation

of Amadeus Basin, Australia (Hill et al., 2000) and subsequently found in rocks of Svalbard (Halverson et al., 2005, 2007) and across northwestern Canada (Macdonald et al., 2010). Age constraints were recently established for the Bitter Springs stage; in the central Ogilvie Mountains of Canada a U-Pb date of 811.51 ± 0.25 Ma was obtained from a bedded tuff deposited just as $\delta^{13}C_{carb}$ values began to fall (Macdonald et al., 2010). The minimum age constraint is less robust, stratigraphically higher in the same succession a U-Pb date of 717.43 ± 0.14 Ma has been obtained from a rhyolite (Macdonald et al., 2010) and in the nearby Coal Creek Inlier of the Ogilvie Mountains a Re-Os date of 739.9 ± 6.1 Ma (Strauss et al., 2014) has been established, both of these are well above the return to normal, high $\delta^{13}C$ values.

The Islay carbon isotopic excursion, the younger of the two isotopic events of the early to middle Neoproterozoic, was named for the Islay Limestone in southwestern Scotland where it was first recognized (Brasier and Shields, 2000; Prave et al., 2009). The Islay negative excursion has not been as widely documented as the Bitter Springs stage, which appears to have had a more protracted negative interval, but it has been recorded in fossiliferous units in Svalbard (Halverson et al., 2004; Hoffman et al., 2012) and in northwestern Canada (Macdonald et al., 2010, Strauss et al., 2014). The Islay isotopic event precedes and has been thought to presage the onset of the Sturtian glaciation, the first of the Cryogenian Snowball Earth glacial events (Halverson and Shields-Zhou, 2011). As with the Bitter Springs stage, the maximum age constraint on the Islay isotopic excursion was

determined from rocks deposited in the initial stages of the event as values had begun to fall. The same 739.9 ± 6.1 Ma Re-Os age that constrains the Bitter Springs stage down-section was obtained from a silicified black shale of the Callison Lake Dolostone in the Coal Creek Inlier of the Ogilvie Mountains and it records the earliest interval of the Islay event. The minimum age of the Islay isotopic event also comes from the Ogilvie Mountains where a U-Pb age of 717.43± 0.14 Ma from a rhyolite underlies a dated (716.4 ± 0.24 Ma) brecciated tuff within a Sturtian correlative glacial unit (Macdonald et al., 2010).

Both the Bitter Springs stage and Islay isotopic excursion were broken into three slightly overlapping intervals for inclusion in our dataset; these include the decrease in $\delta^{13}C_{carb}$ values, a peak or plateau, and increase to previous levels. In the decreasing and increasing intervals a portion of the base "typical Neoproterozoic" values were included and each overlapped slightly with the peak or plateau interval. This applies conservative uncertainty ranges to different parts of the anomalies, increasing the likelihood of robust correlation (Sadler, 2012) and making it possible to utilize isotopic data even if the anomaly is truncated in a section (e.g. only the bottom and middle intervals Islay excursion are recorded in the Russøya Member of the Polarisbreen Group, Svalbard). These carbon isotopic excursion intervals were coded onto existing fossiliferous sections, often by utilizing stratigraphic positions of distinctive marker beds described in both paleontological and geochemical literature to determine meterage scaled to fossil occurrence depths. An example of this is seen in the extrapolated Backlundtoppen Formation and Russøya Member

section derived from paleontological work by Knoll and colleagues (1989) that allowed placement of the Islay isotopic excursion from data of Hoffman et al. (2012) due to both papers' description and position of the distinctive Dartboard Dolomite Member.

Glacial Tillites

During the early to middle Neoproterozoic Era two globally synchronous glaciations are hypothesized to have occurred and are commonly referred to as the Sturtian and Marinoan glaciations, respectively (Hoffman and Li, 2009). When these glacial tillites occur in or are associated with fossiliferous sections, they have been included as additional constraints.

The CONOP algorithm

The CONOP program was used here to develop the best-fit hypothetical ordination of species FAD and LAD, radiometric ages, carbon isotopic events and deposition of tillites. At the start of a run, events without *a priori* order (i.e. species FAD and LAD) are randomly assembled by the program with FAD grouped in the first half and LAD in the second half of the sequence. Other events are placed in known order between FAD and LAD groups. The CONOP algorithm proceeds by introducing successive changes (mutations) in the sequence and assessing the quality of the new sequence relative to all of the field data. Mutations must honor all known coexistences. The quality of the mutated time line is assessed by two

criteria: 1) How much shrinking and stretching of locally observed ranges and uncertainty intervals is needed to make all sections fit the time-line; and 2) How many unobserved coexistences does it introduce? The weighted sum of these two criteria is the measure of misfit between data and hypothetical time-lines that CONOP minimizes (Sadler, 2010). Mutations that reduce misfit are always kept. Most of those that increase misfit are rejected but, in order to avoid suboptimal outcomes, some bad mutations must be accepted. As a run progresses the algorithm's tolerance for bad mutations decreases from >50% to ~0% and a best-fit ordination solution results.

Thus CONOP produces good hypothetical solutions for large and locally contradictory datasets. Multiple runs with the same starting conditions can produce different, equally or nearly equally well-fit solutions. The differences in the solutions are caused by difficulty in locating a unique best-placement of local taxa or sections that do not provide enough information to be easily constrained. This is typically due to either long-lived taxa in short sections or rare taxa in too few sections. If all of the taxa recorded in a local section have stratigraphic ranges that exceed that section, there will be little context for placement of that section in sequence. This is an unsurprisingly common occurrence in Neoproterozoic biostratigraphy given the long stratigraphic ranges of several taxa (Butterfield, 2007). Fortunately, several sections that would perform this way can be placed into stratigraphic context of "better behaved" sections. For example, both the Russøya and Macdonaldryggen members of the Elbobreen Formation of Svalbard preserve only species of *Leiosphaeridia*, a

tremendously long-lived form-genus (see below), but the stratigraphic position of these units can be "stitched" to the more fossiliferous and informative units in the Akademikerbreen Group + Polarisbreen Group succession, forcing the position of the problematic sections.

Within the CONOP algorithm these four types of data: biostratigraphic ranges, isotopic excursions, radiometric age constraints, and glacial sedimentary features are assigned to four different logical categories of relative age information that operate differently. The local first and last observations of a species are biased estimators of the true first and last appearance data (FAD and LAD). They do not represent the times of actual speciation and extinction events, but tend to underestimate the true duration of the species. Accordingly, CONOP allows local biostratigraphic ranges to stretch to bring all local species successions into agreement with a single time-line of events (i.e. the local FAD estimator may stretch to a lower point in the section and the local LAD estimator may stretch to a higher one). The composite species range includes times when the species occurs *anywhere*. Conversely, isotopic excursions are better input as uncertainty intervals. The recognition of isotopic excursions depends upon the abruptness of the chemical changes and the sample spacing. The excursion may be treated as two or three, movable and overlapping intervals (e.g. fall, rise, and plateau) designed to ensure a given interval will capture at least one common point in time where it occurs in local sections. This data type is allowed shrink to fit in a correlation, as they are purposefully input as looser depth constraints (e.g. the bottom interval of a negative excursion includes typical $\delta^{13}C$ values from before the fall to

negative values). The final composite uncertainty interval estimates where that part of the excursion is seen *everywhere*. Glacial tillites may be treated as uncertainty intervals or as immovable marker horizons; we treat them as uncertainty intervals. A radiometric date is treated as an immovable marker event in the section where it was collected. The same date is entered as an uncertainty interval (2-sigma analytical uncertainty) in a hypothetical age-scaled section; that section represents the knowledge of the relative age of samples from separate sections. The different approaches to these different data types are taken in data entry so that as much information as possible is used without overstating the precision of any of it (Sadler et al., 2014).

For this study it was determined that ten runs of the program were sufficient. Eight of these ten converged on very similar solutions, the remaining two runs differed from the consensus on minor details but still expressed the same major features (Figs. 2 and 3). The differences are inevitable because the problem is still underdetermined; i.e. too many unknowns. By superimposing multiple outcomes, this limitation is turned into explicit uncertainty statements.

The ten different ordination solutions disagree about the species richness in the earliest portions of this curve (Fig. 2). This is largely due to the poorly constrained sections that can be placed in different positions in the ordinal composite with equally good fits (alternatively seen as equal penalties). It is worth noting here, an artifact that results from selecting a portion of time rather than the whole span of existence of the eukaryotes: taxa

that originated before 1Ga have their local FAD at the beginning of our interval (or somewhat after the beginning for less than common taxa) so there is a certain amount of run-up time required to reach standing richness. This could also be seen in reverse at the end of an interval of interest as species LAD occur. Artificial truncations of our interval boundaries can create the appearance of speciation and extinction events. To mitigate this edge-effect we added buffer regions of time by including some Mesoproterozoic and Ediacaran sections to pull the spurious range-end events away from the boundaries of our interval of interest (Fig. 2). This approach insures the run-up into and run-down out of standing richness occur outside of our interval of interest. Please note that these buffer regions should not be read as richness records for the Mesoproterozoic Era and Ediacaran Period due to incomplete data and the same edge-effect mentioned above.

It is important to understand the limitations of our data and if sampling unevenness affects our results. From the dataset the CONOP program can produce a curve illustrating section richness through time and can apply a rarefaction algorithm. Whereas rarefaction in modern ecological studies addresses a sample size as numbers of individuals in space, paleoecological studies require the additional dimension of time. Our sample size is measured as the number of all local taxon ranges that range-through each event level in our composite (thus, taxa that appear in many sections are counted many times). In this way we consider both the number sections, and the number and evenness of distribution of taxon ranges through time. The rarefaction algorithm estimates how many different taxa we would

see if the sample size had been a lower, constant size– one near our lowest actual sample size. Thus if all of our taxa are seen in many places, halving the sample size might capture the same number of them. But if all taxa are seen only once, halving the count might halve the richness and if one taxon is seen everywhere and the others only once, halving the sample size might drop the observed richness to the one cosmopolitan taxon and very few others.

Results

Species Richness Record

Despite a few poorly constrained sections, major features of the eukaryote species richness record persist in each of the ordination solutions (Figs. 2 and 3). The species richness records presented here overlay ten best-fit solutions of ordination utilizing the same parameters and input of biostratigraphic, carbon isotopic and radiometric data. These records differ only in presentation: one (Fig. 2) illustrates an ordinal composite sequence of events and the other (Fig. 3) is the same composite scaled to the geologic time scale. Functionally, this means that figure 2 is scaled in terms of the occurrence of events, as if biological turnover (speciation and extinction) maintained an even pace—for example few events such as species FAD and LAD occur in the 1Ga to 811 Ma time span, thus this is a compressed region of the graph. Conversely, figure 3 is scaled linearly by time and this same 189 Ma interval, the entirety of the Tonian and a portion of the Cryogenian periods (as currently defined; Shields-Zhou et al., 2012), is much expanded (Fig. 3a).

The process of creating a time-scaled composite is explained in detail by Sadler and colleagues (2009). Briefly, this proceeds from the ordinal composite that is first scaled using local section thicknesses that have been normalized based on the number of events a section spans (but does not necessarily observe), and the average thicknesses between events in those sections. This creates a scaled composite in which events inherit their order from the ordinal composite and their proportional stratigraphic placements from the average spacing between individual events in the normalized sections. Thus the scaled composite should look like a single hypothetical section that records all events in their order and with proportional occurrences. The scaled composite is then calibrated using piece-wise linear interpolation between the external age constraint events imbedded within the composite.

Major Features of species richness record

One of the first major features of the Neoproterozoic species richness record is an increase between 805 and 800 Ma, which is temporally associated with the second interval, or plateau, of the Bitter Springs carbon isotopic stage. This is followed by a drop ~770 Ma and then another increase in species richness starting ~760 Ma. Previous estimates of species richness (Knoll, 1994; Vidal and Moczydłowska-Vidal, 1997; Knoll et al., 2006) suggested a similar increase near this time but did not differentiate between what appears be two peaks with an intervening drop in richness. The drop in richness between 770 and 760 Ma is driven by the last appearances of a number of acritarch taxa such as *C. buickii* and *V. lophostriata*

and the peak that follows ~760 Ma results from several first appearances of vase-shaped microfossil taxa such as *Bonniea dacruchares* and *Melanocyrillium hexodiadema.* These VSM taxa are short-lived however; their last appearances result in the steep drop in richness ~750 Ma. This drop is well-supported by the multiple CONOP solutions and has been suggested by previous studies (Knoll, 1994; Vidal and Moczydłowska-Vidal, 1997; Knoll et al., 2006; Nagy et al., 2009; Riedman et al., 2014). Although previously hypothesized to have been precipitated by the onset of the Sturtian glaciation, these data indicate the drop in richness— and indeed extinction, as these taxa are never again seen— occurred well before any lithological evidence of glaciation. This low level of species richness continued through the Sturtian and Marinoan glaciations, recovering in the Ediacaran Period with the appearance of a new suite of taxa.

Section Correlations

The same ordination solutions that were used to generate the species richness record can also provide section correlations (Fig. 4) and local and composite ranges of individual taxa (discussed below; Fig. 5).

The correlation of section ranges (Fig. 4) is illustrated on a vertical scale of the sequence of events for one of the ordinal solutions. Here each local section is drawn as a rectangle, the vertical length of which is dictated by the number of events spanned by that section; it does not necessarily correlate with thickness of a section or duration of

deposition. Events that are actually observed in that section are indicated by black horizontal bars; these bars can be seen as a sort of degree of support for a section's relative position. Where these bars are instead grey, there was an event that was recorded somewhere– that occurred during the duration of this section– but was just not recorded here. For sections that record only long-lived taxa and no external age constraints, the length of the rectangle indicated by the algorithm is often exaggerated, reflecting the total uncertainty in the age of the poorly-constrained taxa. The FAD and LAD of those long-lived taxa are well outside of the section bounds and do nothing to constrain the section. To reduce this effect the long-lived genus *Leiosphaeridia* was removed for the purposes of correlation (but was included for purposes of the richness record).

The correlation of sections presented here (Fig. 4), although the best estimate of the algorithm from the current dataset, is likely to have some minor anomalies. One eye-catching feature is the occurrence of the mineralized scale microfossils of the upper Fifteenmile Group of the western Ogilvie Mountains (previously Tindir Group; Allison and Awramik, 1989; Cohen and Knoll, 2012) in the Sturtian–Marinoan interglacial period. Based on regional correlations these fossils are understood to be older than the Sturtian glacial event (~716 Ma) and most likely just younger than the Bitter Springs stage—but without those external age constraints attached to the section and the fact that the scale microfossils are found nowhere else, the algorithm chose to place the section to minimize forced co-occurrences with other taxa. This usually means that a unique fauna will be placed

in an interval of minimum richness. This can be corrected in the dataset by providing the western Ogilvie Mountains section with the regionally established age constraint and by including the Sturtian and Marinoan glacial units up-section from the fossils. The nature of this error, however, is telling—the fact that the algorithm placed these singleton fossils in the interglacial interval speaks to the depauperate condition of the assemblage extant during that time; there were only a few long-ranging taxa present, thus conflict would be minimal. Proper placement of this section will likely result in an increase of the current richness peak between 805 and 775 Ma.

This section correlation provides testable predictions of potential positions of the Bitter Springs and Islay negative carbon isotopic excursions and suggests sections as targets for future paleontological study of specific time intervals and of specific taxa. For example, upper portions of the Chuar Group, and possibly the Visingsö Group may record the Islay carbon isotope anomaly and geochemical analyses of the Miroyedikha and Alinya formations could reveal the Bitter Springs carbon isotopic stage. Similarly, the Alinya Formation and portions of the Chuar Group share new acritarch taxa that may shed light on acritarch affinities and with this new section correlation, additional localities of study have been identified.

Potential index taxa

Index taxa should be common, globally distributed and short-lived. None of the species suggested in the literature or discovered during this study can approach the Phanerozoic standard for index fossils. Nonetheless, several species previously suggested as having biostratigraphic utility do appear to have been relatively short-lived (Fig. 5a). *Cerebrosphaera buickii*, a distinctive and robust acritarch does show promise for biostratigraphic use, as do the VSMs. The stratigraphic range of *C. buickii* (Fig. 5b) is rather restricted (~805 to 750 Ma) as compared with *Trachyhystrichosphaera aimika* (~1114 to 750 Ma; Fig. 5c), another candidate index taxon. As noted in the local ranges above the composite histogram for *C. buickii* (Fig. 5b), this fossil is cosmopolitan, having been recovered in units of northern Baltica, Svalbard, Siberia, northern Laurentia and Australia.

The composite range of the total VSM group (Fig. 5d) is similarly restricted and the paleogeographic distribution of these fossils is similarly broad; they have been recovered in northern Baltica, Greenland, Svalbard, northern Laurentia and Australia (Australian occurrence not included in the database due to lack of stratigraphic context; Saito et al, 1988). Although currently supported by only a few fossil finds, it appears that individual VSM species may offer tighter stratigraphic resolution. The composite ranges of two of the most common VSM species, *Bonniea dacruchares* and *Melanocyrillium hexodiadema*, have been plotted upon the VSM total group composite range (Fig. 5d). These plots indicate a relatively short stratigraphic range for the VSM total group, appearing at about 774 Ma and disappearing ~750 Ma. Within the VSM total group, *B. dacruchares* and *M. hexodiadema*

appear towards the end of this interval, at about 760 Ma, and survive for only about 10 million years before their last appearances during the drop in richness ~750 Ma.

Caveats and Biases

Sampling

Sampling bias is a major concern in biostratigraphic analyses, raising questions about whether the features of a richness curve result from uneven sampling and if sampling is paleogeographically even.

In the section correlation diagram (Fig. 4), sections have been grouped by paleogeographic region (Fig. 1) allowing assessment of possible geographic and temporal biases. Given the broad distribution of sections it appears that this dataset does represent global fossil distribution; the resulting species richness record can justifiably called a "global" record. The main geographically driven trend seen here (other than a discomfiting lack of South American and African sections) is the loss of global coverage from just before the Islay isotopic excursion through the Marinoan glaciation. Indeed there appear to be fewer sections overall recording this interval. This is contrasted by the more numerous and geographically evenly distributed sections recording deposition before during and after the Bitter Springs stage.

This temporal unevenness in sampling trends with peaks and troughs of the richness record, a worrying finding for purposes of developing a species richness record. However,

we have found this pattern is also seen in individual section richness through time (Fig. 6); that is, sections in the richness peak intervals tend to be richer, themselves, than sections in trough intervals—the global richness pattern is accurately echoing the local richness pattern. Thus, even if there were the same number of sections through time, the richness curve would retain its features. This is seen in the rarefied richness curve (Fig. 7) in which unevenness of sampling is corrected.

Time averaging

During data entry much consideration was given to what constitutes species co-occurrence. Even within a single sample, time averaging can create false co-occurrences of individual fossils separated by millions of years in the span of a few centimeters. This problem is exacerbated by the fact that sampling protocols vary from worker to worker and from field to drillcore and are not always detailed in publications. Certainly, higher resolution paleontological sampling is a laudable goal and will result in refined stratigraphic ranges of some taxa. That being said, however, the tendency of most Neoproterozoic taxa to be very long-lived will dictate a short journey to the point of diminishing returns. Here the long-lived nature of Neoproterozoic taxa can be seen as advantageous—if the time-averaging caused by slow sedimentation, erosion or large samples represents less than a few million years, it is unlikely to significantly affect the species richness record.

Conclusions and remaining questions

Paleontological, geochemical and radiometric data have been combined and analyzed using the CONOP seriation and correlation algorithm, resulting in a high-resolution eukaryotic species richness record for the early to middle Neoproterozoic Era (1 Ga to 635 Ma). Major features of this record include an increase in species richness at ~805 Ma, sustained high richness levels until a decrease ~770 Ma and then a sharp and short-lived increase at ~760 Ma before falling to and maintaining—for an extended time—the lowest richness levels recorded in this interval. These findings are in keeping with those of previous studies of eukaryotic species richness but with the addition of a double-dip extinction, first of diverse ornamented and process-bearing acritarchs, followed by the rapid appearance and then extinction of vase-shaped microfossil taxa. Additionally, stratigraphic ranges and occurrence data for individual species that had been previously suggested as potential index taxa have been evaluated utilizing the correlation and seriation of fossiliferous sections. Of these taxa, *Cerebrosphaera buickii* and the vase-shaped microfossils appear to have the most biostratigraphic promise. In addition to providing insight into the biota of the Neoproterozoic Era, both the eukaryotic species richness record and section correlations generated here provide testable predictions for future paleontological and geochemical study.

References Cited

Allison. C. W. and Awramik., S., 1989, Organic-walled microfossils from the earliest Cambrian or latest Proterozoic Tindir Group rocks, northwestern Canada: Precambrian Research, v. 43, p. 253–294.

Brasier, M. D. and Shields, G., 2000, Neoproterozoic chemostratigraphy and correlation of the Port Askaig glaciation, Dalradian Supergroup of Scotland: Journal of the Geological Society, London, v. 157, p. 909–914.

Butterfield, N. J., 2004, A vaucheriacean alga from the middle Neoproterozoic of Spitsbergen: implications for the evolution of Proterozoic eukaryotes and the Cambrian explosion: Paleobiology, v. 30, p. 231–252.

Butterfield, N. J., 2005a, Reconstructing a complex early Neoproterozoic eukaryote, Wynniatt Formation, arctic Canada: Lethaia, v. 38, p. 155–169.

Butterfield, N. J., 2005b, Probably Proterozoic Fungi: Paleobiology, v. 31, p. 165–182.

Butterfield, N. J., 2007, Macroevolution and macroecology through deep time: Palaeontology, v. 50, p. 41–55.

Butterfield, N. J. and Grotzinger, J. P., 2012, Palynology of the Huqf Supergroup, Oman, *in* Bhat, G. M., Craig, J. Thurow, J. W., Thusu, B. and Cozzi, A. (eds.) Geology and

Hydrocarbon Potential of Neoproterozoic–Cambrian Basins in Asia Geological Society of London Special Publications, v. 366.

Butterfield, N. J., Knoll, A. H. and Swett, K., 1994, Paleobiology of the Neoproterozoic Svanbergfjellet Formation, Spitsbergen: Fossils and Strata, no. 34, p. 1–84.

Butterfield, N. J. and Rainbird, R. H., 1998, Diverse organic-walled fossils, including "possible dinoflagellates", from the early Neoproterozoic of arctic Canada: Geology, v. 26, p. 963–966.

Canfield, D. E., 2014, Oxygen: a four billion year history: Princeton University Press, 224 p.

Cohen, P. and Knoll, A. H., 2012, Scale microfossils from the mid-Neoproterozoic Fifteenmile Group, Yukon Territory: Journal of Paleontology, v. 86, p. 775–800.

Condon, D. J. and Bowring, S. A., 2011, A user's guide to Neoproterozoic geochronology: *in* Arnaud, E., Halverson, G. P. and Shields-Zhou, G. (eds.) The Geological Record of Neoproterozoic Glaciations: Geological Society, London, Memoirs, no. 36, p. 139–149.

Condon, D. J., Zhu, M., Bowring, S., Wang, W., Yang, A. and Jin, Y., 2005, U-Pb ages from the Neoproterozoic Doushantuo Formation, China: Science, v. 308, p. 95–98.

Cotter, K., 1997, Neoproterozoic microfossils from the Officer Basin, Western Australia: Alcheringa, v. 21, p. 247–270.

Cotter, K., 1999, Microfossils from Neoproterozoic Supersequence 1 of the Officer Basin, Western Australia: Alcheringa, v. 23, p. 63–86.

Dong, L., Xiao, S., Shen, B., Yuan, X., Yan, X., Peng, Y., 2008, Restudy of the worm-like carbonaceous compression fossils Protoarenicola, Pararenicola, and Sinosabellidites from early Neoproterozoic successions in North China: Palaeogeography, Palaeoclimatology, Palaeoecology, v. 258, p. 138–161.

Du, Rulin and Tian Lifu, 1985, Algal macrofossils from the Qingbaikou System in the Yanshan Range of North China: Precambrian Research, v. 29, p. 5–14.

Grey, K., 1999, Proterozoic palynology of samples from Empress 1A, *in* Stevens, M. K. and Apak, S. N., eds., GSWA Empress1 and 1A well completion report Yowalga Sub-basin, Officer Basin, Western Australia: Geological Survey of Western Australia, record 1999/4, p. 68–69.

Grey, K., Hill, A. C., Calver, C., 2011, Biostratigraphy and stratigraphic subdivision of Cryogenian successions of Australia in a global context, *in* Arnaud, E., Halverson, G. P. and Shields-Zhou, G. (eds.) The Geological Record of Neoproterozoic Glaciations: Geological Society, London, Memoirs, no. 36, p. 113–134.

Halverson, G. P., Hoffman, P. F., Schrag, D. P., Maloof, A. C. and Rice, A. H. N., 2007, Toward a Neoproterozoic composite carbon-isotope record: GSA Bulletin, v. 117, p. 1181–1207.

Halverson, G. P., Maloof, A. C. and Hoffman, P. F., 2004, The Marinoan glaciation (Neoproterozoic) in northeast Svalbard: Basin Research, v. 16, p. 297–324.

Halverson, G. P., Maloof, A. C., Schrag, D. P., Dudás, F. Ö. and Hurtgen, M., 2005, Stratigraphy and geochemistry of a ca 800 Ma negative isotope interval in northeastern Svalbard: Chemical Geology, v. 237, p. 5–27.

Halverson, G. P., Wade, B. P., Hurtgen, M. T., Barovich, K. M., 2010, Neoproterozoic chemostratigraphy: Precambrian Research, v. 182, 337–350.

Halverson, G. P. and Shields-Zhou, G., 2011, Chemostratigraphy and the Neoproterozoic glaciations, *in in* Arnaud, E., Halverson, G. P. and Shields-Zhou, G. (eds.) The Geological Record of Neoproterozoic Glaciations: Geological Society, London, Memoirs, no. 36, p. 51–66.

Hill, A. C. and Walter, M. R., 2000, Mid-Proterozoic (~830–750 Ma) isotope stratigraphy of Australia and global correlation: Precambrian Research, v. 100, p. 181–211.

Hill, A. C., Cotter, K. L. and Grey, K., 2000, Mid-Neoproterozoic biostratigraphy and isotope stratigraphy in Australia: Precambrian Research, v. 100, p. 281–298.

Hoffman, P. F., Halverson, G. P., Domack, E. W., Maloof, A. C., Swanson-Hysell, N. L. and Cox, G., 2012, Cryogenian glaciations on the southern tropical paleomargin of Laurentia (NE Svalbard and East Greenland), and a primary origin for the upper Russøya (Islay) carbon isotope excursion: Precambrian Research, v. 206–207, p. 137–158.

Hoffman, P. F. and Li, Z-X., 2009, A palaeogeographic context for Neoproterozoic glaciation: Palaeogeography, Palaeoclimatology, Palaeoecology, v. 277, p158–172.

Hofmann, H. J., 1985, The mid-Proterozoic Little Dal Macrobiota, Mackenzie Mountains, north-west Canada: Palaeontology, v. 28, p. 331–354.

Hofmann, H. J., 1999, Global distribution of the Proterozoic sphaeromorph acritarch *Valeria lophostriata* (Jankauskas): Acta Micropalaeontologica Sinica, v. 16, p. 215–224.

Hofmann, H.J. and Aitken, J. D., 1979, Precambrian biota from the Little Dal Group, Mackenzie Mountains, northwestern Canada: Canadian Journal of Earth Sciences, v. 16, p. 150–166.

Hofmann, H. J. and Rainbird, R. H., 1995, Carbonaceous megafossils from the Neoproterozoic Shaler Supergroup of Arctic Canada: Palaeontology, v. 37, p. 721–731.

Hofmann, H. J. and Jackson, G. D., 1994, Shale-facies microfossils from the Proterozoic Bylot Supergroup, Baffin Island, Canada: Paleontological Society Memoir, no. 37, p. 1–39.

Hong, T-Q, Jia, Z-H, Yin, L-M and Zheng, W-W, 2004, Acritarchs from the Neoproterozoic Jiuliqiao Formation, Huainan region, and their biostratigraphic significance: Acta Palaeontologica Sinica, v. 43, p. 377–387.

Huntley, J. W., Xiao, S. and Kowalewski, M., 2006, 1.3 Billion years of acritarch history: An empirical morphospace approach: Precambrian Research, v. 144, p. 52–68.

Jankauskas, T. V., 1978, Riphean plant microfossils from the southern Urals: Doklady Akademii Nauk SSSR, v. 242, p. 98–100 (in Russian).

Jankauskas, T. V., 1979, Middle Riphean microbiota of the southern Urals and the Ural region of Bashkiria: Doklady Akademii Nauk SSSR, v. 248, p. 190–193 (in Russian).

Jankauskas, T. V., Mikhailova, N. S. and Hermann, T. N. (eds.), 1989. Mikrofossilii Dokembria SSSR: Nauka, Leningrad, p. 191.

Karlstrom. K, Bowring, S., Dehler, C., Knoll, A. H., Porter, S., Des Marais, D., Weil, A., and Sharp, Z., 2000, Chuar Group of the Grand Canyon: record of breakup of Rodinia, associated change in the global carbon cycle, and ecosystem expansion by 740 Ma: Geology, v. 28, p. 619–622.

Kaufman, A. J., Knoll, A. H. and Awramik, S. M., 1992, Biostratigraphic and chemostratigraphic correlation of Neoproterozoic sedimentary succession: Upper Tindir Group, northwestern Canada, as a test case: Geology, v. 20, p. 181–185.

Knoll, A. H., 1984, Microbiotas of the Late Precambrian Hunnberg Formation, Nordaustalndet, Svalbard: Journal of Paleontology, v. 58, p. 131–162.

Knoll, A., 1994, Proterozoic and early Cambrian protists: evidence for accelerating evolutionary tempo: Proceedings of the National Academy of Sciences, v. 91, p. 6743–6750.

Knoll, A. H., 1996, Chapter 4: Archean and Proterozoic paleontology, p. 51–80. *In* J. Jansonius and D. C. McGregor (eds.), Palynology: principles and applications. American Association of Stratigraphic Palynologists Foundation, Vol 1.

Knoll, A. H. and Calder, S., 1983, Microbiotas of the Late Precambrian Ryssö Formation, Nordaustlandet, Svalbard: Palaeontology, v. 26, p. 467–496.

Knoll A. H., Javaux, E. J., Hewitt, D. and Cohen, P., 2006, Eukaryotic organisms in Proterozoic oceans: Philosophical Transactions of the Royal Society B, v. 361, p. 1023–1038.

Knoll, A. H. and Swett, K., 1985, Micropaleontology of the late Proterozoic Veteranen Group, Spitsbergen: Palaeontology, v. 28, p. 51–53.

Knoll, A. H., Swett, K. and Burkhardt, E., 1989, Paleoenvironmental distribution of microfossils and stromatolites in the upper Proterozoic Backlundtoppen Formation, Spitsbergen: Journal of Paleontology, v. 63, p. 129–145.

Knoll, A. H., Swett, K. and Mark, J., 1991, Paleobiology of a Neoproterozoic Tidal Flat/Lagoonal Complex: The Draken Conglomerate Formation, Spitsbergen: Journal of Paleontology, v. 65, p. 531–570.

Knoll, A. H. and Vidal, G., 1980, Late Proterozoic vase-shaped microfossils fromt eh Visingsö Beds, Sweden: Geologiska Föreningens I Stockholm Förhanlingar, v. 102, p. 207–211.

Li, Z. X., Bogdanova, S. V., Collins, A. S., Davidson, A., De Waele, B., Ernst, R. E., Fitzsimons, I. C. W., Fuck, R. A., Gladkochub, D. P., Jacobs, J., Karlstrom, K. E., Lu, S.. Natapov, L. M., Pease, V., Pisarevsky, S. A., Thrane, K. and Vernikovsky, V., 2008, Assembly, configuration, and break-up history of Rodinia: a synthesis: Precambrian Research, v. 160, p. 179–210.

Li, Z-X., Evans, D. A. D. and Halverson, G. P., 2013, Neoproterozoic glaciations in a revised global palaeogeography from the breakup of Rodinia to the assembly of Gondwanaland: Sedimentary Geology, v. 294, p. 219–232.

Macdonald, F. A., Prave, A. R., Petterson, R., Smith, E. F., Pruss, S., Oates, K., Waechter, F., Trotzuk, D. and Fallick, A. E., 2013, The Laurentian record of Neoproterozoic glaciation, tectonism, and eukaryotic evolution in Death Valley, California: GSA Bulletin, v. 125, p. 1203–1223.

Macdonald, F. A., Schmitz, M. D., Crowley, J. L., Roots, C. F., Jones, D. S., Maloof, A. C., Strauss, J. V., Cohen, P. A., Johnston, D. T. and Schrag, D. P., 2010, Calibrating the Cryogenian: Science, v. 327, p. 1241–1243.

Martí Mus, M. and Moczydłowska, M., 2000, Internal morphology and taphonomic history of the Neoproterozoic vase-shaped microfossils from the Visingsö Group, Sweden: Norsk Geologisk Tidsskrift, v. 80, p. 213–228.

McFadden, K., Xiao, S., Zhou, C. and Kowalewski, M., 2009, Quantitative evaluation of the biostratigraphic distribution of acanthomorphic acritarchs in the Ediacaran Doushantuo Formation in the Yangtze Gorges area, South China: Precambrian Research, v. 173, p. 170–190.

Meyer, K. M. and Kump, L. R., 2008, Oceanic euxinia in Earth history: Causes and Consequences: Annual Review of Earth and Planetary Sciences, v. 36, p. 251–288.

Nagy, R. M., Porter, S. M., Dehler, C. M. and Shen, Y., 2009, Biotic turnover driven by eutrophication before the Sturtian low-latitude glaciation: Nature Geoscience, v. 2, 415–418.

Nyberg, A. V. and Schopf, J. W., 1984, Microfossils in stromatolitic cherts from the upper Proterozoic Min'yar Formations, southern Ural Mountains, USSR: Journal of Paleontology, v. 58, p. 738–772.

Parfrey, L. W., Lahr, D. J. G., Knoll, A. H. and Katz, L. A., 2011, Estimating the timing of early eukaryotic diversification with multigene molecular clocks: Proceedings of the National Academy of Sciences, v. 108, p. 13624–13629.

Petrov, P. Yu and Veis, A. F., 1995, Facial-ecological structure of the Derevnya Formation microbiota: upper Riphean, Turukhansk Uplift, Siberia: Stratigraphy and Geological Correlations, v. 3, p. 435–460.

Porter, S. M. and Knoll, A. H., 2000, Testate amoebae in the Neoproterozoic Era: evidence form vase-shaped microfossils in the Chuar Group, Grand Canyon: Paleobiology, v. 26, p. 360–385.

Porter, S. M., Meisterfeld, R. and Knoll, A. H., 2003, Vase-shaped microfossils from the Neoproterozoic Chuar Group, Grand Canyon: a classification guided by modern testate amoebae: Journal of Paleontology, v. 77, p. 409–429.

Prasad. B., Uniyal, S. N. and Asher, R., 2005, Organic-walled microfossils from the Proterozoic Vindhyan Supergroup of Son Valley, Madhya Pradesh, India: Palaeobotanist, v. 54, p. 13–60.

Prave, A. R., Fallick, A. E., Thomas, C. W., and Graham, C. M., 2009, A composite C-isotope profiles for the Neoproterozoic of Scotalns and Ireland: Journal do the Geological Society, London, v. 166, p. 845–857.

Qian, M-P, Jiang, Y. and Yu, M-G., 2009, Neoproterozoic millimetric-centimetric carbonaceous fossils form northern Anhui and Jiangsu, China: Acta Palaeontologica Sinica, v. 48, p. 74–88.

Riedman, L. A., Porter, S. M., Halverson, G. P., Hurtgen, M. T. and Junium, C. 2014, Organic-walled microfossil assemblages from glacial and interglacial Neoproterozoic units of Australia and Svalbard: Geology, v. 42, p. 1011–1014.

Riedman, L.A. and Porter, S.M., *in press*. Organic-walled microfossils of the mid-Neoproterozoic Alinya Formation, Officer Basin, Australia: Journal of Paleontology.

Sadler, P. M., 2010, Brute-force biochronology: sequencing paleobiologic first- and last-appearance events by trial-and-error, *in* Alroy, J. and Hunt, G. (eds.), Quantitaive Methods in Paleobiology: Paleontological Society short course, Paleontological Society Papers, v. 16, p. 271–289.

Sadler, P. M., Cooper, R. A. and Crampton, J. S., 2014, High-resolution geobiologica time-lines: progress and potential, fifty years after the advent of graphic correlation: The Sedimentary Record, v. 12, p. 4–9.

Sadler, P. M., Cooper, R. A. and Melchin, M., 2009, High-resolution, early Paleozoic (Ordovician-Silurian) time scales: GSA Bulletin, v. 121, p. 887–906.

Saito, Y., Tiba, T. and Matsubara, S., 1988, Precambrian and Cambrian cherts in northwestern Tasmania: Bulletin of the National Museum of Tokyo, Series C, v. 14, p. 59–70.

Samuelsson, J., 1997, Biostratigraphy and palaeobiology of early Neoproterozoic strata of the Kola peninsula, Northwest Russia: Norsk Geologisk Tidsskrift, v. 77, p. 165–192.

Samuelsson, J. and Butterfield, N. J., 2001, Neoproterozoic fossils from the Franklin Mountains, northwestern Canada: stratigraphic and palaeobiological implications: Precambrian Research, v. 107, p. 235–251.

Samuelsson, J., Dawes, P. R. and Vidal, G., 1999, Organic-walled microfossils from the Proterozoic Thule Supergroup, northwestern Greenland: Precambrian Research, v. 96, p. 1–23.

Sergeev, V. N., 2001, Paleobiology of the Neoproterozoic (upper Riphean) Shorikha and Burovaya silicified microbiotas, Turukhansk Uplift, Siberia: Journal of Paleontology, v. 75, p. 427–448.

Sergeev, V., Knoll, A. and Grotzinger, J., 1995, Paleobiology of the Mesoproterozoic Billyakh Group, Anabar Uplift, Northern Siberia: Memoir of the Paleontological Society, no. 39, p. 1–37.

Sergeev, T. V., Knoll, A. H. and Petrov, P. Yu., 1997, Paleobiology of the Mesoproterozoic-Neoproterozoic transition: the Sukhaya Tunguska Formation, Turukhansk Uplift, Siberia: Precambrian Research, v. 85, p. 201-239.

Sergeev, V. N. and Lee Seong-Joo, 2006, Real eukaryotes and precipitates first found in the middle Riphean stratotype, southern Urals: Stratigraphy and Geological Correlation, v. 14, p. 1–18.

Sergeev, V. N. and Schopf, J. W., 2010, Taxonomy, paleoecology and biostratigraphy of the late Neoproterozoic Chichkan microbiota of south Kazakhstan: the marine biosphere on the eve of metazoan radiation: Journal of Paleontology, v. 84, p. 363–401.

Shields-Zhou, G., Hill, A. C. and Macgabhann, B. A., 2012, The Cryogenian Period, *in* Gradstein, F., Ogg, J., Schmitz, M. and Ogg, G. (eds.) The Geologic Time Scale 2012: Elsevier, p. 393–411.

Singh, V. K., Babu, R. and Shukla, M., 2009, Discovery of carbonaceous remains from the Neoproterozoic shales of Vindhyan Supergoup, India: Journal of Evolutionary Biology Research, v. 1, p. 1–17.

Srivastava, P., 2002, Carbonaceous megafossils from the Dholpura shale, uppermost Vindhyan Supergroup, Rajasthan: an age implication: Journal of the Palaeontological Society of India, v. 47, p. 97–105.

Srivastava, P., 2009, Trachyhystrichosphaera: an age-marker acanthomorph from the Bhander Group, upper Vindhyan, Rajasthan: Journal of Earth System Sciences, v. 118, p. 575–582.

Strauss, J., Rooney, A. D., Macdonald, F. A., Brandon, A. D and Knoll, A.H., 2014, 740 Ma vase-shaped microfossils from Yukon, Canada: Implications for Neoproterozoic chronology and biostratigraphy: Geology, v. 42, p. 659–662.

Tang, Q., Pang, K., Xiao, S., Yuan, X., Ou, Z. and Wan, B., 2013, Organic-walled microfossils from the early Neoproterozoic Liulaobei Formation in the Huainan region of North China and the biostratigraphic significance: Precambrian Research, v. 236, p. 157–181.

Veis, A. F., Petrov, P. U. and Vorob'eva, N. G., 1998, Miroedikha mikrobiota Verkhnego Rifeya Sibiri: Stratigrafiya. Geologicheskaya Korreliatsiya, v. 6, p. 15–37.

Vidal, G., 1976a, Late Precambrian microfossils from the Visingsö beds in Southern Sweden: Fossils and Strata, no. 9, p. 1–37.

Vidal, G., 1976b, Late Precambrian acritarchs from the Eleonore Bay Group and Tillite Group in East Greenland: Grønlands Geologiske Undersøgelse Rapport, no. 78, p. 1–19.

Vidal, G., 1979, Acritarchs from the upper Proterozoic and lower Cambrian of East Greenland: Grønlands Geologiske Undersøgelse Bulletin, no. 134, p. 1–40.

Vidal, G., 1981a, Aspects of problematic acid-resistant, organic-walled microfossils (acritarchs) in the upper Proterozoic of the North Atlantic region: Precambrian Research, v. 15, P. 9–23.

Vidal, G., 1981b, Micropaleontology and biostratigraphy of the Upper Proterozoic and Lower Cambrian sequence in East Finnmark, northern Norway: Norges Geologiske Undersøkelse, v. 362, p. 1–53.

Vidal, G. and Ford, T. D., 1985, Microbiotas from the Late Proterozoic Chuar Groups (Northern Arizona) and Uinta Mountain Group (Utah) and their chronostratigraphic implications: Precambrian Research, v. 28, p. 349–389.

Vidal, G. and Siedlecka, A., 1983, Planktonic, acid-resistant microfossils from the upper Proterozoic strata of the Barents Sea region of Varanger Peninsula, east Finnmark, northern Norway: Norges Geologiske Undersøkelse, v. 382, p. 45–79.

Vidal, G. and Moczydłowska-Vidal, M., 1997, Biodiversity, speciation and extinction trends of Proterozoic and Cambrian phytoplankton: Paleobiology, v. 23, p. 230–246.

Vidal, G., Moczydłowska, M. and Rudavskaya, V. A., 1993, Biostratigraphic implications of a *Chuaria-Tawuia* assemblage and associated acritarchs from the Neoproterozoic of Yakutia: Palaeontology, v. 36, p. 387–402.

Vorob'eva, N., Sergeev, V. N. and Knoll., A., 2009, Neoproterozoic microfossils from the northeastern margin of the East European Platform: Journal of Paleontology, v. 83, p. 161–196.

Xiao, S., Knoll, A. H., Kaufman, A. J., Yin L. and Zhang Y., 1997, Neoproterozoic fossils in Mesoproterozoic rocks? Chemostratigraphic resolution of a biostratigraphic conundrum from the North China Platform: Precambrian Research, v. 84, p. 197–220.

Yin, L. and Sun, W., 1994, Microbiota from the Neoproterozoic Liulaobei Formation in the Huainan region, northern Anhui, China: Precambrian Research, v. 65, p. 95-114.

Yin, C., Liu, P., Awramik, S. M., Chen, S., Tang, F., Gao, L., Wang, Z., Riedman, L. A., 2011, Acanthomorphic biostratigraphic succession of the Ediacaran Doushantuo Formation in the East Yangtze Gorges, South China: Acta Geologica Sinica, v. 85, p. 283–295.

Zang, W-L and Walter, M., 1992a, Late Proterozoic and Early Cambrian microfossils and biostratigraphy, northern Anhui and Jiangsu, central-eastern China: Precambrian Research, v. 57, p. 243–323.

Zang, W-L and Walter, M., 1992b, Late Proterozoic and Cambrian microfossils and biostratigraphy, Amadeus Basin, central Australia: Association of Australiasian Palaeontologists Memoir, no. 12, p. 1–132.

Figure Captions

Figure 1. Paleogeographic locations of sections. A paleogeographic reconstruction at ~780 Ma showing the general locations of the units sampled in red stars. Craton/terrance abbreviations: A = Amazonia; Ae--Avalonia (east); Aw--Avalonia (west); B--Baltica; C--Congo; EA--East Antarctica; ES--East Svalbard; G--Greenland; I--India; K--Kalahari; L--Laurentia; NA--Northern Australia; NC--North China; R--Rio Plata; S--Sahara; SA--Southern Australia; SC--South China; Sf--Sao Francisco; Si--Siberia; T--Tarim; WA--West Africa. Modified from Li et al. 2013.

Table 1. Table of Fossiliferous Sections. Arranged by paleocontinent from southeast to northwest. References are primary paleontological literature.

Figure 2. Species Richness on Ordinal Composite Timeline. Ten overlapping species richness solutions on X-axis of ordinal succession of events. Greyed areas to the far left and right of figure are buffer regions included to reduce edge-effects (see text) and are not to be taken as representations of species richness in Mesoproterozoic Era or Ediacaran Period.

Figure 3. Species Richness on Time-scale axis. A. the 1 Ga to 635 Ma interval and B. close-up on 850 Ma to 675 Ma interval. Ten overlapping species richness solutions on X-axis of geologic time. Three overlapping intervals of Bitter Springs carbon isotopic stage and Islay carbon isotopic anomaly indicated in blue and purple boxes, respectively. Red triangles indicate radiometric ages: from left to right 811.51 ± 0.25 Ma (Macdonald et al., 2010), 742 ± 6 Ma (Karlstrom et al., 2000), 739.9 ± 6.1 Ma (Strauss et al., 2014), 717.43 ± 0.14 Ma and 716.4 ± 0.24 Ma (Macdonald et al., 2010).

Figure 4. Correlation of Sections. Rectangles representing fossiliferous sections on ordinal scale created without inclusion of *Leiosphaeridia* species. Sections that recorded only *L. spp.* are omitted. Sections are grouped by paleogeographic location from

southeastern to northwestern Rodinia (Fig.1; Li et al., 2013). Length of sections indicates the number of events (FAD, LAD, ages, isotopic events) that occur within a section, which is not necessarily correlated with stratigraphic thickness or duration of deposition. Black bars on sections indicate an event that is actually recorded in a given section and can be taken as degree of support for a section's relative placement. Blue and green regions indicate Bitter Springs carbon isotopic stage and Islay carbon isotopic anomaly, respectively; these events are each represented by three overlapping intervals, the darker color indicates the peak or plateau of the negative excursion. Red lines indicate radiometric ages: 811 Ma and 716 Ma from Macdonald et al., 2010; 742 Ma from Karlstrom et al., 2000; 635 Ma from Condon et al., 2005.

Figure 5. Local support for global composite ranges of selected taxa. Grey blocks indicate composite range of taxa on ordinal scale; height of blocks reflects number of sections in which that taxon occurs. Thin black lines above indicate taxon ranges in local sections. Blue vertical line indicates position of 811.5 Ma age from Fifteenmile Group (Macdonald et al., 2010), purple vertical line indicates position of 742 Ma age from Chuar Group (Karlstrom et al., 2000). A. *Leiosphaeridia crassa*, B. *Cerebrosphaera buickii*, C. *Trachyhystrichosphaera aimika*, D. Vase-shaped microfossils as a group and individual taxa. Total blocks on ordinal composite represent range of VSM total group, black blocks

indicate range of *Melanocyrillium hexodiadema* and textured grey box indicates overlapping ranges of *Bonniea dacruchares* and *M. hexodiadema*. Local ranges are for total group VSM.

Figure 6. Average Section Richness on Ordinal Composite Timeline. Average number of taxa per section on an X-axis of ordinal composite of events from a single solution. Indicates the richness of individual sections across the ordination of events. Note that local section richness echoes the species richness record, indicating high average section richness in intervals of peak species richness, thus the global (species richness) record duplicates the local record. This can be taken to mean that even if sampling were even across time, the features of the species richness record are retained. Blue line indicates 811.5 Ma age from Fifteenmile Group (Macdonald et al., 2010), purple vertical line indicates position of 742 Ma age from Chuar Group (Karlstrom et al., 2000), first set of vertical grey bands indicates overlapping intervals (see text) of Bitter Springs isotopic stage, second set of vertical grey bands indicates Islay carbon isotopic anomaly.

Figure 7. Rarefied Species Richness on Ordinal Composite Timeline. Species richness on ordinal composite from a single solution corrected for uneven abundance of samples. Grey zones indicate buffer regions (discussed in text), Blue and purple vertical lines indicate Bitter Springs carbon isotopic stage and Islay carbon isotopic anomaly, respectively. Correction for sampling as determined from numbers of local ranges on ordinal

scale and held to twenty-five taxa per interval of composite. Lighter blue lines indicate 95% confidence band. Where the three curves meet the sampling is below the 25 taxa threshold and too sparse for rarefaction at this level. Note this echoes the species richness; all major features of species richness record are maintained.

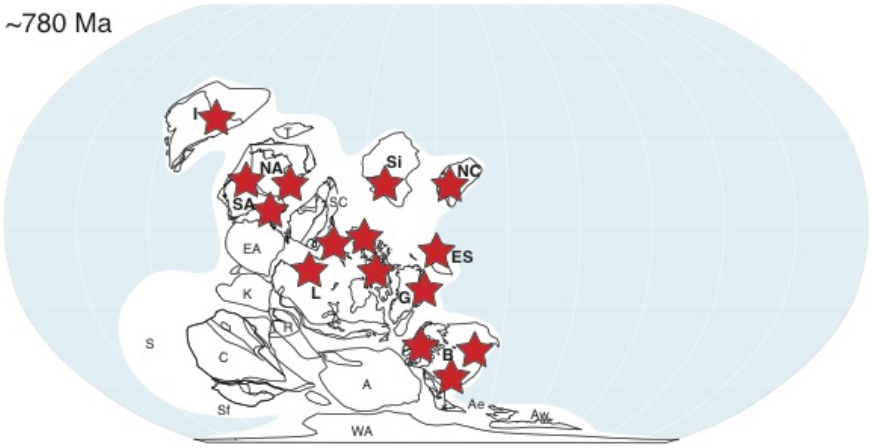

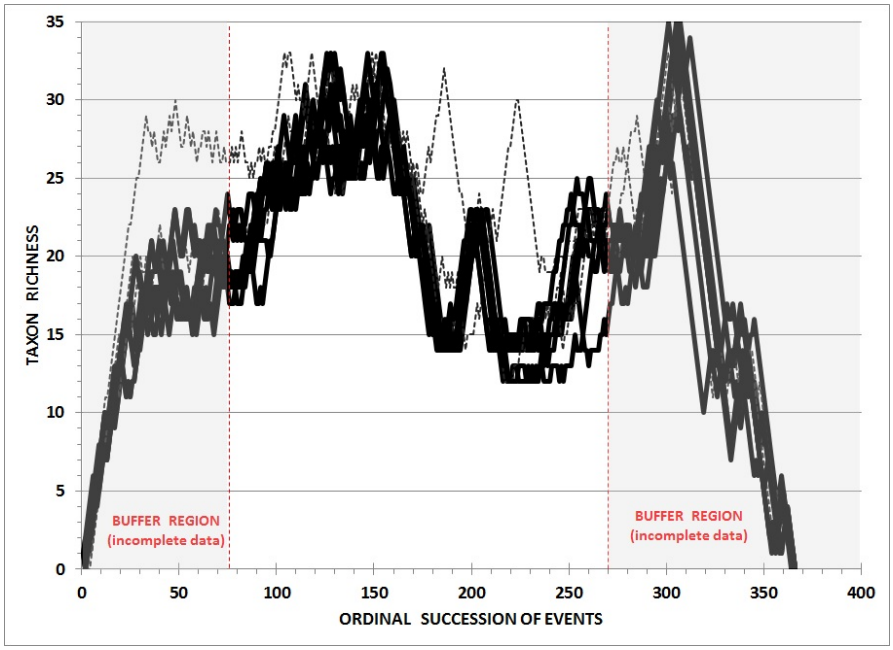

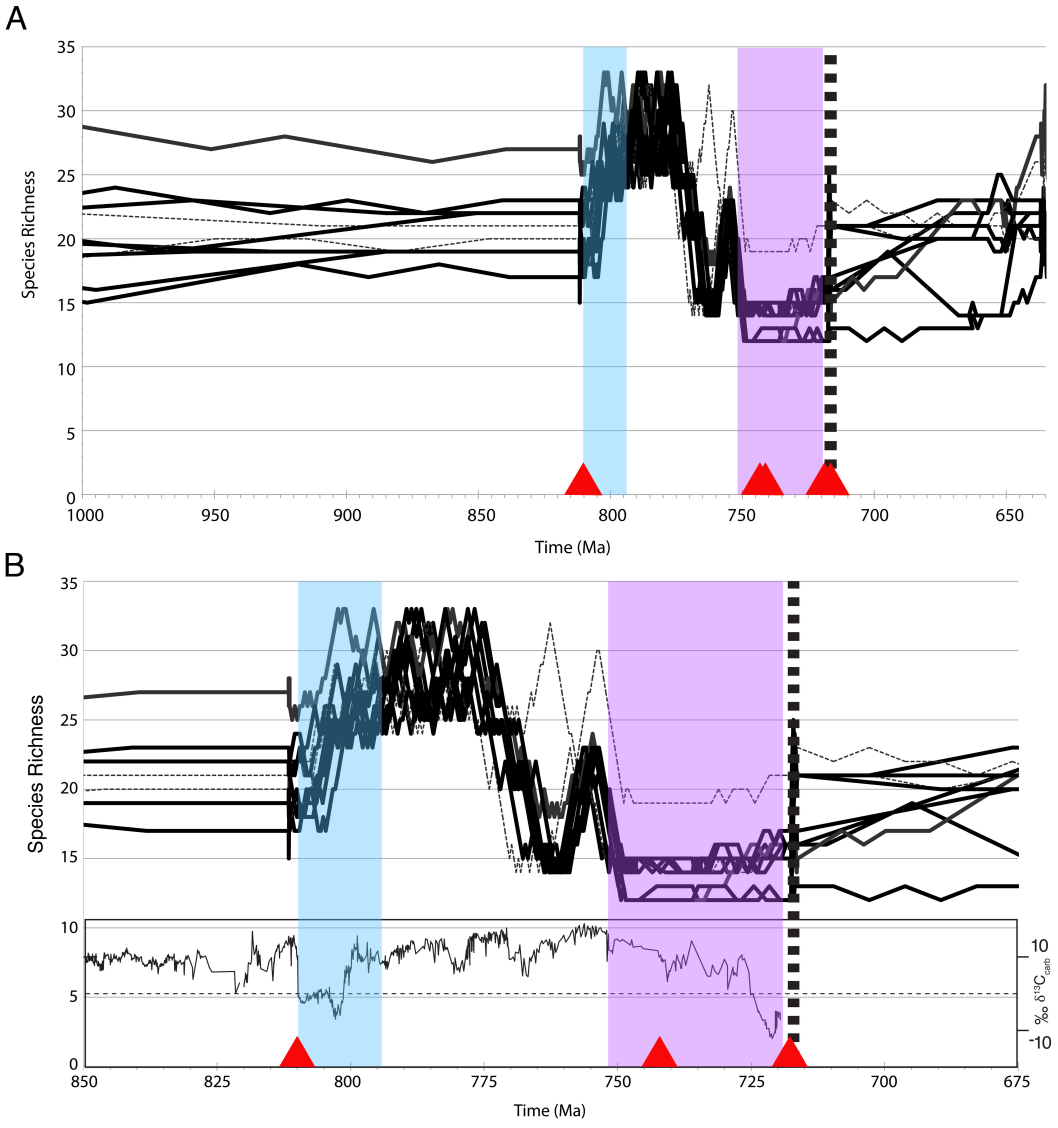
A
Species Richness
35
30
25
20
15
10
5
0
1000
950
900
850
800
750
700
650
Time (Ma)
B
Species Richness
35
30
25
20
15
10
5
0
10
5
0
‰ $\delta^{13}C_{carb}$
10
−10
850
825
800
775
750
725
700
675
Time (Ma)

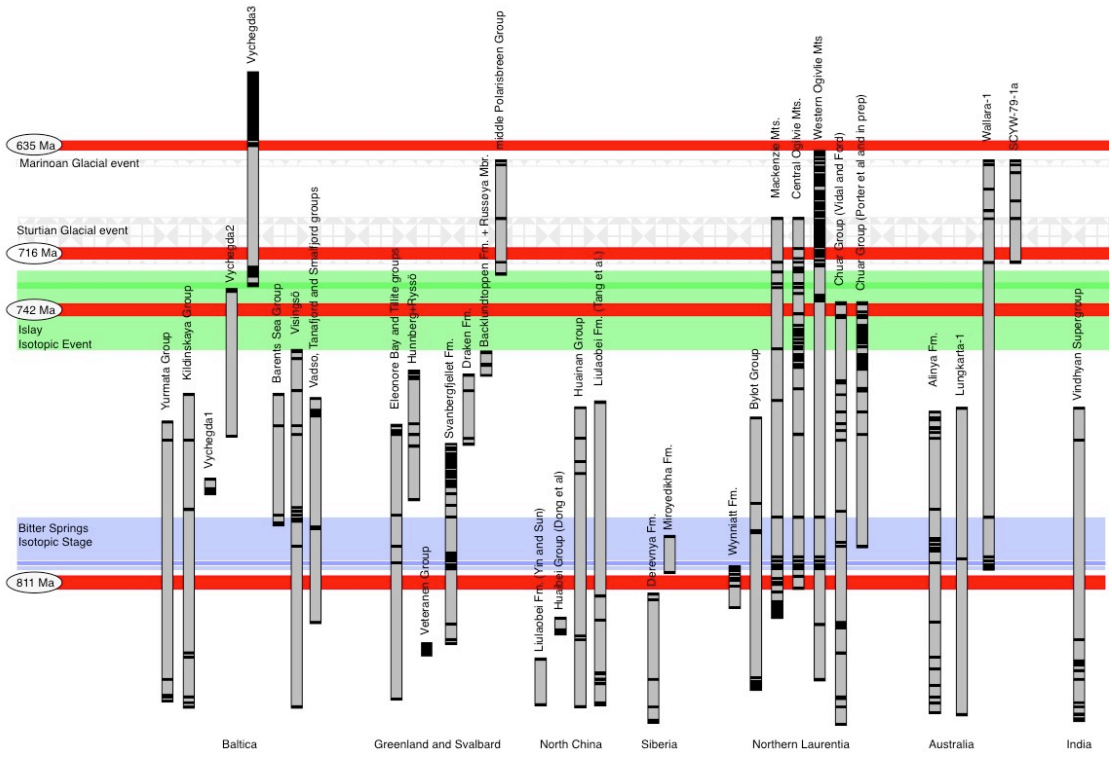
635 Ma
Marinoan Glacial event
Sturtian Glacial event
716 Ma
742 Ma
Islay
Isotopic Event
Bitter Springs
Isotopic Stage
811 Ma
Vychegda3
Vychegda2
Vychegda1
Yurmata Group
Kildinskaya Group
Barents Sea Group
Visingsö
Vadsø, Tanafjord and Smalfjord groups
Eleonore Bay and Tillite groups
Humberg-Ryssö
Veteranen Group
Svanbergfjellet Fm.
Draken Fm.
Backlundtoppen Fm. + Russøya Mbr.
middle Polarisbreen Group
Liulaobei Fm. (Yin and Sun)
Huabei Group (Dong et al)
Huainan Group
Liulaobei Fm. (Tang et al.)
Debengda Fm.
Mirgoyedkha Fm.
Wynniatt Fm.
Bylot Group
Mackenzie Mts.
Central Ogilvie Mts.
Western Ogilvie Mts
Chuar Group (Vidal and Field)
Chuar Group (Porter et al and in prep)
Wallara-1
ICYW-79-1a
Alinya Fm.
Lungkarta-1
Vindhyan Supergroup
Baltica
Greenland and Svalbard
North China
Siberia
Northern Laurentia
Australia
India

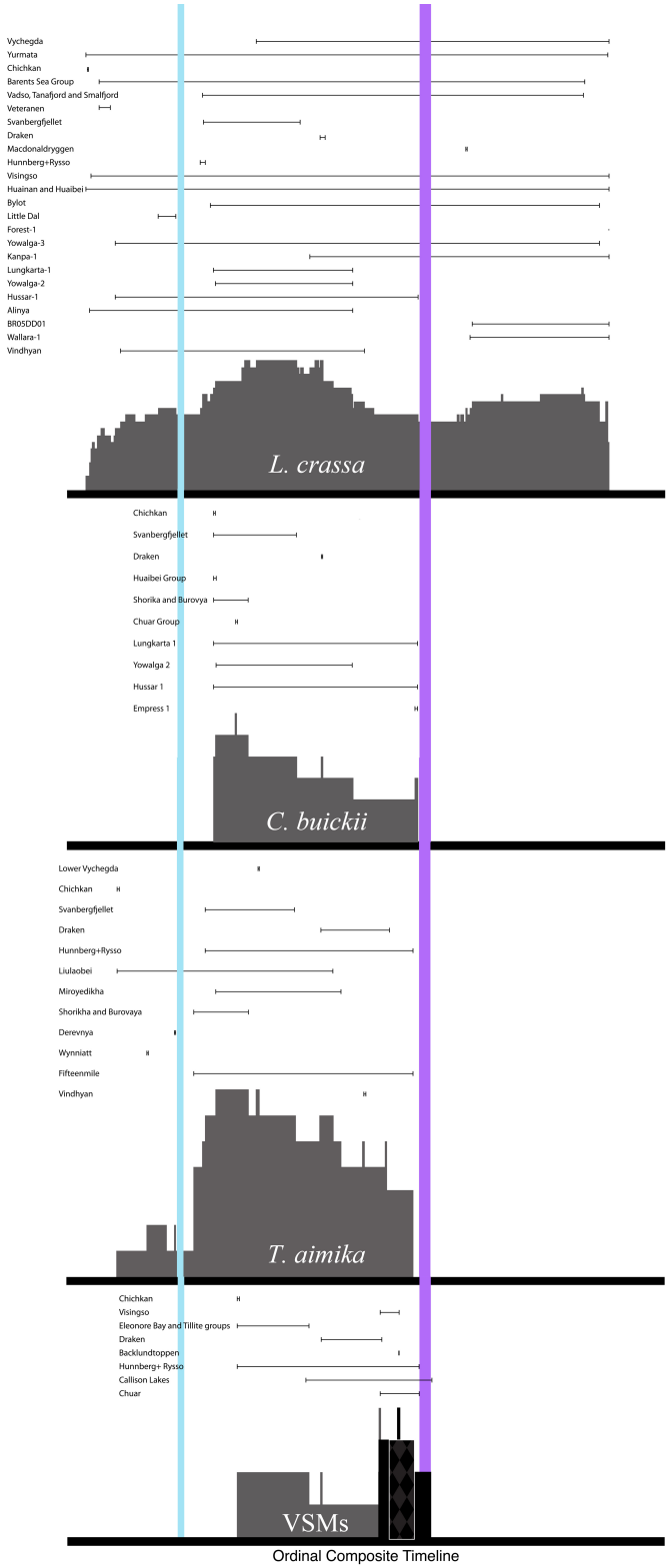

Ordinal Composite Timeline

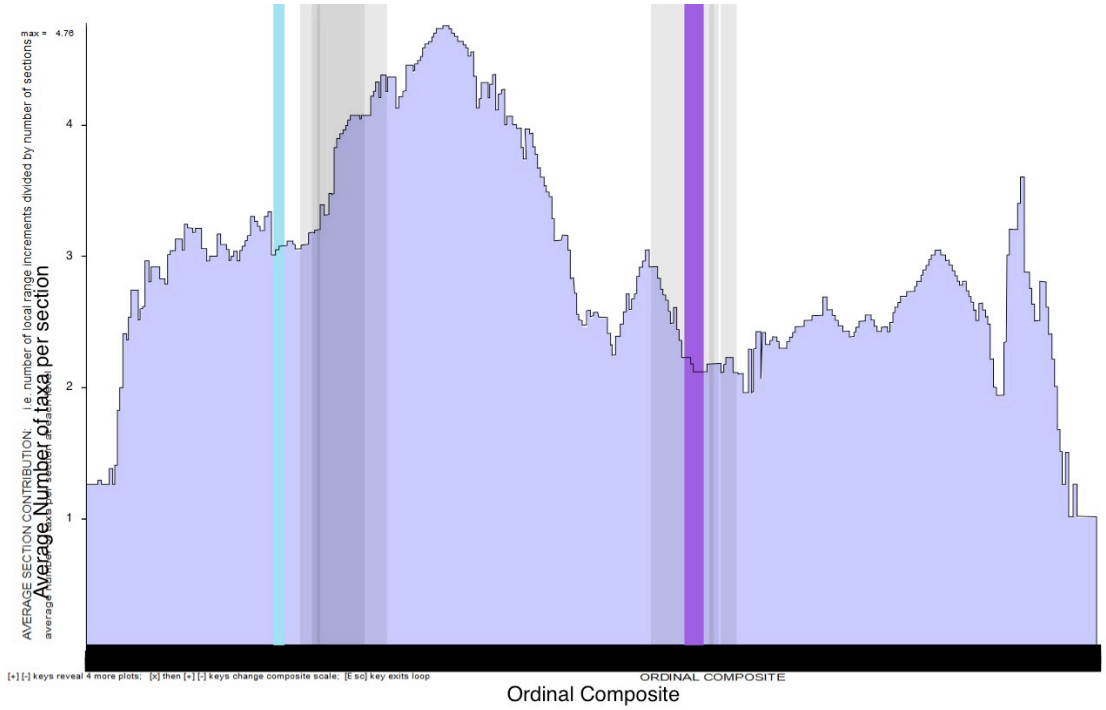
max = 4.78
AVERAGE SECTION CONTRIBUTION i.e. number of local range increments divided by number of sections
Average Number of taxa per section
4
3
2
1
[+] [-] keys reveal 4 more plots; [x] then [+] [-] keys change composite scale; [Esc] key exits loop
ORDINAL COMPOSITE
Ordinal Composite

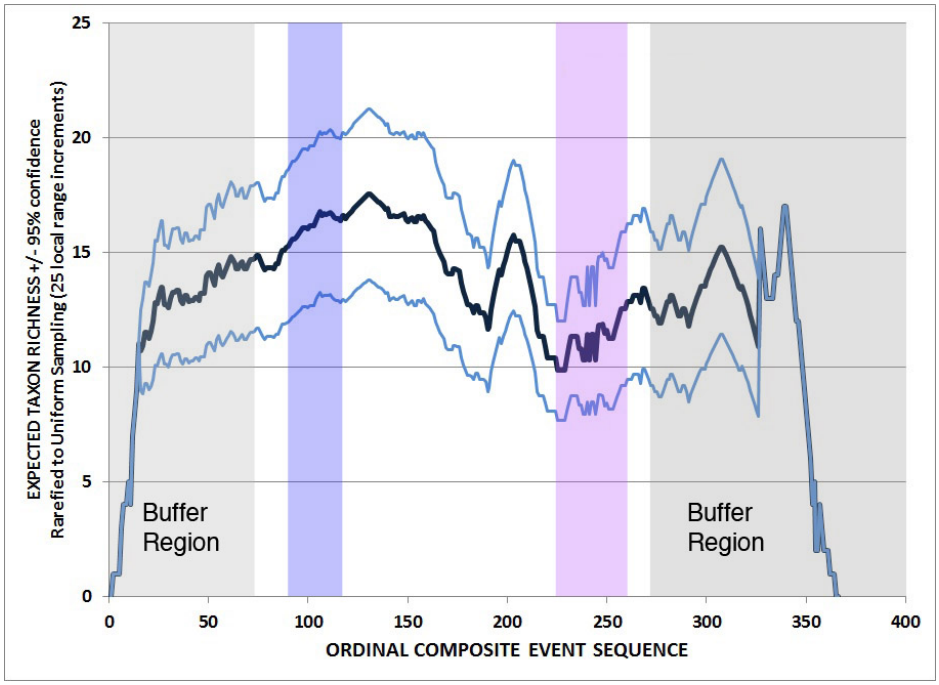
EXPECTED TAXON RICHNESS +/- 95% confidence
Rarefied to Uniform Sampling (25 local range increments)
25
20
15
10
5
0
Buffer Region
Buffer Region
0
50
100
150
200
250
300
350
400
ORDINAL COMPOSITE EVENT SEQUENCE